Critical Reviews in Biochemistry and Molecular Biology, 39:217–259, 2004

ISSN: 1040-9238 print / 1549-7798 online
DOI: 10.1080/10409230490514008

Taylor & Francis
Taylor & Francis Group

Structure-Function Relationships in Unusual Nonvertebrate Globins

Keiji Shikama

Biological Institute, Graduate School of Life Sciences, Tohoku University, Sendai, Japan; PHP Laboratory for Molecular Biology, Nakayama-Yoshinari, Sendai, Japan

Ariki Matsuoka

Department of Biology, Fukushima Medical University, Fukushima, Japan

Based on the literature and our own results, this review summarizes the most recent state of nonvertebrate myoglobin (Mb) and hemoglobin (Hb) research, not as a general survey of the subject but as a case study. For this purpose, we have selected here four typical globins to discuss their unique structures and properties in detail. These include *Aplysia* myoglobin, which served as a prototype for the unusual globins lacking the distal histidine residue; midge larval hemoglobin showing a high degree of polymorphism; *Tetrahymena* hemoglobin evolved with a truncated structure; and yeast flavohemoglobin carrying an enigmatic two-domain structure. These proteins are not grouped by any common features other than the fact they have globin domains and heme groups. As a matter of course, various biochemical functions other than the conventional oxygen transport or storage have been proposed so far to these primitive or ancient hemoglobins or myoglobins, but the precise *in vivo* activity is still unclear.

In this review, special emphasis is placed on the stability properties of the heme-bound O_2. Whatever the possible roles of nonvertebrate myoglobins and hemoglobins may be (or might have been), the binding of molecular oxygen to iron(II) must be the primary event to manifest their physiological functions *in vivo*. However, the reversible and stable binding of O_2 to iron(II) is not a simple process, since the oxygenated form of Mb or Hb is oxidized easily to its ferric met-form with the generation of superoxide anion. The metmyoglobin or methemoglobin thus produced cannot bind molecular oxygen and is therefore physiologically inactive. In this respect, protozoan ciliate myoglobin and yeast flavohemoglobin are of particular interest in their very unique structures. Indeed, both proteins have been found to have completely different strategies for overcoming many difficulties in the reversible and stable binding of molecular oxygen, as opposed to the irreversible oxidation of heme iron(II). Such comparative studies of the stability of MbO_2 or HbO_2 are of primary importance, not only for a full understanding of the globin evolution, but also for planning new molecular designs for synthetic oxygen carriers that may be able to function in aqueous solution and at physiological temperature.

Keywords globins, heme oxidation, evolution, insect (midge), mollusc (*Aplysia*), protozoan (Ciliate), yeast (*Candida*)

Address correspondence to Keiji Shikama, PHP Laboratory for Molecular Biology, Nakayama-Yoshinari 1-16-8, Sendai 989-3203, Japan. E-mail: shikama@mail.tains.tohoku.ac.jp

INTRODUCTION

We do not know exactly when and how free oxygen began to appear on the earth, but it is our common belief that about 2 or 3 billion years ago, molecular oxygen was produced mostly from decomposition of water by photosynthetic cyanobacteria. With increasing amounts of dioxygen on the primitive earth, living cells adapted themselves from the anaerobic form to the aerobic one so as to extend their inhabitable environment. This was really a dramatic change in life. In the anaerobic environment in which primordial life arose glycolysis, for example, represented a successful attempt to extract some of the chemical energy of glucose. In contrast to this, the complete oxidation of glucose to CO_2 and H_2O by utilizing oxygen molecule was the most significant and crucial advancement in cellular metabolic pathways. It thus allowed organisms to enhance greatly their ability to extract the chemical energy of the sugar for use in all living processes.

In light of the high efficiency of energy conservation, this dramatic change from the anaerobic system to the aerobic one may well be designated as an "oxygen (r)evolution." In this evolution, molecular oxygen serves as the

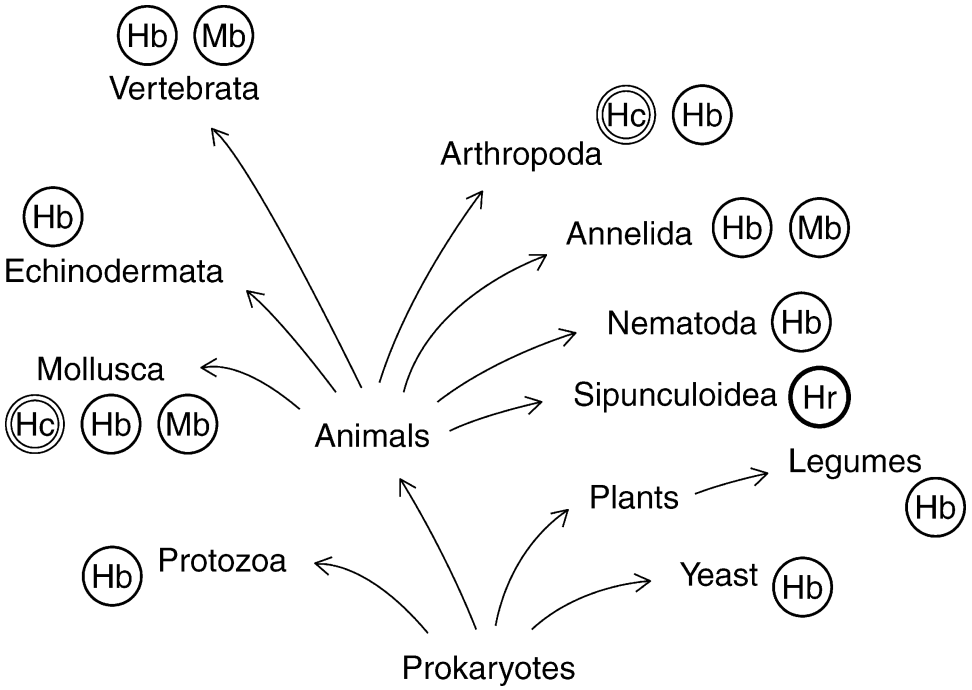

FIG. 1. A phylogenetic tree for the distribution of oxygen-carrying proteins in nature. The carriers include Hb, Mb, Hc, and Hr. Redrawn from Shikama *et al*. (1995).

ultimate electron acceptor to respiratory substrates:

$$\text{Anaerobic} \xrightarrow[\text{Oxygen (R)evolution}]{O_2} \text{Aerobic.} \qquad [1.1]$$

For living cells, however, it was not such a simple process to command molecular oxygen for safe usage, since O_2 gas has a triplet ground state, $^3\Sigma_g^-$, whose biradical electronic configuration is described by the notation

$$O_2(s1s)^2(s^*1s)^2(s2s)^2(s^*2s)^2(s2p_z)^2(p2p_x)^2(p2p_y)^2$$
$$(p^*2p_x)^1(p^*2p_y)^1(s^*2p_z)^0$$

Dioxygen therefore has a very strong tendency to take electrons from other substances and to make the complete electron pairing in its unoccupied orbitals. This leads to the sequential formation of highly reactive or toxic oxygen species such as the superoxide anion (O_2^-), peroxide anion ($O_2^=$), and hydroxyl radical ($HO^{\cdot}$), as by-products of many normal cellular metabolisms. Consequently, the development of enzymes to protect cells against such "oxidant stress" was of great urgency to aerobic organisms. This resulted in the ubiquitous occurrence of superoxide dismutase, catalase, peroxidase, and so on. In these circumstances, hemoglobin (Hb) and myoglobin (Mb) play an essential role in stabilizing molecular oxygen for transport and storage. In these proteins, the iron(II)-dioxygen bond does a vital function in their physiology.

However, the Hb and Mb pair is not always the answer to the problem of carrying molecular oxygen. Other oxygen transport pigments are found in invertebrates. Figure 1 illustrates a phylogenetic tree for the distribution of oxygen-carrying proteins in nature, including hemocyanin (Hc) and hemerythrin (Hr). Nevertheless, the recent discovery of Mb- or Hb-like proteins in virtually all the kingdoms of living organisms has led us to conclude that the gene for Mb or Hb must be very ancient (Hardison, 1998; Couture *et al*., 1999; Wittenberg *et al*., 2002).

For nonvertebrate hemoglobins and myoglobins, Weber and Vinogradov (2001) have made an extensive review from the point of view of the physiological functions and molecular adaptations. Their survey ranges from single-chain globins found in bacteria, algae, protozoa, and plants, to large, multisubunit Hbs found in nematodes, mollusks, and crustaceans, to the giant annelid Hbs comprised of globin and nonglobin subunits. Chimeric Hbs found in bacteria and fungi are also included. As a result, they remarked that the evolutionary trends evident in the structures and functions of nonvertebrate globins appear to be adaptive in extending the inhabitable environment available to Hb- (or Mb-)containing organisms. This review also focuses on the extensive variation in the functional properties of nonvertebrate Hbs and Mbs. In addition to transporting and storing O_2, several novel Hb

functions have emerged, including control of nitric oxide (NO) levels in microorganisms, use of NO to control the level of O_2 in nematodes, binding and transport of sulfide in endosymbiont-harboring species, protection against sulfide, scavenging of O_2 in symbiotic leguminous plants, O_2 sensing in bacteria, and so forth. Their voluminous work is indeed a treasure house of literature in this research field (Weber & Vinogradov, 2001).

More recently, Hargrove and coworkers have presented a critical review for both symbiotic and nonsymbiotic plant Hbs (Kundu *et al*., 2003). In contrast to symbiotic leghemoglobins present in the nitrogen-fixing soybean root nodules, nonsymbiotic Hbs are expressed at low concentrations in nonnodular, rapidly growing, and metabolizing plant tissues and occur widely in both mono- and dicotyledonous plants. In their review, the rate and affinity constants have been compared for oxygen binding to sperm whale Mb, soybean leghemoglobin, and rice nonsymbiotic Hb in conjunction with their different heme pocket structures. As a result, both Mb and leghemoglobin were found to meet the physical requirements to facilitate oxygen diffusion in their respective environments, although leghemoglobin regulates oxygen affinity through a mechanism somewhat different from that of Mb. In rice nonsymbiotic Hb, on the other hand, the heme is hexacoordinated with the distal histidine serving as the sixth ligand. This differs markedly from pentacoordinate leghemoglobin with its open binding site for exogenous ligands, as the usual Mbs and Hbs do so (see Figure 2 of Section II). Nevertheless, nonsymbiotic plant hemoglobins have so far demonstrated extremely high oxygen affinities accompanied with very slow oxygen dissociation rates. The evolutionary origin and physiological role of such hexacoordinate plant hemoglobins still remain a mystery (Kundu *et al*., 2003).

In contrast to these review articles, we have attempted here to provide other aspects of the nonvertebrate globin research. In our case studies, we would like to limit our discussion to a few but very unique globins which are selected in light of the particular importance to the molecular diversity in globin evolution. These include *Aplysia* Mb, which served as a prototype for the unusual globins lacking the distal histidine residue; midge larval Hb showing a high degree of polymorphism; *Tetrahymena* Hb evolved with a truncated structure; and yeast flavohemoglobin carrying an enigmatic two-domain structure. These proteins are not grouped by any common features other than the fact they have globin domains and heme groups. Each topic will be treated broadly enough to interest a general audience yet narrow enough to be within the competence of the authors. In describing these hemoproteins, special focus will also be placed on the stability property of the heme-bound dioxygen. Whatever the possible roles of such primitive or ancient globins may be (or might have been), the reversible binding of molecular oxygen to iron(II) must be the primary event to manifest their physiological functions *in vivo*.

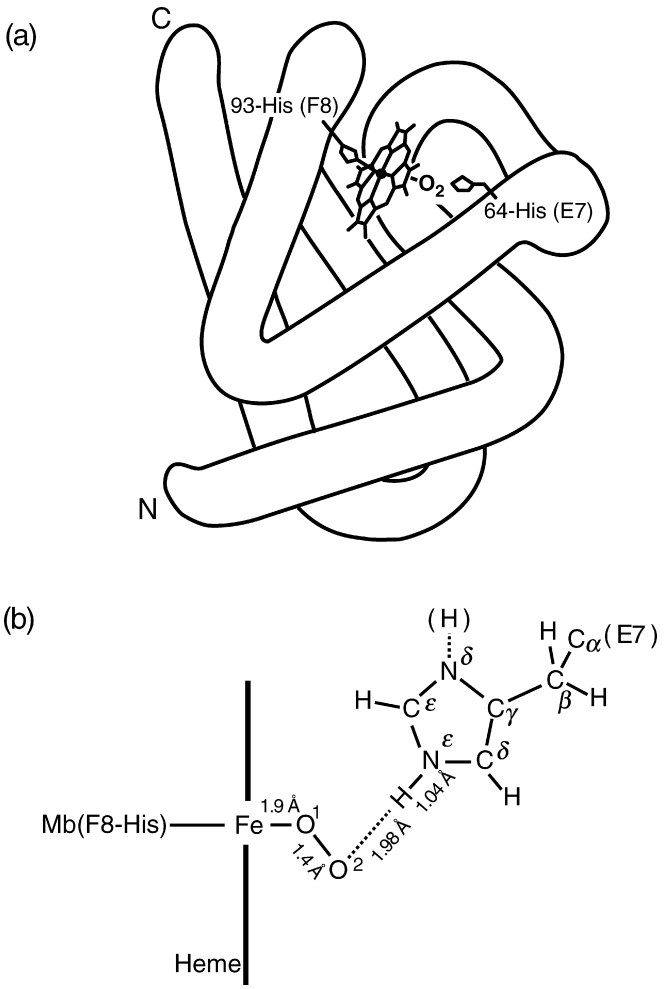

FIG. 2. Schematic representations for the tertiary structure of sperm whale Mb. (a) A pseudo-3D drawing of the whole molecule, showing the two histidine residues that are strongly involved in its function. (b) A detailed geometry of the FeO_2 bond in the molecule (Phillips & Schoenborn, 1981). The bound dioxygen is bent, held end-on, and forms a hydrogen bond to the distal (E7) histidine at position 64, with the angles of $\angle Fe{-}O{-}O = 115 \pm 5^\circ$ and $\angle O{-}O\cdots H = 96^\circ$.

MOLLUSCAN MYOGLOBIN FROM *APLYSIA KURODAI:* AN UNUSUAL LACK OF THE DISTAL HISTIDINE

Discovery of a New Type of Myoglobin from *Aplysia*

Almost the entire Mb molecule has two completely distinct histidines that are deeply involved in its function. Sperm whale Mb, for example, consists of 153 amino acid residues and contains totally 12 histidines. Of these,

one is the heme-binding proximal (F8) histidine at position 93, another is the distal (E7) histidine at position 64. In general, the Mb (or globin) fold consists of eight α-helices wrapped around the heme iron, which lies in a hydrophobic cleft or pocket. The helices are labelled A to H from the N terminus, the corners between them AB to GH, and the N- and C-terminal coil regions are called NA and HC, respectively. Individual residues are numbered, beginning at the N-terminal end of the helix or corner of which they form a part. Accordingly, E7 is the seventh residue from the N-terminal end of the E helix. The two sides of the heme are referred to as proximal or the His F8 side, and distal or the His E7 side to which ligands such as O_2, H_2O, and OH^- can bind, as illustrated in Figure 2.

Recently much attention has been directed to the possible roles of the distal histidine residue in Mb and Hb molecules. It has been suggested that it acts as a gate (Karplus & McCammon, 1986) or a swinging door (Johnson *et al*., 1989; Scott *et al*., 2001) for ligand entry into the heme pocket and that it stabilizes the bound dioxygen by hydrogen-bond formation (Phillips & Schoenborn, 1981) as well as stabilizing the axial water molecule of the ferric, high-spin species (Matsuoka *et al*., 1992; Shikama & Matsuoka, 1994; Quillin *et al*., 1993). Furthermore, the distal histidine *via* its imidazole ring participates in a proton-relay mechanism as a catalytic residue for the acidic oxidation of MbO_2 and HbO_2 (Tsuruga *et al.*, 1998; Shikama, 1988, 1998; Yasuda *et al*., 2002). A detailed geometry of the FeO_2 bond in sperm whale MbO_2, which was revealed by X-ray and neutron diffraction studies (Phillips & Schoenborn, 1981), is also given in Figure 2.

However, there are a few interesting Mbs in which the usual distal histidine is lacking. This new type of Mb was first isolated by Rossi-Fanelli and Antonini (1957) from *Aplysia limacina*, a common gastropod mollusc from the Mediterranean. The crystallographic structure of this molecule is now available at 1.6 Å resolution, and the distal (E7) residue is recognized as Val at position 63 (Bolognesi *et al*., 1989). In relation to these structural results, the stability characteristics of the bound dioxygen of *Aplysia* Mb should be of the most interest and primary concern, but these were little understood. To elucidate these questions, native oxymyoglobin has been isolated directly from the radular muscle of *Aplysia kurodai*, a common species found around the Japanese coast. Its spectral and stability properties have thus been studied extensively and, compared with those of sperm whale Mb that served as a reference. Such an examination should facilitate a fuller understanding of the role of the distal histidine residue in Mb and Hb biochemistry as well as in the evolution of these molecules.

Mb occurs exclusively in red muscles such as those of the cardiac and skeletal tissues of vertebrates. In invertebrates, on the other hand, one of the most remarkable red muscles may be the radular muscle of *Aplysia*, the so-called sea hare with a prominent front pair of tentacles and a rudimentary internal shell. Although the animal carries hemocyanin in its blood (Ghiretti-Magaldi *et al*., 1979), two large, red-colored masses can be clearly seen in a ventral section: one is the buccal apparatus which contains a radula, and the other is the triturating stomach which has a dozen gastric teeth arrayed in it. In the buccal apparatus, the radular muscle works to tear up seaweeds as they enter the oral cavity and become the animal's food. In *Aplysia*, only the two red organs have Mb, its high content being almost comparable to those in cardiac and skeletal muscles of mammals.

As we shall see in later sections, the oxygenated form of *Aplysia* Mb is extremely unstable, and special care must be taken in its preparation (Shikama & Katagiri, 1984): Fresh buccal masses were freed from radula and mucous membrane carefully, and homogenized in 3 volumes of cold distilled water containing 0.5 mM EDTA. After insoluble materials had been removed by centrifugation, the extract was fractionated with ammonium sulfate between 70 and 100% saturation. After gel filtration on Sephadex G-75, the essential step was the chromatographic separation of the oxy form (MbO_2) from its ferric met form (metMb) on a DEAE-cellulose column.

Structural Properties of *Aplysia* Myoglobin

Tentori *et al.* (1968, 1973) were the first to study the amino acid sequence of the myoglobin from *Aplysia limacina*, a Mediterranean species. Subsequently, we also determined the complete amino acid sequence of the myoglobins from *A. kurodai*, a species found around the Japanese coast, and *Aplysia juliana*, a species distributed worldwide (Suzuki *et al*., 1981; Takagi *et al*., 1984). As shown in Figure 3, the Mb from *A. kurodai* is composed of 144 amino acid residues with a calculated molecular mass of 15,940 daltons including the heme moiety. Thus it is smaller than sperm whale Mb by nine residues. When compared with that of *A. limacina*, it contains 21 amino acid replacements and one deletion. In so far as examined, *Aplysia* Mbs are all acetylated at the N terminus and have only a single histidine residue at position 95 that corresponds to the heme-binding proximal (F8) one, consequently lacking the usual distal (E7) histidine.

To predict the secondary structure in solution, we have carried out circular dichroism (CD) measurements for *A. kurodai* Mb in 10 mM buffer, pH 7.4 (Shikama *et al*., 1982). As a result, the mean residue molar ellipticity at 222 nm was found to be $[\theta]^{MRW} = -18{,}500$ deg cm^2 dmol^{-1}. Consequently, *Aplysia* Mb has a considerably low helical content as compared with sperm whale Mb, which has a value of $-24{,}500$ deg cm^2 dmol^{-1}.

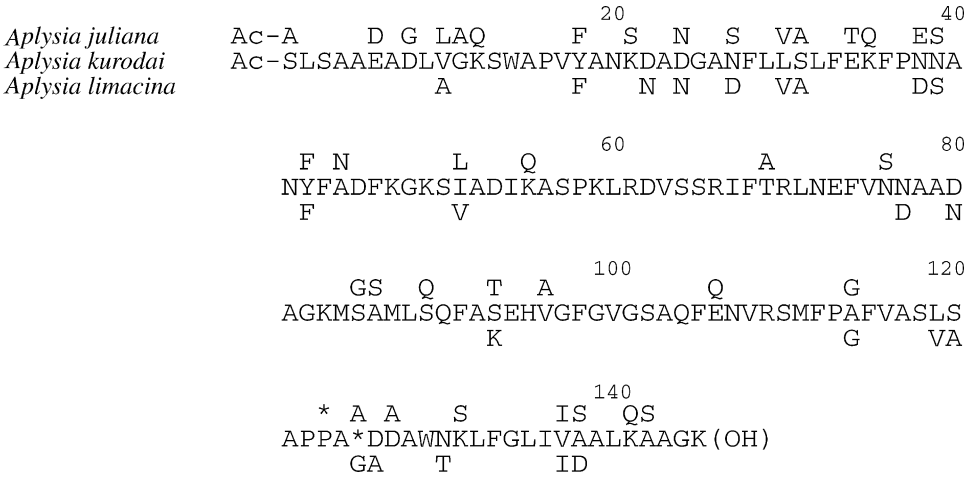

FIG. 3. Primary structure of *Aplysia* Mbs. Amino acid sequence of the Mb from *A. kurodai* is compared with those of *A. juliana* and *A. limacina*. Residues that differ in *A. juliana* and in *A. limacina* are shown above and below the center sequence, respectively, and a deletion is indicated by an asterisk. Sequence data are taken from Suzuki *et al*. (1981) for *A. kurodai*, from Tentori *et al*. (1973) for *A. limacina*, and from Takagi *et al*. (1984) for *A. juliana*.

The X-ray crystal structure of *A. limacina* metmyoglobin was first studied by Ungaretti *et al*. (1978) at 5 Å resolution. Subsequently, the protein was refined to 2.0 Å and then to 1.6 Å resolution by Bolognesi *et al*. (1985, 1989). They showed that the tertiary structure of *A. limacina* Mb conforms to the common globin fold consisting of eight α-helices and that these helices can be well overlaid with those of sperm whale Mb in shape and position to the heme group. Of the 145 amino acid residues, 112 are found in helical conformation. This fraction seems to be 30% higher than the value estimated from circular dichroism measurements for *A. kurodai* Mb in 10 mM buffer, pH 7.4 (Shikama *et al*., 1982). This strongly suggests that *Aplysia* Mb is in helical fluctuations in solution.

In the crystal, the distal residue is recognized as Val-63 (E7), and the sixth (distal) coordinate position of the heme iron is not occupied by a water molecule at neutrality, *i.e*., below the acid-alkaline transition point (p$K \sim 7.5$). Rather, a water molecule is found at 4.6 Å apart from the heme iron in the ferric met form. Moreover, this solvent water molecule is kept in position by a hydrogen bond to the carbonyl oxygen of residue Val-63. The absence of an axial water molecule in *A. limacina* metmyoglobin was also proposed by Pande *et al*. (1986) from solution ^{1}H NMR study on the basis of the hyperfine shift of the heme mesoproton. The crystal structure at alkaline pH, on the other hand, indicates that a hydroxyl ion is bound to the sixth coordinate position of the ferric iron. It should also be noted that the heme propionates of *A. limacina* Mb are not making intramolecular salt-bridges to protein residues and thus stick out of the heme pocket into the surrounding solvent (Bolognesi *et al*., 1989). In sperm whale Mb, the two propionic acid groups are involved in polar interactions with Arg-45 (CD3) and His-97 (FG2), respectively, forming salt bridges (Fermi & Perutz, 1981).

Spectral Properties of *Aplysia* Myoglobin: Different Positioning of the Soret Peak

Since there is a strong tendency for oxymyoglobin (MbO_2) to become oxidized easily during isolation procedures, all early Mb preparations were obtained in the ferric met form. Accordingly, if needed, MbO_2 must have been produced from metmyoglobin (metMb) by reduction with a strong reagent such as sodium hydrosulfite. However, there have been a number of reports that such chemically generated MbO_2 showed various artifacts attributable to side reactions with this reducing agent. Instead of preparing MbO_2 from metMb, therefore, modern procedures for isolating native MbO_2 directly from muscle tissues all stem from the method of Shikama and coworkers (Yamazaki *et al*., 1964), which has been improved with some refinements and controls using various muscle sources. Along with these lines of evidence, Shikama and Katagiri (1984) have succeeded, for the first time, in isolating native MbO_2 from the radular muscle of *Aplysia* and have examined its spectral properties.

Figure 4 shows the absorption spectrum of native MbO_2 from *A. kurodai* with that of its acidic met form. *A. juliana*, another common species, showed an almost identical spectrum. It thus became evident that the visible spectrum of *Aplysia* MbO_2 is very similar to those of mammalian MbO_2, the α-peak being higher than the β-peak and the absorbance ratio (α/β ratio) being 1.03. In contrast to the oxy form, the acidic met form of *Aplysia* Mb showed remarkable spectral differences from that of mammalian Mbs,

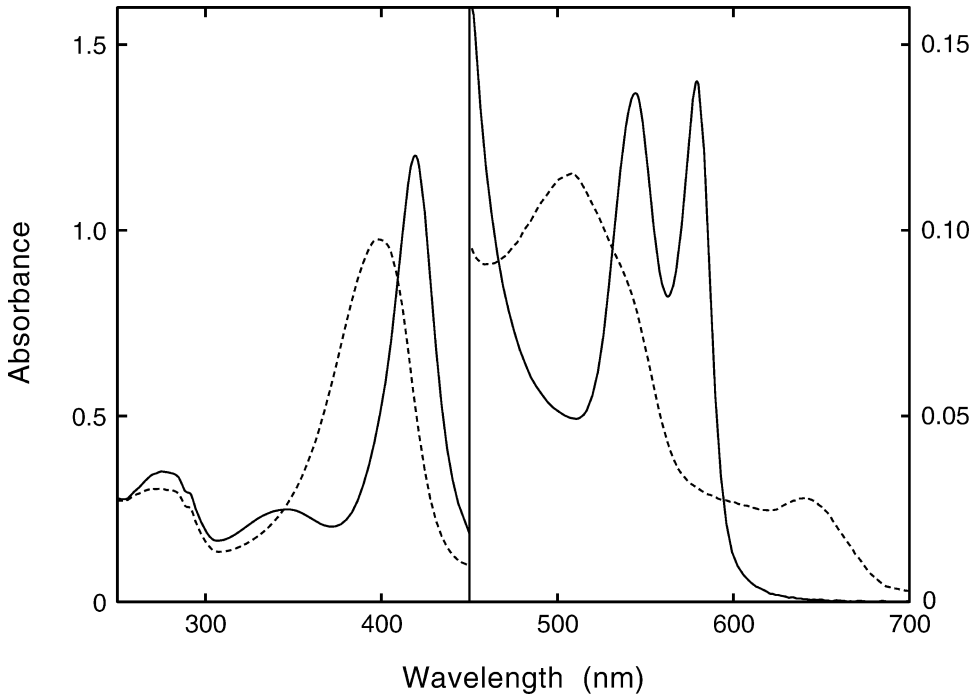

FIG. 4. Absorption spectra of *A. kurodai* MbO_2 (continuous line) and acidic metMb (broken line). The concentration was 10 μM for each form in 10 mM Tris-HCl buffer; the pH was 7.5 for MbO_2 and 6.4 for metMb. The expanded scale was used for the visible spectra. Redrawn from Shikama and Matsuoka (1989).

particularly in the Soret region (350–450 nm). As is clear in Figure 4, its Soret peak is profoundly blue shifted and accompanied by a marked decrease in intensity, probably due to a broadening of the spectrum. This is just the reverse of what is observed in sperm whale Mb (Figure 5).

Shikama and Matsuoka (1989, 1994) have examined a dozen Mbs from various species for their spectrophotometric properties and have found that the proteins can be divided into two groups on the basis of the absorbance ratio of the Soret peak of the acidic met form to that of the oxy form, i.e., the $\gamma_{met}/\gamma_{oxy}$ ratio, as listed in Table 1. Values higher than 1.0 (ranging from 1.16 to 1.41) were obtained for the usual type of Mbs, whereas those of less than 1.0 (ranging from 0.79 to 0.84) were seen for the ratio for the Mbs lacking the distal histidine residue. In place of histidine, the distal residue is assigned to be Val-63 for *Aplysia* and *Dolabella* Mbs (Bolognesi *et al*., 1989; Takagi *et al*., 1984; Suzuki, 1986), and to Gln-59 for the Mbs from two kinds of sharks, *Galeorhinus japonicus* and *Galeus nipponensis* (Suzuki, 1987; Suzuki *et al*., 1988).

The differences in spectral features of myoglobins may become much more evident if their Soret peaks are plotted on a map of extinction coefficient ε (mM^{-1} cm^{-1}) *versus* wavelength λ (nm). As is also clear in Table 1, the MbO_2 peaks are all in very close positions, whereas the acidic met forms have separate peak positions in two different ranges depending upon the presence or absence of the distal histidine residue. For these different positions of the Soret peak, a possible explanation is as follows. In the acidic metMbs, the sixth coordinate position of the ferric heme iron is usually occupied by a water molecule, which is stabilized by hydrogen-bond formation with the distal histidine residue. In the case of Mbs lacking the E7 histidine, however, the sixth coordinate position is vacant in the acidic met form (Giacometti *et al*., 1981). In *A. limacina* Mb, for instance, a water molecule is found near Val-63 at the E7 position, but far from the heme iron by 4.6 Å (Bolognesi *et al*., 1989).

To check up further on the spectral criterion for identifying two types of Mbs, we have prepared an E7His-modified derivative of sperm whale Mb and examined for its Soret absorption. For this purpose, the imidazole NH site of the distal histidine was cyanated to break open the ring by the addition of BrCN in a 10-fold molar excess at pH 6.0, according to the specifications of Shiro and Morishima (1984). As a result, the Soret peak of CN-modified sperm whale Mb was profoundly blue-shifted from 409 to 393 nm and accompanied by a marked decrease in intensity from 168 to 104 mM^{-1} cm^{-1}. At the same time, our explanation has been reinforced by the Soret magnetic circular dichroism (MCD) spectroscopy. Its Soret signal is known to reflect more directly the presence or absence of an axial

TABLE 1
Spectroscopic parameters of the Soret peak both in the oxy form and the acidic met form of Mbs from various sources

Source	His (E7)	Absorption maximum (nm) (Extinction coefficient ($mM^{-1}cm^{-1}$)) Acidic met form	Oxy form	$\gamma_{met}/\gamma_{oxy}$	Reference
Sperm whale	(+)	409 (168)	418 (129)	1.30	Shikama and Matsuoka (1989)
Horse	(+)	408 (188)	418 (133)	1.41	Yamazaki *et al*. (1964)
Bovine	(+)	409 (176)	418 (134)	1.31	Shikama and Matsuoka (1989)
Chicken	(+)	409 (164)	418 (129)	1.27	Shikama and Matsuoka (1989)
Bigeye tuna	(+)	406 (151)	415 (130)	1.16	Shikama and Matsuoka (1989)
Tetrahymena pyriformis	(+)	406 (161)	414 (123)	1.31	Korenaga *et al*. (2000)
Aplysia kurodai	(−)	395 (97)	418 (120)	0.80	Shikama and Katagiri (1984)
Aplysia juliana	(−)	395 (94)	418 (118)	0.79	Shikama and Matsuoka (1989)
Dolabella auricularia	(−)	402 (97)	418 (117)	0.83	Suzuki (1987)
Galeorhinus japonicus	(−)	398 (105)	418 (127)	0.82	Suzuki (1987)
Galeus nipponensis	(−)	393 (104)	417 (124)	0.84	Shikama *et al.* (1988)
BrCN-modified sperm whale Mb	(−)	393 (104)			Matsuoka *et al.* (1992)

His (E7) denotes the presence (+) or absence (−) of the distal histidine residue.

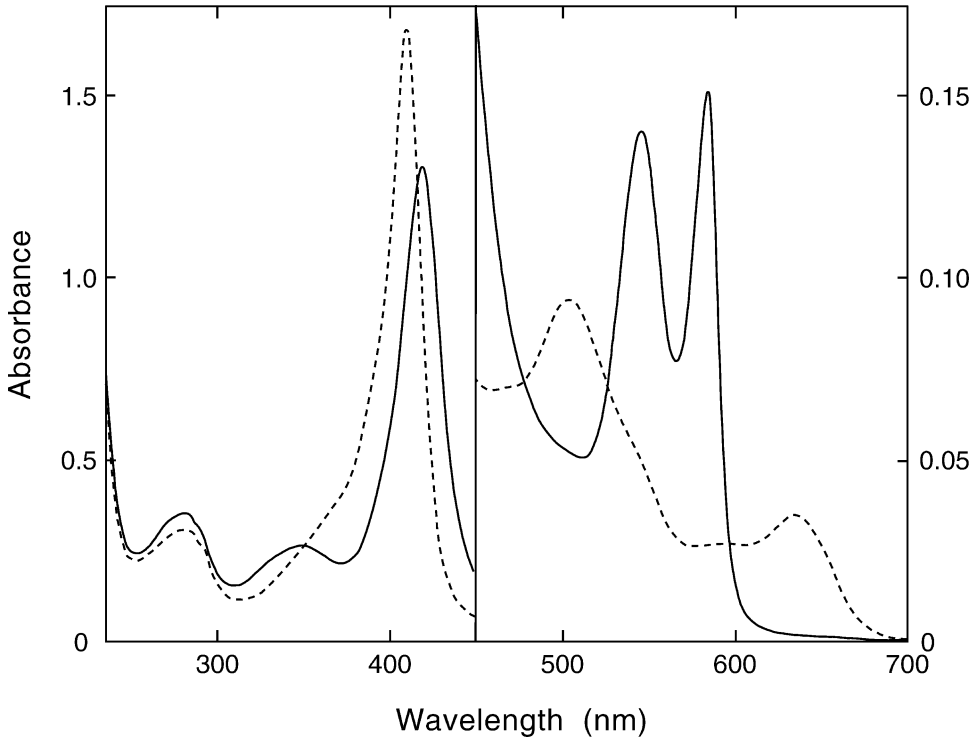

FIG. 5. Absorption spectra of sperm whale MbO_2 (continuous line) and acidic metMb (broken line). The concentration was 10 μM for each form in 10 mM Tris-HCl buffer; the pH was 7.5 for MbO_2 and 6.3 for metMb. Redrawn from Shikama and Matsuoka (1989).

water ligand at the sixth coordinate position of the ferric heme iron (Matsuoka *et al*., 1992).

Stability Properties of *Aplysia* Oxymyoglobin

Oxygen Binding. *Aplysia* Mb has a much lower affinity for oxygen than do mammalian Mbs. In order to unravel the on-rate and off-rate constants for the oxygen binding, Wittenberg *et al*. (1965) have made a kinetic analysis on *A. limacina* Mb in terms of the following equation:

$$\mathrm{Mb} + \mathrm{O_2} \underset{k_{\mathrm{off}}}{\overset{k_{\mathrm{on}}}{\rightleftharpoons}} \mathrm{MbO_2}. \qquad [2.1]$$

In 0.1 M buffer (pH 7.0) at 20°C, they obtained a value of 1.5×10^7 $\mathrm{M^{-1}\ s^{-1}}$ for k_{on}, this being essentially the same as that of horse Mb. However, a value of $k_{\mathrm{off}} = 70\ \mathrm{s^{-1}}$ for the O_2 dissociation was much larger than a value of $10\ \mathrm{s^{-1}}$ for horse Mb. Consequently, this large off-rate constant is responsible for the lower affinity of *Aplysia* Mb for O_2. It would come mainly from the absence of hydrogen bonding capacity of the E7 residue (Val) to the heme-bound dioxygen (Wittenberg *et al*., 1965). The lack of the distal histidine has also a profound effect on the stability of *Aplysia* Mb.

Autoxidation Reaction: Lack of the Acid-Catalysis. It is in the ferrous form that Mb can bind molecular oxygen reversibly and carry out its physiological function. However, the oxygenated form (MbO_2) is known to be oxidized easily to the ferric met form (metMb) with generation of the superoxide anion as

$$\mathrm{MbO_2} \xrightarrow{k_{\mathrm{obs}}} \mathrm{metMb} + \mathrm{O_2^-}, \qquad [2.2]$$

where k_{obs} represents the first-order rate constant observed at a given pH value (Gotoh & Shikama, 1976). The rate of the autoxidation is therefore written as:

$$\frac{-\mathrm{d[MbO_2]}}{\mathrm{d}t} = k_{\mathrm{obs}}[\mathrm{MbO_2}] \qquad [2.3]$$

This process was followed up by a plot of experimental data as $-\ln([\mathrm{MbO_2}]_t/[\mathrm{MbO_2}]_0)$ *versus* time t, where the ratio of MbO_2 concentration after time t to that at time $t = 0$ can be monitored by the absorbance changes at α-peak of the protein (578 nm in the case of *Aplysia* MbO_2). From the slope of each straight line the observed first-order rate constant, k_{obs} in $\mathrm{h^{-1}}$, was thus determined. In 0.1 M buffer at pH 7.2 and 25°C, for instance, its value was $0.50 \times 10^{-2}\ \mathrm{h^{-1}}$ for sperm whale MbO_2, 0.83×10^{-2} $\mathrm{h^{-1}}$ for human psoas MbO_2, $0.31 \times 10^{-1}\ \mathrm{h^{-1}}$ for *Paramecium* MbO_2, and $0.11\ \mathrm{h^{-1}}$ for *Aplysia* MbO_2 (Tsubamoto *et al.*, 1990; Korenaga *et al*., 2000). As the ferric met-species produced in this way cannot bind molecular oxygen, the rate constant (k_{obs}) for the autoxidation reaction provides us with an important measure for the stability of the bound dioxygen in myoglobin or hemoglobin molecule.

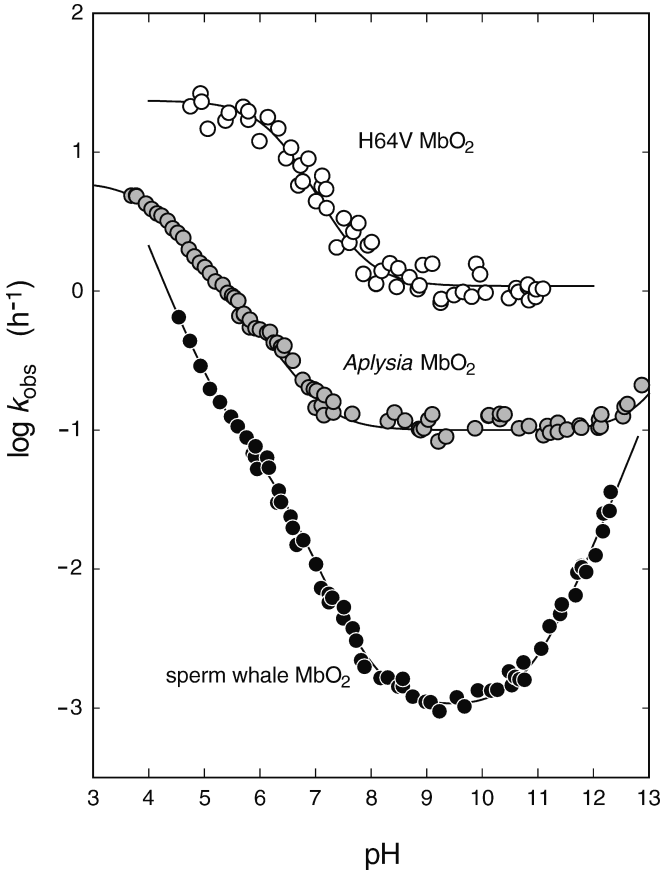

FIG. 6. pH-dependence of the stability of *Aplysia* MbO_2 with those of sperm whale and its H64V mutant oxymyoglobins in 0.1 M buffer at 25°C. The logarithmic values of the observed rate constant, k_{obs}, for the autoxidation reaction are plotted against the pH of the solution. The computed curve (——) was obtained by a least-squares fitting to the experimental points over the whole range of pH studied, based on Equation (2.8) for sperm whale MbO_2, Equation (2.11) for *Aplysia* MbO_2, and Equation (2.13) for the H64V mutant protein, respectively. MbO_2 concentration: 25 μM for *A. kurodai*; 50 μM for sperm whale; 10 μM for the H64V mutant. Taken from our previous data (Shikama & Matsuoka, 1994; Suzuki *et al*., 2000).

If the values of k_{obs} are plotted against the pH of the solution, a profile of the stability of oxymyoglobin can be obtained. Figure 6 shows such a profile for *Aplysia* MbO_2, with those of sperm whale MbO_2 and its H64 → V (H64V) mutant protein, under air-saturated conditions in 0.1 M buffer at 25°C. When compared with the sperm whale MbO_2 that served as a reference, it is quite clear that *Aplysia* MbO_2 is extremely susceptible to autoxidation over the whole range of pH studied. Furthermore, its

pH dependence is also unusual and much less steep than that of sperm whale MbO_2 (Shikama & Matsuoka, 1986, 1994).

In the autoxidation reaction, pH can affect the rate in many different ways. In a recent article that appeared in *Chemical Reviews*, Shikama (1998) has carefully evaluated various mechanisms proposed so far for the autoxidation reaction of Mb and Hb, including the effects of pH, oxygen pressure, and subsequent side reactions. As a result, he concluded that a displacement mechanism is needed to make it possible to yield O_2^- so readily from the FeO_2 center. Incidentally, the O_2^- production was observed not only in the native proteins but also in the mutant proteins such as H64V, the analogue of *Aplysia* Mb (Brantley *et al.*, 1993). At any rate, the essence is that the autoxidation reaction is not a simple, dissociative loss of O_2^- from MbO_2 but is due to a nucleophilic displacement of O_2^- from MbO_2 by a water molecule or a hydroxyl ion that can enter the heme pocket from the surrounding solvent. The iron is thus converted to the ferric met form, and the water molecule or the hydroxyl ion remains bound to the Fe(III) at the sixth coordinate position to form aqua- or hydroxide-metMb. Even the complicated pH-dependence for the autoxidation rate can thereby be explained primarily in terms of the following three types of displacement processes (Shikama, 1984, 1988, 1998):

$$\mathrm{Mb(II)(O_2) + H_2O \xrightarrow{k_0} Mb(III)(OH_2) + O_2^-}, \qquad [2.4]$$

$$\mathrm{Mb(II)(O_2) + H_2O + H^+ \xrightarrow{k_H} Mb(III)(OH_2) + HO_2}, \qquad [2.5]$$

$$\mathrm{Mb(II)(O_2) + OH^- \xrightarrow{k_{OH}} Mb(III)(OH^-) + O_2^-}. \qquad [2.6]$$

In these equations, k_0 is the rate constant for the basal displacement by H_2O, k_H is the rate constant for the proton-catalyzed displacement by H_2O, and k_{OH} is the rate constant for the displacement by OH^-. The contribution of these elementary processes to the observed or overall autoxidation rate, k_{obs} in Equation (2.3), can vary with the concentrations of H^+ or OH^- ions. Consequently, the stability of MbO_2 shows a very strong pH dependence that has a parabolic part, as seen in Figure 6 for sperm whale Mb. In order to know definitely the kinetic and thermodynamic parameters contributing to each k_{obs}*versus* pH profile, we have proposed some mechanistic models for each case. The rate equations derived therefrom were tested for their fit to the experimental data with the aid of a computer, according to our previous specifications (Shikama & Matsuoka, 1986, 1994; Tsuruga *et al.*, 1998).

As a typical example, the pH profile for the autoxidation rate of sperm whale MbO_2 has been analyzed completely in terms of an "acid-catalyzed two-state model" (Shikama & Matsuoka, 1986, 1994). In this model, it is assumed that a single, dissociable group, XH with pK_1, is involved in the reaction. Consequently, there are two forms of the MbO_2, represented by A and B, at molar fractions of α and β $(= 1-\alpha)$, espectively, that are in equilibrium with each other but that differ in dissociation state for the group XH. These forms can be oxidized to metMb by displacement of O_2^- from MbO_2 by an entering water molecule or hydroxyl ion. Using the rate constants defined above, the reaction scheme may therefore be written as:

$$\begin{array}{ccc} \mathrm{MbO_2(XH)} & \overset{K_1}{\rightleftharpoons} & \mathrm{MbO_2(X^-)} \\ k_0^{\mathrm{A}} \downarrow k_{\mathrm{H}}^{\mathrm{A}} \downarrow & & k_0^{\mathrm{B}} \downarrow k_{\mathrm{H}}^{\mathrm{B}} \downarrow k_{\mathrm{OH}}^{\mathrm{B}} \downarrow \\ \text{metMb} & & \text{metMb} \end{array}. \qquad [2.7]$$

For the mechanism delineated in Equation (2.7), the observed rate constant, k_{obs} in Equation (2.3), can be reduced to

$$k_{\mathrm{obs}} = \left\{k_0^{\mathrm{A}}[\mathrm{H_2O}] + k_{\mathrm{H}}^{\mathrm{A}}[\mathrm{H_2O}][\mathrm{H^+}]\right\}(\alpha) + \left\{k_0^{\mathrm{B}}[\mathrm{H_2O}] + k_{\mathrm{H}}^{\mathrm{B}}[\mathrm{H_2O}][\mathrm{H^+}] + k_{\mathrm{OH}}^{\mathrm{B}}[\mathrm{OH^-}]\right\}(\beta), \qquad [2.8]$$

where

$$\alpha = \frac{[\mathrm{H^+}]}{[\mathrm{H^+}] + K_1}$$

and

$$\beta = (1-\alpha) = \frac{K_1}{[\mathrm{H^+}] + K_1}. \qquad [2.9]$$

By iterative least-squares procedures inserting various values for K_1, the adjustable parameter in Equation (2.9), the best fit to the experimental values of k_{obs} was obtained as a function of pH (see Figure 6). In this way, the rate constants and the acid dissociation constant involved in the autoxidation reaction of sperm whale MbO_2 were evaluated in 0.1 M buffer at 25°C and are given in Table 2.

From these results it becomes evident that the proton-catalyzed processes with the rate constants k_H^A and k_H^B dramatically promote the autoxidation reaction of sperm whale MbO_2 above the basal processes in water with the rate constants k_0^A and k_0^B. The reductive displacement of the bound dioxygen as O_2^- by H_2O can proceed without any protonation, but it is clear that the rate is enormously accelerated with the proton assistance, by a factor of $4.7 \times 10^6 \mathrm{mol}^{-1}$ for state A and by a factor of $1.1 \times 10^8\ \mathrm{mol}^{-1}$ for state B. In this proton catalysis formulated

TABLE 2
Rate constants and acid dissociation constants obtained from the pH dependence curves for the autoxidation rate of *Aplysia* MbO_2, sperm whale MbO_2, and its H64V MbO_2 in 0.1 M buffer at 25°C

Source	State of MbO_2	k_0 ($h^{-1}M^{-1}$)	k_H ($h^{-1}M^{-2}$)	k_{OH} ($h^{-1}M^{-1}$)	pK
Aplysia kurodai MbO_2	A(XH, YH)	0.11	—	—	
	⇓ K_1				4.3
	$B(X^-, YH)$	0.13×10^{-1}	—	—	
	⇓ K_2				6.1
	$C(X^-, Y^-)$	0.18×10^{-2}	—	0.83	
Sperm whale MbO_2	A(XH)	0.78×10^{-4}	0.37×10^{3}	—	
	⇓ K_1				6.2
	$B(X^-)$	0.18×10^{-4}	0.20×10^{4}	0.14×10	
Sperm whale H64V	A(XH)	0.42	—	—	
mutant MbO_2	⇓ K_1				6.3
	$B(X^-)$	0.20×10^{-1}	—	—	

Taken from Shikama and Matsuoka (1994) and from Suzuki *et al*. (2000).

by Equation (2.5), the distal (E7) histidine (the dissociable group XH with $pK_1 = 6.2$ in this case), which forms a hydrogen bond to the bound dioxygen (Phillips & Schoenborn, 1981), appears to facilitate the effective movement of a catalytic proton from the solvent to the bound, polarized dioxygen *via* its imidazole ring by a proton-relay mechanism (Shikama & Matsuoka, 1986, 1994; Shikama, 1988, 1998; Suzuki *et al*., 2000).

In sharp contrast to sperm whale MbO_2, *Aplysia* MbO_2 is oxidized to metMb at an almost constant rate over a wide range of pH 7–12, its value being 100 times higher than that of sperm whale MbO_2 at pH 9.0. In the acidic range of pH 7–4, the rate of autoxidation of *Aplysia* MbO_2 also increases rapidly with increasing hydrogen ion concentration, but much less so than for sperm whale MbO_2, the latter protein having a value close to $n = -1$ for the slope of $\log(k_{obs})$ *versus* pH, as is clear in Figure 6. This strongly suggests that the mode of action of the proton is different in *Aplysia* Mb. We have finally concluded that the unusual pH-profile of *Aplysia* MbO_2 can best be explained in terms of a "three-state model" (Shikama & Matsuoka, 1986, 1994).

In this scheme, it is assumed that two kinds of dissociable groups, XH with pK_1 and YH with pK_2, are involved in the reaction. Consequently, there are three forms of MbO_2, represented by A, B, and C, at molar fractions of α, β, and γ $(= 1 - \alpha - \beta)$ respectively, which are in equilibrium with each other but differ in dissociation states for the groups XH and YH. These forms can be oxidized to metMb by displacement of O_2^- from MbO_2 by an entering water molecule and, at extremely high pH values, by an entering hydroxyl ion. Using the rate constants defined previously, the autoxidation reaction of *Aplysia* MbO_2 may therefore be written as:

$$\begin{array}{ccccc} MbO_2(XH, YH) & \overset{K_1}{\rightleftharpoons} & MbO_2(X^-, YH) & \overset{K_2}{\rightleftharpoons} & MbO_2(X^-, Y^-) \\ k_0^A\downarrow & & k_0^B\downarrow & & k_O^C\downarrow \quad k_{OH}^C\downarrow \\ \text{metMb} & & \text{metMb} & & \text{metMb} \end{array} \qquad [2.10]$$

For this reaction, the observed rate constant, k_{obs} in Equation (2.3), is given by

$$k_{obs} = \left\{k_0^A[H_2O]\right\}(\alpha) + \left\{k_0^B[H_2O]\right\}(\beta) + \left\{k_O^C[H_2O] + k_{OH}^C[OH^-]\right\}(\gamma), \qquad [2.11]$$

where

$$\alpha = \frac{[H^+]^2}{[H^+]^2 + K_1[H^+] + K_1K_2},$$
$$\beta = \frac{K_1[H^+]}{[H^+]^2 + K_1[H^+] + K_1K_2}, \qquad [2.12]$$

and

$$\gamma = (1 - \alpha - \beta) = \frac{K_1K_2}{[H^+]^2 + K_1[H^+] + K_1K_2}.$$

In this way, the rate constants and the acid dissociation constants involved in the autoxidation reaction of *Aplysia* MbO_2 were obtained in 0.1 M buffer at 25°C and are also summarized in Table 2 (Shikama & Matsuoka, 1994).

In these kinetic formulations, one of the most remarkable features is that *Aplysia* oxymyoglobin does not show any proton-catalyzed process having the term of $k_H[H_2O][H^+]$, such as the one that can play a dominant role in the autoxidation reaction of sperm whale MbO_2 by involving the distal histidine as its catalytic residue. Instead, *Aplysia* MbO_2 contains two kinds of dissociable groups with $pK_a = 4.3$ and 6.1, respectively, each being responsible for an additional increase in its autoxidation rate on the acidic pH side. Indeed, the extreme susceptibility of *Aplysia* MbO_2 to autoxidation comes not from the acid catalysis but mainly due to a large value of $k_0^C = 0.18 \times 10^{-2}$ h^{-1} M^{-1}, this being 100 times higher than the corresponding value of $k_0^B = 0.18 \times 10^{-4}$ h^{-1} M^{-1} for sperm whale MbO_2.

As described in the previous section, X-ray crystallography of *A. limacina* Mb has shown that the sixth coordinate position of the heme iron is vacant in its acidic met form (Bolognesi *et al*., 1989). In our context, this structural observation may be interpreted as follows. In displacing O_2^- from *Aplysia* MbO_2 by an entering water molecule, the Fe(III)(OH_2) species can also be formed transiently, as a matter of course, but the bonding is probably too weak to retain the axial water ligand due to lack of the distal histidine residue. In the crystal structure, in fact, a water molecule is found near the distal Val-63, apart from the iron by 4.6 Å (Bolognesi *et al*., 1989).

For the two kinds of dissociable groups involved in the autoxidation of *Aplysia* MbO_2, we have concluded that both are carboxyl groups; one (YH with $pK_2 = 6.1$) is a heme propionate and the other (XH with $pK_1 = 4.3$) is a protein residue, probably of Glu-94 just before the heme-binding proximal His-95. This identification is based on the thermodynamic characterization of the dissociation processes and the effect of esterification of the heme propionates as well (Matsuoka & Shikama, 1988, 1992).

Dual Role of the Distal Histidine Residue. A single mutation at position 64 dramatically changed the stability property of sperm whale MbO_2 (Suzuki *et al*., 2000). In H64V mutation, for example, the distal His-64 was replaced by Val having a smaller side chain of R = –CH$(CH_3)_2$. As demonstrated in Figure 6, the H64V MbO_2 was oxidized to metMb at an almost constant rate over the wide range of pH 8–11, its value being nearly 1000 times higher than that of the native MbO_2 at pH 9.0. Another unusual feature was also found on the acidic side of pH 7–4. Certainly, the oxidation rate of the H64V MbO_2 increased with increasing hydrogen ion concentration but much less so (n = −0.5) than for the native or wildtype (H64H) MbO_2 (n = −1), and it exhibited a distinct saturation level below pH 6. In formulating such pH profile, the follwing "two-state" mechanism,

$$k_{obs} = \{k_0^A[H_2O]\}(\alpha) + \{k_0^B[H_2O]\}(\beta), \qquad [2.13]$$

was satisfactory by involving a single, dissociable group (XH) with $pK_1 = 6.3$. From the thermodynamic characterization of the XH group, Suzuki *et al*. (2000) have concluded that the most probable candidate is a carboxyl group of the heme propionates, although its pK_a value does not lie in the normal range. The numerical results are given in Table 2.

When the distal (E7) histidine was replaced by other amino-acid residues, all such mutant oxymyoglobins have completely lost the acid-catalyzed processes with the rate constants k_H^A and k_H^B. Indeed, the extreme susceptibility of the H64V MbO_2 to autoxidation comes mainly from a large value of k_0^A as well as of k_0^B, the same as is *Aplysia* MbO_2. However, it is also true that a single H64V mutation was not adequate to mimic all the unique properties of *Aplysia* Mb. This situation seems to underscore the difficulty of explaining the properties of invertebrate Hbs or Mbs based on mutagenesis of the vertebrate proteins.

At any rate, the distal histidine residue can play a dual role in the nucleophilic displacement of O_2^- from MbO_2 or HbO_2 (Suzuki *et al*., 2000). One is in a proton-relay mechanism *via* its imidazole ring at acidic pH. Insofar as it is examined for more than a dozen Mbs, such a proton-catalyzed process could never be observed in the autoxidation reaction for Mbs lacking the usual distal histidine residue, no matter whether the protein is the naturally occurring or the distal His mutant. The other role of the distal histidine is in the maximum protection of the FeO_2 center against a water molecule or a hydroxyl ion that can enter the heme poket from the surrounding solvent. This is particularly important to the considerable stability of MbO_2 and HbO_2 in neutral pH range (Brantley *et al*., 1993). In this way, the distal histidine provides the delicate balance of catalytic and steric factors necessary for controlling the reversible oxygen binding to Mb and Hb in protic, aqueous solvent.

Concluding Remarks: Another Prototype of Myoglobin

Unlike mammalian oxymyoglobins, *Aplysia* MbO_2 is oxidized very quickly to the ferric met form over a wide range of pH 4–13. Kinetic analysis has revealed that the extreme susceptibility of *Aplysia* Mb to autoxidation comes mainly from a large value of k_0^C, the rate constant for the basal displacement by H_2O in the neutral pH range. In regard to the structural evidence, a high value of k_0^C implies that the heme pocket of *Aplysia* Mb is sufficiently open to allow easier attack of the solvent water molecule on the FeO_2

center, with a consequent very rapid formation of metMb. This may be due mostly to replacement of the distal histidine residue by a valine of much smaller size, since the distal His is in a location where it can act just like a gate or a swinging door for the ligand entry into the heme pocket.

Due to lack of the distal histidine residue, *Aplysia* MbO_2 did not show any proton-catalyzed process, such as the one that can play a dominant role in the heme oxidation of mammalian oxymyoglobins. A lack of the distal histidine also provides a profound effect on the absorption spectra of *Aplysia* Mb. In the ferric met form, its Soret peak is considerably blue shifted and accompanied by a marked intensity decrease. Insofar as we have examined, this spectral feature is unique for all the Mbs lacking the usual distal histidine residue and can be explained by the concomitant absence of an axial water molecule at the sixth coordinate position of the ferric heme iron. This simple, spectral criterion is extremely useful for predicting whether the usual distal histidine is present in Mb or Hb molecules in particular, such as those from lower organisms, including midge larva (Fukuda *et al*., 1993), ciliated protozoa (Korenaga *et al*., 2000), and yeast (Kobayashi *et al*., 2002). These primitive globins show no notable degree of sequence similarity with the mammalian Mbs or Hbs that served as a reference.

With regard to the distal (E7) residue, mollusca appear to present a very unique phylum in which both types of Mbs are involved. We have already isolated a dimeric Mb from the radular muscle of *Cerithidea rhizophorarum* (Takagi *et al*., 1983). This species is also a common gastropodic mollusc found on the Japanese coast but belongs to a different subclass (the prosobranchia) than *Aplysia* (the opisthobranchia). Unlike *Aplysia* myoglobin with a single histidine at position 95, *Cerithidea* myoglobin contains three histidine residues at positions 48, 66, and 98 in its monomer, and His-66 has been assigned to the distal position (Takagi *et al*., 1983). In this respect, it should be noted that at least a two-base exchange of the coding triplet is needed for the replacement of His [CAU, CAC] to Val [GUU, GUC] as is in the cases of *Aplysia* and *Dolabella* Mbs, whereas the other possible, distal replacements to Asp [GAU, GAC], Leu [CUU, CUC], and Gln [CAA, CAG] can be caused by only one-base exchange. Among these, the last replacement is most frequently found in a number of Mbs and Hbs from various sources.

We do not know at the present time whether there is (or was) any evolutionary advantage for *Aplysia* Mb to have Val in place of the distal His. Nevertheless, it is true that *Aplysia* Mb provides us with another important prototype for probing the possible roles of the distal histidine residue in Mb and Hb biochemistry as well as in the evolution of these globin molecules.

INSECT HEMOGLOBIN FROM *TOKUNAGAYUSURIKA AKAMUSI*: A HIGH DEGREE OF POLYMORPHISM

Ecological Life Cycle of the Midge *Tokunagayusurika akamusi*

Some insects have a globin in their fast-growing larval stage but lose it after metamorphosis in favor of the diffusion of gaseous oxygen through hollow tracheal tubes. This is the case in the midge (Diptera, Chironomidae), and the Chironomidae is one of the largest insect families. For the midge larval Hb, extensive work has been carried out with several species of Chironominae, such as C*hironomus thummi thummi* (Di Iori *et al*., 1997; Huber *et al*., 1971; Steigemann & Weber, 1979; Weber *et al.*, 1985) and *C. thummi piger* (Hankeln *et al.*, 1988; Rozynek *et al*., 1988). Their hemoglobins are of low molecular mass, found as both monomeric and dimeric forms in the larval hemolymph, and they show a high degree of polymorphism. Among these, the C. *thummi thummi* (CTT) Hb-III was the first invertebrate Hb whose X-ray structure was determined at high resolution. In its crystal structure, displaying the common globin fold, the heme group is rotated by 180° and the heme cavity in the deoxy form has an unusual open gate conformation at pH 7.0, with the distal His able to swing out of the cavity (Huber *et al*., 1971; Steigemann & Weber, 1979). This Hb has therefore been the subject of structural, spectral, and functional studies, accordingly (Di Iori *et al.*, 1997; Weber *et al.*, 1985).

On the other hand, *Tokunagayusurika akamusi*, a common species found in eutrophic lakes in Japan, belongs to a different subfamily (Orthocladiinae) from Chironominae, and its larva is unique in morphology and ecological behavior. In the Chironomid group, the young hatch from the colorless, transparent egg as wormlike larvae. The larva grows through four instars (stages separated by a molt) without change of shape. As for *T. akamusi*, the Japanese word "*akamusi*" means bloodworm, which comes from the fact that a large amount of Hb is synthesized into the hemolymph of the fourth-instar larva. This small bloodworm (15–18 mm in length and 1.5 mm in diameter) begins to burrow into polluted and extremely hypoxic mud flats of lakes to have a long period (more than half a year) of diapause. The burrow can reach up to 80 cm in depth, and $\varepsilon^{\circ\prime} = 0$ volts in the oxidation-reduction potential. After diapause, the matured and sex-differentiated larva crawls up above the ground again and undergoes a pupal molt in which the shape alters completely. The brown pupa is encased in a cuticle, and the pupal stage terminates with a final or imaginal molt in which the adult, winged midge emerges from the pupal case. The life of the adult midge is restricted to roughly a one-month period.

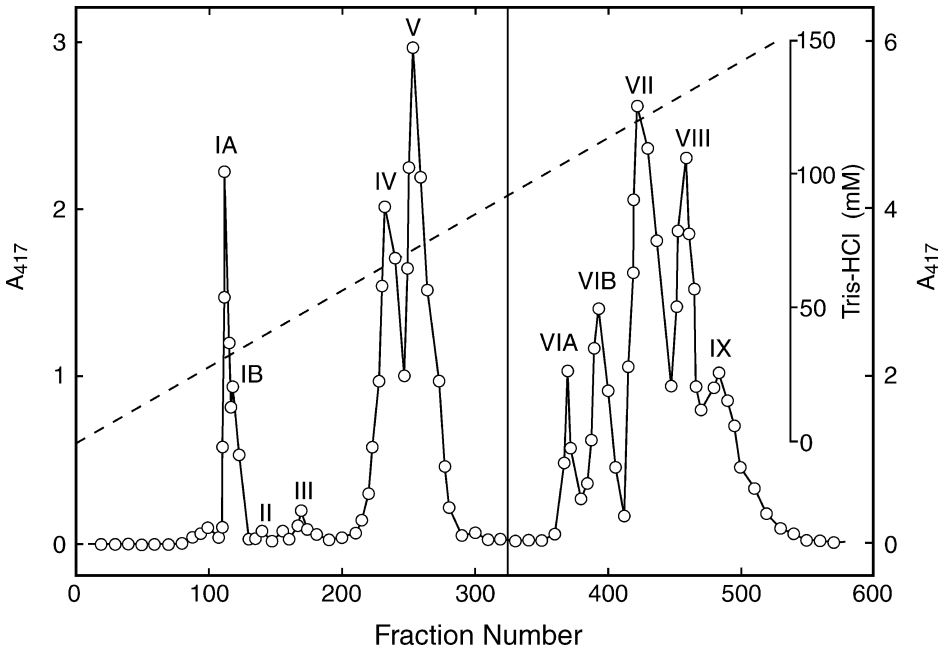

FIG. 7. DEAE-cellulose chromatography of *T. akamusi* Hb. Hb solution (250 ml, 500 mg) was applied to a DEAE-cellulose column (4 × 16 cm) equilibrated with 5 mM Tris-HCl buffer (pH 8.4). The elution was carried out with a linear concentration gradient of Tris-HCl buffer from 5 to 150 mM at pH 7.9. The heme protein level was monitored by the absorbance at 417 nm (O), and the expanded scale was used until the fraction number 325. Fraction size, 10 ml. Redrawn from Fukuda *et al*. (1993).

In this section, we will describe some molecular properties of the polymorphic hemoglobin from *T. akamusi* in light of a very unique ecological behavior of the fourth-instar larva. Among the eleven separable components, special focus will be placed on the Hb VII, a major component in the larval hemolymph. In this protein we have observed, for the first time, the pH-dependent swinging movement of the distal histidine residue. To demonstrate any unusual character of midge larval Hb, we will also examine the autoxidation rate over a wide range of pH, as well as the oxygen equilibrium property.

Polymorphic Hemoglobin from the Fourth-Instar Larva of *T. akamusi*

Chromatographic and Spectral Characterization. Frozen larvae were thawed quickly and homogenized with Teflon-glass homogenizer in a 3-volume of 5 mM Tris-HCl buffer (pH 8.4) containing 0.1 mM phenylmethylsulfonyl fluoride (PMSF) and 0.5 mM EDTA to prevent endogenous protease digestion. After insoluble materials had been removed by centrifugation, the Hb extract was fractionated with ammonium sulfate between 55 and 100% saturation, and passed through a Sephadex G-50 column. The essential step was the chromatographic separation of the Hb components on a DEAE-cellulose column equilibrated with 5 mM Tris-HCl buffer (pH 8.4). The subsequent elution was carried out with a linear concentration gradient of Tris-HCl buffer from 5 to 150 mM at pH 7.9 (Fukuda *et al.*, 1993).

As shown in Figure 7, the hemoglobin from the fourth-instar larva of *T. akamusi* was separated into as many as eleven components on a DEAE-cellulose column, these being named IA, IB, II, III, IV, V, VIA, VIB, VII, VIII, and IX according to the order of elution. In this elution profile, the expanded scale is used for the concentration of the early eluted components I to V. In SDS-polyacrylamide gel electrophoresis, each component showed almost the same mobility indicative of a molecular mass of approximately 15 kDa. In buffer alone, however, the components VI to IX were found as dimeric form.

We have examined all the components for their spectrophotometric property, and found that these can be classified into two groups on the basis of their different positioning of the Soret peak. As mentioned in the preceding section, an absorbance ratio of the Soret peak of the acidic met form to that of the oxy form, namely the $\gamma_{met}/\gamma_{oxy}$ ratio, provides us with a simple criterion for predicting whether or not a Mb (or a Hb) has the distal (E7) histidine residue: The values higher than 1.0 are found for the usual type of Mbs such as sperm whale Mb, whereas those of less than 1.0 are the ratio for the Mbs lacking the distal histidine, as in *Aplysia* Mb. In this context, the component VII exhibited a value of $\gamma_{met}/\gamma_{oxy} = 1.19$ with almost the

same visible spectrum as sperm whale Mb (see Figure 5). Such a spectral feature was common to all the components VI to IX. In the component V, on the other hand, the Soret peak of the acidic met form showed a considerable blue-shift accompanied with a marked decrease in intensity, giving a $\gamma_{met}/\gamma_{oxy}$ ratio of less than 1.0. This spectral feature was similar to that of *Aplysia* Mb (see Figure 4) and common to all the early eluted components I to V.

These spectral observations strongly suggest that the *T. akamusi* larval hemoglobin is comprised of two distinct groups; one having the usual distal histidine and the other lacking in it. Amino acid sequence study will confirm this prediction.

Amino Acid Sequence. Among the eleven separable components, Hbs V and VII are the major ones in each different group, and make up 15 and 30%, respectively, of the total hemoglobin concentration in the fourth-instar larval hemolymph. Figure 8 represents the complete amino acid sequences of both Hbs. As is clear, *T. akamusi* Hb V (Ta-V) was composed of 152 amino acid residues, while the component VII (Ta-VII) was of 150 residues. As predicted from the spectral criterion, the component VII contained the usual distal (E7) histidine at position 64, whereas the component V replaced it by an isoleucine at position 66. The sequence similarity between the components V and VII was only 27%, and the hydropathy profiles also suggested that their heme environment is different. In their molecular alignment, Phe-46 and His-98 of the component V, as well as Phe-44 and His-99 of the component VII, could be placed as the invariant Phe (CD1) and the heme-binding proximal histidine (F8), respectively. The B10 residues appear to be Phe-32 in Ta-V and Leu-30 in Ta-VII, based on the structure of *Chironomus* Hb.

Phylogenetic Tree. A matrix analysis was carried out to test the sequence homology of *T. akamusi* Hb components V and VII with other midge Hbs, including 10 components from *C. thummi thummi* (Huber *et al.*, 1971; Weber *et al.*, 1985) and 3 components from *C. thummi piger* (Hankeln *et al.*, 1988; Rozynek *et al.*, 1988). As a result, Ta-VII Hb has higher percentage identities (40–48%) with the *Chironomus* Hb components than has Ta-V Hb (26–27%). Because all the *Chironomus* Hbs have a distal histidine residue, appearance of the V-type (or *Aplysia* Mb-type) components may be very specific to the genus *Tokunagayusurika*.

The sequence of 42–44 N-terminal residues can be determined by an automated sequencer for all the components of *T. akamusi* hemoglobin, as these proteins were not blocked at N-terminus. The similarity of each component was then calculated according to an unweighted pair-group clustering method (Nei *et al.*, 1985). As depicted by a phylogenetic tree in Figure 9, all the VII-type components (VIA, VIB, VII, VIII, and IX) were found in the same cluster and showed a very high degree of homology (more than 80%) with each other. The V-type components (IA, IB, II, III, IV, and V) fell into the other cluster but showed a wide variety of similarity (35–90%) among them. Since sequence homology between the two clusters was very low (20–30%), the two types of *T. akamusi* Hb

Amino acid sequence of *Tokunagayusurika akamusi* Hb

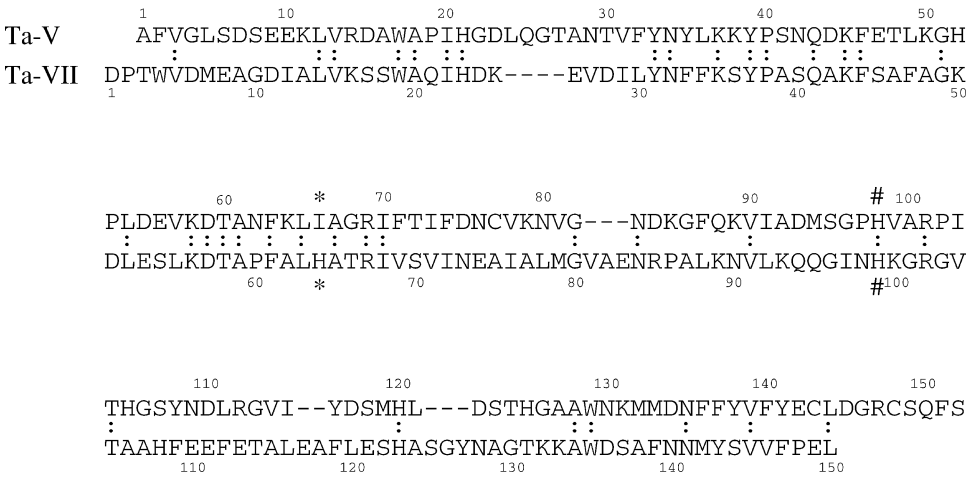

FIG. 8. Amino acid sequences of *T. akamusi* Hb components V and VII. The markers are used to indicate the proximal F8-His (#), the distal E7 residue (*), and the identical residues between both components (:). The B10 residues appear to be Phe-32 in Ta-V and Leu-30 in Ta-VII. Taken from Kamimura *et al*. (2003).

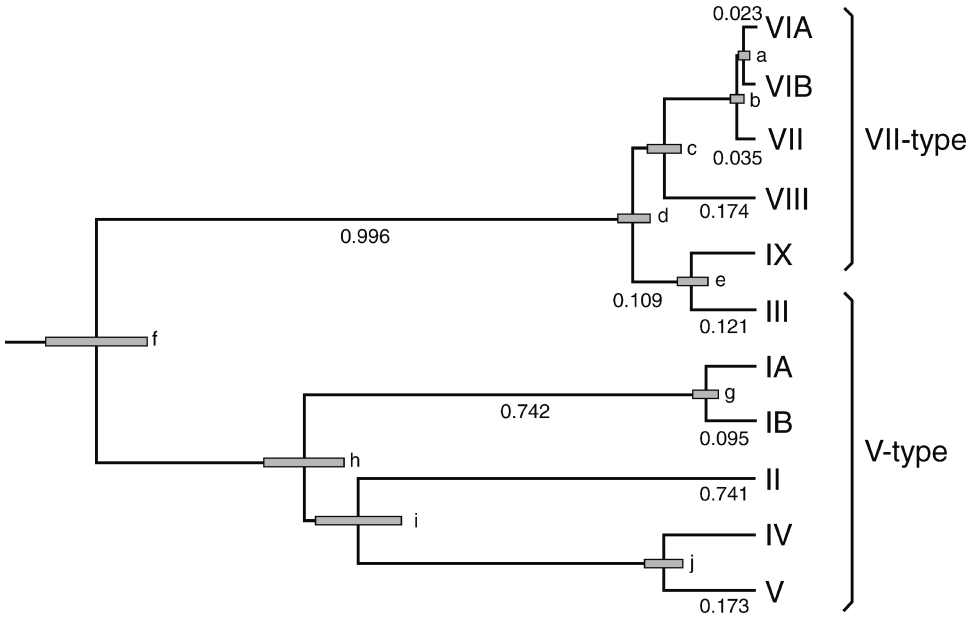

FIG. 9. A phylogenetic tree of eleven components of *T. akamusi* Hb. The tree was constructed on the basis of the Poisson-corrected values for the amino acid replacement, which are given along each branch by an unweighted pair-group clustering method. Standard errors at the branching points (a–j) were 0.011, 0.013, 0.032, 0.032, 0.027, 0.091, 0.029, 0.072, 0.076, and 0.033, respectively, and are represented by the hatched boxes. Redrawn from Fukuda *et al*. (1993).

seem to have a different origin or a very early separation in the phylogenetic tree. The VII-type components may have resulted from much more recent gene duplications than in the V-type components.

Recently, Burmester and Hankeln (1999) found a Hb-like gene in cDNA databases of the fruit fly *Drosophila melanogaster*, and isolated the gene named *dmeglob*1 (*Drosophila melanogaster* globin 1). The *dmeglob*1 gene had an open reading frame of 153 codons that is arranged on three exons. The derived protein sequence revealed the eight-helix structure that is typical for vertebrate globins, and it contained the characteristic distal and proximal histidines at positions 61 and 96. As hypoxic conditions do not appear in the life cycle of *Drosophila,* its globin remains obscure in the physiological role. To understand globin evolution in insects, however, they have constructed a neighbor-joining tree of selected globins and found that *Drosophila* globin tends to group most closely with a midge Hb-V from *T. akamusi* and with a botfly Hb from *Gasterophilus intestinalis*. Incidentally, our test of sequence similarity shows that *Drosophila* globin scores 26% to *T. akamusi* Hb V.

Swinging Movement of the Distal Histidine Residue in *T. akamusi* Hemoglobin VII

Soret Absorption Spectroscopy. In the polymorphic Hb comprised of 11 separable components, Hb VII (Ta-VII) is of particular interest. In neutral pH range, its absorption spectrum is essentially the same as that of sperm whale Mb both in the oxy and met forms (see Figure 5). When the met form of Ta-VII Hb was placed in acidic pH range, however, its spectrum changed dramatically depending upon the pH of the solution, particularly in the Soret region (Akiyama *et al*., 1994). Figure 10 represents such spectral changes with pH in 0.1 M KCl at 25°C. With lowering pH, the Soret peak was considerably blue-shifted from 406 to 397 nm, and accompanied by a marked decrease in intensity from 145 to 95 $mM^{-1}cm^{-1}$, probably due to a broadening of the spectrum.

Judging from the spectral criterion proposed in the preceding section, Ta-VII Hb, when exposed to acidic pH, seemed to be converted from a sperm whale Mb-type structure to a *Aplysia* Mb-type form. The Soret MCD spectra also revealed that Ta-VII Hb is in a pH-dependent equilibrium between a hexacoordinate and a pentacoordinate structure for its ferric heme iron (Akiyama *et al.*, 1994).

Stopped-Flow and Rapid-Scan Spectroscopy. It was therefore interesting to study the isomerization process of *T. akamusi* Hb VII (Ta-VII) in detail, using stopped-flow rapid mixing techniques, in 0.1 M buffer at 25°C (Kamimura *et al*., 2003). Figure 11 shows such time-resolved Soret absorption spectra of ferric Ta-VII Hb, when its pH was changed from 7.2 to 5.0 in a stopped-flow

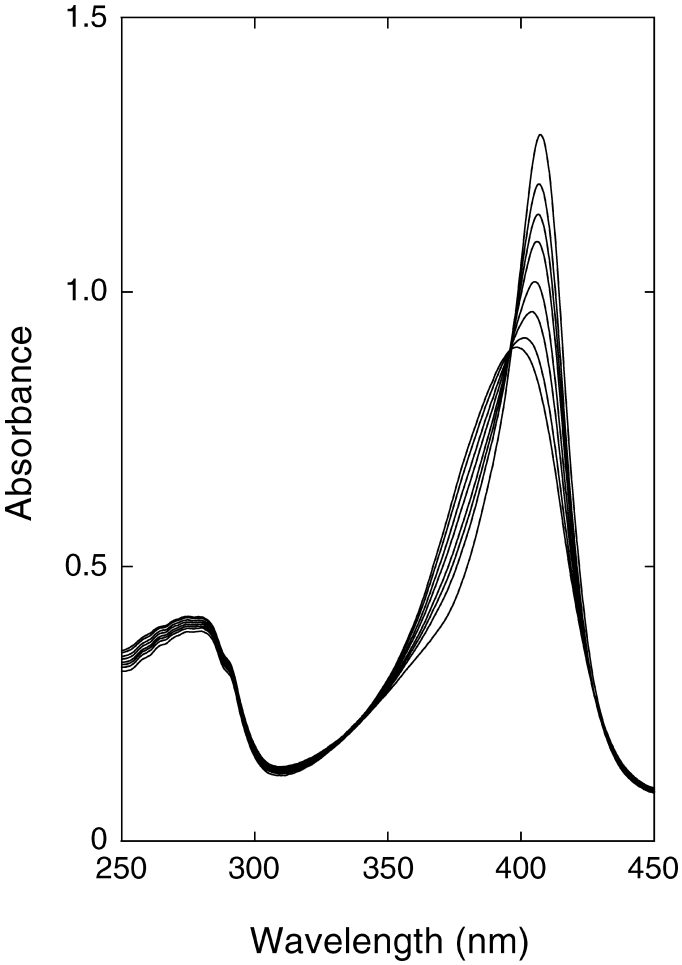

FIG. 10. Spectral changes with pH for the Soret peak of *T. akamusi* ferric Hb VII in 0.1 M KCl at 25°C. The pH was changed from 7.1 (top) to 6.7, 6.5, 6.3, 6.1, 5.8, 5.5, and to 5.0 by adding small amounts of 0.1 M HCl so as to keep its final volume within 1% of the original hemoglobin solution (3 ml). Heme concentration, 10 μM. Redrawn from Akiyama *et al*. (1994).

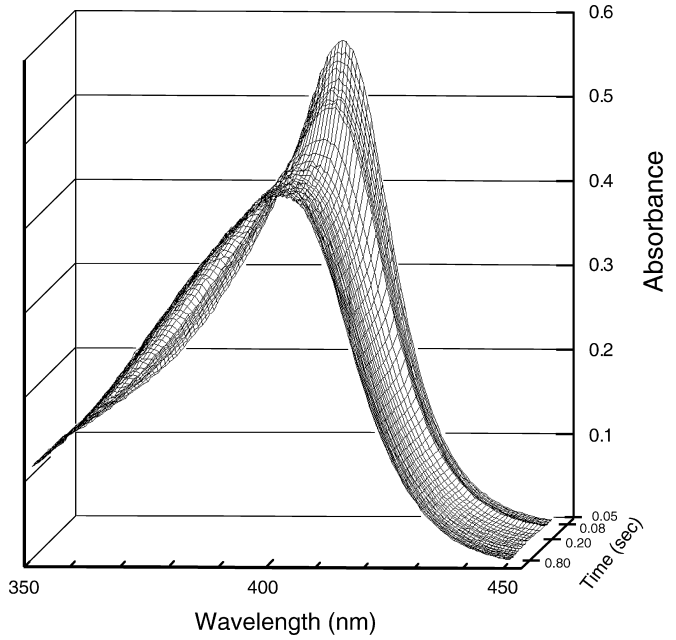

FIG. 11. Time-resolved Soret absorption spectra of *T. akamusi* Hb VII after the pH drops from 7.2 to 5.0 at 25°C. The ferric met species in 10 mM Tris buffer (pH 7.2) was mixed with an equal volume of 0.2 M Mes buffer (pH 5.0) in the stopped-flow apparatus. The first spectrum was for the Soret band scanned 0.05 s after mixing, while the last one is for 0.8 s later. The final heme concentration was 4.1 μM at pH 5.0. Redrawn from Kamimura *et al*. (2003).

spectrophotometer (Otsuka, RA-2000). This apparatus is equipped with a 10 mm light path cell and two sample reservoirs (3 ml). After the pH was jumped down, the spectra were recorded every 3 ms over a 500 s period and a range of 350–450 nm.

In the three-dimensional display, the spectrum scanned 0.05 s after mixing still retained the usual Soret absorption with maximum centered at 407 nm, characteristic of the six-coordinate ferric species. After 0.80 s, however, the peak was dramatically shifted to 397 nm with a set of isosbestic points at 396 and 426 nm, and accompanied by a marked decrease in intensity. All of these features indicate that the protein was converted completely into a five-coordinate species (Shikama & Matsuoka, 1989, 1994; Matsuoka *et al.*, 1992). These spectral changes of Ta-VII were totally reversible with pH. We conclude therefore that the observed Soret absorbance changes can be attributed to a transition of an iron-ligated water molecule, which is hydrogen-bonded to the distal histidine at position 64, to a water-free iron with the histidine swung away from the E7 position.

Figure 12 represents such a swinging movement of the distal histidine residue in a very schematic way. Unfortunately, we cannot indicate where the distal histidine moves to in *T. akamusi* Hb VII, as the X-ray crystal structure is not yet available. However, it is interesting to note that this transformation reaction is accompanied by a complete reversal of the sign of the Soret CD signal. At pH 7.0, ferric Ta-VII gave the CD spectrum containing a weak but distinct negative Soret signal. At pH 5.0, on the other hand, the protein exhibited a well-developed, positive CD lobe with maximum centered at 406 nm. These findings strongly suggest that the swinging movement of the distal histidine would exert effects on the amino-acid chromophores in the very vicinity of the heme moiety, so as to change the optical rotatory dispersion of the Soret band. No such pH-dependent reversal of the CD signal (or the Cotton effect) was observed in another component Ta-V, as well as in sperm whale Mb (Kamimura *et al*., 2003).

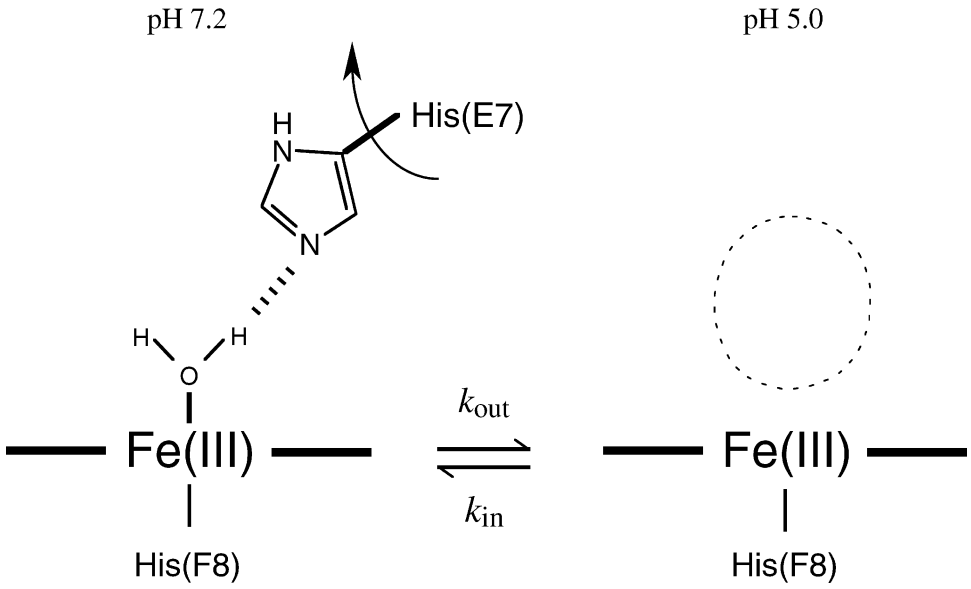

FIG. 12. A schematic representation for the pH-dependent swinging-out of the distal histidine residue. By a concomitant loss of the axial water molecule, *T. akamusi* Hb VII is transformed from a hexacoordinate to a pentacoordinate (or vacant-type) species. Redrawn from Kamimura *et al*. (2003).

In this transformation reaction, we have found the involvement of a single dissociable group (AH) with $pK_a = 6.3$ at 25°C. At a glance, this pK_a value was likely that of the distal histidine residue, whose protonation would be associated with the rupture of hydrogen bonding to the coordinated water molecule. In sperm whale aquomet-Mb, however, no such spectral change was observed in the Soret peak. From the effect of temperatures on the pK_a value, the AH group involved was found to have thermodynamic parameters characteristic of the ionization of a carboxyl group, although its pK_a value does not fall within the normal range (Akiyama *et al*., 1994). Anyway, our next step will be to clarify how rapidly the distal histidine swings away from the E7 position in *T. akamusi* Hb VII.

Rapid-Flow Kinetics. If we measure the absorbance changes at selected wavelengths, we can observe the time courses of the transformation reaction of ferric Hb VII more directly. Figure 13 shows such an example for the spectral track followed up at 407 nm (the Soret peak of the ferric high-spin species). In this case, the reaction was started at 25°C by mixing a 10 μM ferric Hb solution in 0.01 M Tris-HCl buffer (pH 7.2) with an equal volume of 0.2 M Mes-NaOH buffer (pH 5.0) to make the pH drop from 7.2 to 5.0. The dead time of the apparatus was 3 ms. As a result, the conversion process was found to obey a single exponential decay without any detectable formation of intermediates. At the same time, it was of importance to know whether the moved residue could swing back again to the original E7 position with pH. For this purpose, similar experiments were carried out at 25°C by mixing a 10 μM ferric Ta-VII solution in 0.01 M Mes-NaOH buffer (pH 5.0) with an equal volume of 0.2 M Tris-HCl buffer (pH 7.2). As soon as the pH was jumped up from 5.0 to 7.2, the absorbance at 407 nm increased exponentially with increasing appearance of the hexacoordinate species.

In formulating the pH-induced swinging movement of the distal histidine residue, at least six kinetic microconstants will be required, as follows:

$$\begin{array}{ccc} \text{hexacoordinate}[-\text{AH}]^* \rightleftharpoons \text{H}^+ + \text{hexacoordinate}[-\text{A}^-](\alpha) \\ k_{out}\downarrow\uparrow ? \qquad\qquad\qquad\qquad \uparrow k_{in}, \\ \text{pentacoordinate}[-\text{AH}](1-\alpha) \rightleftharpoons \text{H}^+ + \text{pentacoordinate}[-\text{A}^-]^* \end{array} \quad [3.1]$$

where AH represents the dissociable group of the regulatory residue (probably a carboxyl group of the heme propionate in this case), and the asterisk is for the unstable intermediate species for each of the two forms. The equilibrium between the hexacoordinte[−AH]* species and the pentacoordinate[−AH] form is not guaranteed because the swung-out histidine is found in a completely different Soret CD environment. The α is the molar fraction of the hexacoordinate form existing at a given pH value. In this reaction scheme, k_{out} represents the apparent first-order rate constant for the outward movement, while k_{in} is for the inward or swing-back movement of the distal histidine

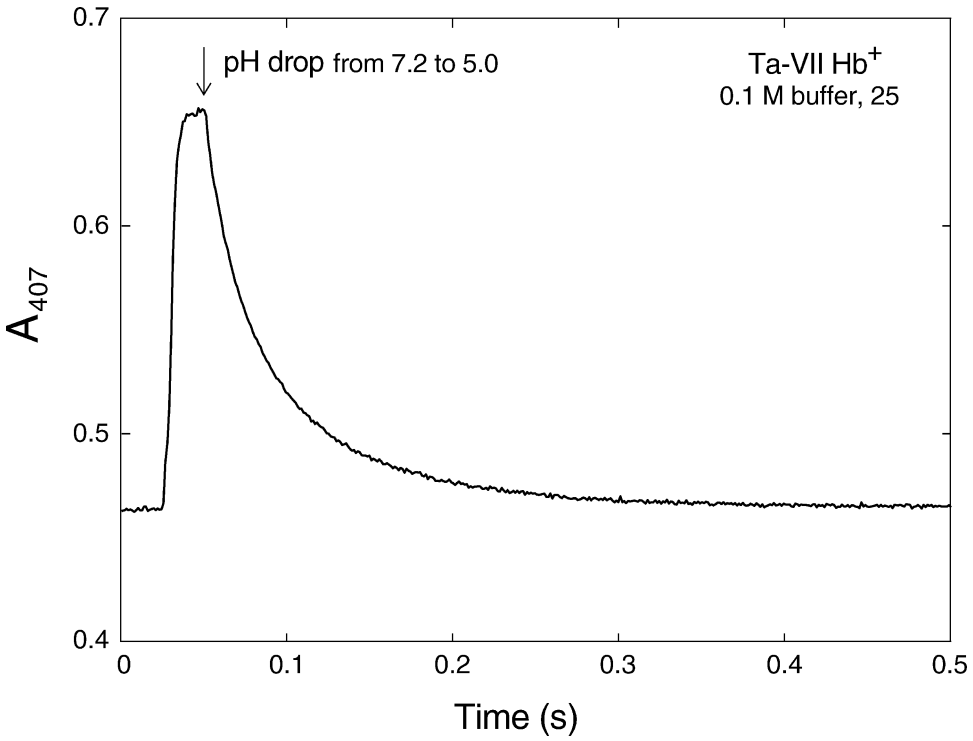

FIG. 13. Time courses for the pH-induced transformation reaction of ferric Hb VII followed by the absorbance changes at 407 nm. The experimental conditions for mixing were the same as is in Figure 11, and the pH was jumped down from 7.2 to 5.0 at 25°C. The final heme concentration was 5 μM. Redrawn from Kamimura *et al*. (2003).

residue, as the protonation and deprotonation processes for the involved AH group would be too fast to become rate-limiting in the swinging movement. In addition, the Soret absorption used here is silent in such protonation and deprotonation processes of a carboxyl group of the heme propionate, so that unstable intermediates, even if produced, could not be detected by the present spectrophotometric techniques.

The swinging process, irrespective of its direction, was therefore followed up by a plot of absorbance data at 407 nm as $-\ln\{(A_t - A_\infty)/(A_0 - A_\infty)\}$ *versus* time t after mixing. Figure 14 represents such first-order plots for the pH-induced conversion reaction of ferric Ta-VII Hb, from a hexacoordinate to a pentacoordinate form and vice versa, in 0.1 M buffer at 25°C. From the slope of each straight line, we have obtained the first-order rate constants of $k_{out} = 25\ s^{-1}$ for the swing-out movement and $k_{in} = 128\ s^{-1}$ for the swing-in process, respectively, of the distal histidine residue (Kamimura *et al*., 2003). Consequently, the swing-away movement takes place with a half-life period of $t_{1/2} = 27$ ms, this being less rapid than the swing-back process with $t_{1/2} = 5$ ms. At present, no mechanistic explanation can be given for this rate difference, as we do not know yet exactly where the distal histidine moved to. Nevertheless, it is true that its new position is in favor of making the residue swing back again to the original E7 position more easily by the pH jump. In such swinging reactions, the ligand water dissociation or association step would be too fast to become rate-limiting.

Oxygen Binding and Stability Properties of *T. akamusi* Hemoglobins

Table 3 summarizes the oxygen equilibrium parameters of *T. akamusi* hemoglobins V and VII at three different pH values and 25°C (Kamimura *et al*., 2003). Overall oxygen

TABLE 3
Oxygen equilibrium parameters of *T. akamusi* Hb in 50 mM Tris buffer plus 0.1 M KCl at 25°C

Hb component	pH	P_{50} (Torr)	δH^+
Ta-V	8.4	0.57	−0.20
	7.4	0.79	
	6.4	1.43	
Ta-VII	8.4	0.63	−0.58
	7.4	1.7	
	6.4	9.1	

Heme concentration: 60 μM.
Taken from Kamimura *et al*. (2003).

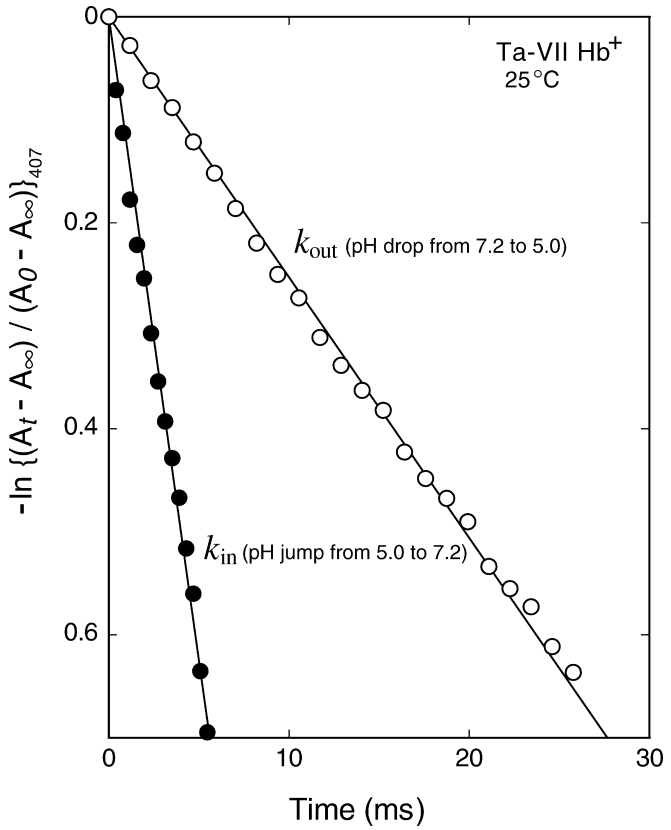

FIG. 14. First-order plots for the pH-dependent transformation reaction of ferric Hb VII in 0.1 M buffer at 25°C. In these plots, k_{out} represents the outward movement of the distal histidine from its E7 position, while k_{in} is for the inward or backward movement to the original position. Redrawn from Kamimura *et al*. (2003).

affinity is expressed in terms of the oxygen pressure to half saturate the protein, P_{50}(Torr). Bohr coefficient was also calculated as δH^+ by the difference in log(P_{50}) between pH 6.4 and 8.4. At neutral pH, both components have P_{50} values quite similar to those of mammalian Mbs. At acidic pH, however, their O_2 affinities became lower, particularly in Hb VII. As a result, Ta-VII Hb was found to have a remarkable Bohr effect almost equal to that of human Hb ($\delta H^+ = -0.48$). In this sense, Hb VII can play a central role in oxygen supply as the major component of the larval hemolymph.

As described previously, it is in the ferrous form that Hb can bind molecular oxygen reversibly and carry out its physiological function. Even in air-saturated conditions, however, the oxygenated form (HbO_2) is oxidized easily to the ferric met form (metHb) with generation of the superoxide anion as follows:

$$Hb(II)(O_2) \overset{k_{obs}}{\rightharpoonup} metHb(III) + O_2^-, \qquad [3.2]$$

where k_{obs} represents the first-order rate constant observed at a given pH value (Gotoh & Shikama, 1976). The rate of the autoxidation reaction is therefore given by

$$\frac{-d[HbO_2]}{dt} = k_{obs}[HbO_2]. \qquad [3.3]$$

In this way, if the values of k_{obs} are plotted against the pH of the solution, a profile of the stability of HbO_2 can be obtained in terms of the autoxidation rate. Figure 15 represents two such profiles for *T. akamusi* hemoglobins V and VII in 0.1 M buffer at 25°C. (Kamimura *et al*., 2003). When compared with sperm whale MbO_2 served as a reference, Ta-V HbO_2 was quite susceptible to autoxidation over the whole range of pH studied. At pH 9.0, for instance, its rate was 25 times higher than that of sperm whale MbO_2. Furthermore, its pH dependence was unusual. The rate also increased with increasing hydrogen ion concentration, but

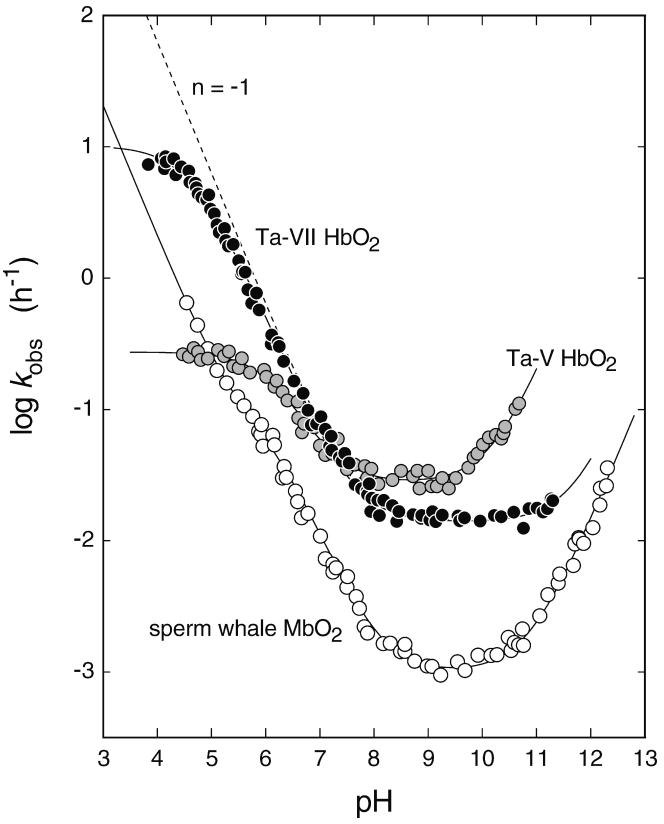

FIG. 15. pH-profiles for the stability of *T. akamusi* HbO_2 and sperm whale MbO_2 in 0.1 M buffer at 25°C. The logarithmic values of the observed first-order rate constant, k_{obs} in h^{-1}, for the autoxidation reaction are plotted against the pH of the solution. The pH-profile of sperm whale MbO_2 is taken from Shikama and Matsuoka (1986, 1994). Heme concentration: 20 μM for midge; 50 μM for sperm whale. Redrawn from Kamimura *et al*. (2003).

much less so than in sperm whale MbO_2. Rather, Ta-V HbO_2 exhibited a distinct rate-saturation below pH 6. This strongly suggests that the mode of action of H^+ ion is different between the two proteins. In sperm whale MbO_2, the rate increases so rapidly at acidic pH that a value close to $n = -1$ is always found for the slope of $\log(k_{obs})$ *versus* pH. As described previously, this is a definite indication of the involvement of a very strong acid catalysis performed by the distal histidine residue through a proton-relay mechanism (Shikama, 1988, 1998).

In marked contrast to sperm whale MbO_2, Ta-V HbO_2 stands with a slope of $n = -0.4$ for the acidic autoxidation. In fact, this protein has an isoleucine at position 66 in place of the usual distal histidine residue (see Figure 8). We have therefore measured the autoxidation rate at more than 70 different pH values from 4 to 12 and finally established the best fit to the experimental values of k_{obs} by a simple "two-state model" (Suzuki *et al*., 2000). In this mechanism, we assumed that a single, dissociable group (XH with pK_1) is also involved in the reaction but in a different way. As a result, the pH profile for the autoxidation rate of this insect protein could be described by the following equation, based on a nucleophilic displacement of O_2^- from the HbO_2 by an entering water molecule or hydroxyl ion:

$$k_{obs} = \left\{k_0^A[H_2O]\right\}(\alpha) + \left\{k_0^B[H_2O] + k_{OH}^B[OH^-]\right\}(\beta). \quad [3.4]$$

In this kinetic formulation, one of the most remarkable features was that Ta-V HbO_2 does not show any proton-catalyzed process that has the term $k_H[H_2O][H^+]$, such as the one that can play a dominant role in the autoxidation reaction of most mammalian myoglobins or hemoglobins carrying the usual distal histidine (Tsuruga *et al.*, 1998; Shikama, 1998; Yasuda *et al.*, 2002). Instead, Ta-V HbO_2 contained a dissociable group (XH with $pK_1 = 6.2$) that is responsible for a small rate-increase saturated at acidic pH side. To characterize this XH group thermodynamically, the effect of temperatures on the K_1 value was investigated by analyzing the pH-profiles obtained at three different temperatures. As a result, the enthalpy change of practically zero was deduced from the slope of the van't Hoff plot. Thus, the resulting thermodynamic parameters were: $\Delta G^\circ = 33.1$ kJ mol^{-1}, $\Delta H^\circ = 0$ kJ mol^{-1}, and $\Delta S^\circ = -111$ J mol^{-1} K^{-1} in 0.1 M buffer at 25°C (Suzuki *et al*., 2000). Although its pK_a value does not lie in the normal range, these parameters are those expected for the ionization of a carboxyl group, and we suggest that the most probable candidate is a carboxyl group of the heme propionates, just as in the previous case of *Aplysia* MbO_2 (Shikama & Matsuoka, 1994).

Along with this line of evidence, our interest was in the stability property of Ta-VII HbO_2, since in its ferric met form the distal histidine was found to swing out from the E7 position at acidic pH. As is clear in Figure 15, the pH profile of Ta-VII HbO_2 featured an intermediate character between sperm whale MbO_2 and Ta-V HbO_2. With increasing hydrogen ion concentration, its oxidation rate increased rapidly as in sperm whale MbO_2 but began to deviate from the theoretical line, having a slope of $n = -1$, and finally reached a saturation level below pH 5 as in Ta-V HbO_2. Among these, the most interesting point is to ask whether the distal histidine swinging occurs in the oxygenated form of Ta-VII as well. However, the Soret absorption spectroscopy is totally silent in this respect. Another approach will be needed for more detailed kinetics of the histidine swinging and autoxidation reactions of Ta-VII HbO_2.

Concluding Remarks: Ecological Adaptation

The hemoglobin from *T. akamusi* consists of at least 11 components that fall into two approximately equal groups: one (VIA, VIB, VII, VIII, and IX) having a distal (E7) histidine and the other (IA, IB, II, III, IV, and V) lacking it. A stage-specific expression of *T. akamusi* hemoglobin appears to be adaptive for the bloodworm to extend its inhabitable environment. By burrowing deeply into lake mud flats, the bloodworm can protect itself from fish and thus have a fairly long period of diapause in safety. The polymorphic forms of *T. akamusi* hemoglobin would also be advantageous to the larval life in O_2 transport and storage under the particular adverse conditions.

For the distal histidine swinging, Johnson *et al.* (1989) observed it in the structure of Mb-ethylisocyanide. They described that when such a bulky ligand bound itself to ferric sperm whale Mb, the distal (E7) histidine swung up and away from the heme iron, just like a swinging door, toward the protein surface. In sperm whale Mb, Tian *et al.* (1993) measured the on and off rate-constants for O_2-binding as a function of pH and reported a dramatic increase in the O_2-dissociation rate at low pH, where the imidazole side chain of the E7-His becomes protonated, loses a hydrogen bond to the bound O_2, and moves outward on a microsecond (μs) timescale. In *T. akamusi* Hb VII, a similar movement of the distal histidine could occur in the ferric met form but on a millisecond (ms) timescale. Consequently, this pH-dependent swinging is quite different from the distal His movement controlling the on and off rate processes of O_2-binding in Mbs and Hbs.

In oxygen equilibrium measurements, the most remarkable result is that O_2 affinities of the components V and VII are almost the same at pH 8.4, but the E7-Ile Hb V shows rather a higher affinity at lower pH. In all the recombinant Mbs reported so far, a His to Ile or Leu mutation at the E7 position is found to cause a dramatic decrease in O_2 affinity, resulting in a very large increase (>10 Torr) in P_{50} value (Springer *et al*., 1994). In this respect, it is possible

that the B10-Phe at position 32 is stabilizing the bound O_2 in Ta-V Hb (see Figure 8). Among the distal heme pocket residues, the B10 is known to be very relevant for the O_2-binding property, in addition to the E7 residue (Zhao *et al.*, 1995).

In light of the oxygen equilibrium parameters and considerable resistance to acidic autoxidation, we conclude that *T. akamusi* Hb VII, the major component, can play an important role in O_2 transport and storage against the extremely acidic and hypoxic adversity. For the pH of the larval hemolymph, there is no report of its direct measurement, but there is a strong possibility that it drops to around pH 4. Under anaerobic conditions, the end-products of carbohydrate metabolism by C*hironomus* larva are known to include large amounts of lactic and succinic acids (Wilps & Zebe, 1976). Multiplicity of *T. akamusi* Hb components in the O_2-binding affinity, Bohr effect, and FeO_2 stability would also be advantageous for this insect larva to overcome various stringent circumstances.

PROTOZOAN MYOGLOBIN FROM *TETRAHYMENA PYRIFORMIS*: A TRUNCATED STRUCTURE

Protozoan Ciliate Myoglobins and Related Globins

The occurrence of a Mb- or Hb-like protein in protozoan ciliates was first reported by Sato and Tamiya (1937) on the basis of spectroscopic observations on cell suspensions of *Paramecium caudatum*. This was later confirmed by Keilin and Ryley (1953) with estimations of its content of 1.12–1.74%. Isolation and characterization of this oxygen-binding protein were thus carried out by several research groups with *P. aurelia* (Smith *et al*., 1962), *P. tetraurelia* (Steers & Davis, 1979), and *P. primaurelia* (Irie & Usuki, 1980). However, the complete amino acid sequence of the so-called *Paramecium* Hb, which is also functionally referred to as Mb (Steers & Davis, 1979), could not be determined over a long period of time.

In those circumstances, we have succeeded in isolating protozoan Mbs (or monomeric Hbs) from three kinds of ciliates, and have determined their complete amino acid sequences. In our study, *Tetrahymena pyriformis* and *T. thermophila* each were cultivated for 5 days at room temperature in a medium of 1% proteose peptone, 0.5% Bacto yeast extract, and 0.87% dextrose. The packed cells of 400 ml were harvested from the mass culture at about 80 l and kept at −80°C until use. *P. caudatum* was also cultivated for 7 days in a bacteria-free Dryl's solution containing 0.4% reddish bean broth. In this case, the packed cells of 450 ml were obtained from the mass culture amounted to 300 l and kept at −80°C. The frozen cells were thawed quickly and ruptured with a Teflon-glass homogenizer in an equal volume of 10 mM Tris-HCl buffer (pH 8.0) containing 1 mM phenylmethylsulfonyl fluoride, 1 mM iodoacetic acid, and 1 mM EDTA to prevent endogenous protease digestion. After insoluble materials had been removed by centrifugation, the Mb extract was fractionated with ammonium sulfate between 50 and 100% saturation, and then subjected to gel filtration on a Sephadex G-50 column. The essential step was the chromatographic separation of MbO_2 from its ferric met form on a CM-cellulose column for *Tetrahymena* species (Korenaga *et al.*, 1996, 2000) and on a DEAE-cellulose column for *Paramecium* species (Tsubamoto *et al*., 1990). The MbO_2 solution thus obtained was condensed and kept at low temperature (0–4°C) until use. The concentration of protozoan Mb was determined, after conversion into cyanomet-form, using an absorption coefficient at 540 nm of 10.8 mM^{-1} cm^{-1} for *T. pyriformis*, 11.2 mM^{-1} cm^{-1} for *T. thermophila*, and 11.9 mM^{-1} cm^{-1} for *P. caudatum* (Korenaga *et al.*, 1996).

As a result, the globin from *P. caudatum* was composed of 116 amino acid residues with a molecular mass of 12,565 Da including the heme moiety (Iwaasa *et al*., 1989), while both *Tetrahymena* proteins consisted of 121 amino acid residues with a molecular mass of 14,343 Da for *T. pyriformis* (Iwaasa *et al*., 1990) and of 14,249 Da for *T. thermophila* (Takagi *et al*., 1993). All of these protozoan Mbs were much smaller than any other globins reported so far, and they were nearly two-thirds of the size of sperm whale Mb (153 amino acid residues). After our findings, several authors reported similar shortened types of Mbs or Hbs, such as those from a cyanobacterium *Nostoc commune* (Potts *et al*., 1992), a unicellular green alga *Chlamydomonas eugametos* (Couture *et al*., 1994), and a pathogenic bacteria *Mycobacterium tuberculosis* (Couture *et al*., 1999). These globins were primarily derived from genomic DNA analysis.

In this way, the contracted or shortened globin class is now established to occur widely in eubacteria, cyanobacteria, protozoa, and plants, and is referred to as truncated hemoglobins (trHbs), which form a distinct group within the globin superfamily. At present, more than 40 putative trHb genes have been identified in particular in aggressively pathogenic bacteria. As a matter of course, various biochemical functions other than the conventional oxygen transport or storage have been proposed so far for these proteins, including nitroxide fixation, terminal oxidation, and photosynthesis (Couture *et al*., 1999), but the precise *in vivo* activity is still unclear. The current state of this topic is given by Wittenberg *et al*. (2002).

In this section, we shall describe the very unique property of *Tetrahymena* Mb, with that of *Paramecium* Mb, by placing focus on the heme environment, autoxidizability, and genomic DNA structure. As truncated Hbs are held to be of very ancient origin, such examinations will

```
                              1                   20                  40
P. caudatum                Ac-SLFEQLGGQAAVQAVTAQFYANIQADATVATFFNGIDMPN
T. pyriformis     Ac-MNKPQTIYEKLGGENAMKAAVPLFYKKVLADERVKHFFKNTDMDH
T. thermophila    Ac-MRKQPTVFEKLGGQAAMHAAVPLFYKKVLADDRVKHYFKNTNMEH

                             41                  60                  80
                             QTNKTAAFLCAALGGPNAWTGRNLKEVHANMGVSNAQFTT
                             QTKQQTDFLTMLLGGPNHYKGKNMTEAHKGMNLQNLHFDA
                             QAKQQEDFLTMLLGGPNHYKGKNMAEAHKGMNLQNSHFDA

                             81                  100             116
                             VIGHLRSALTGAGVAAALVEQTVAVAETVRGDVVTV
                             IIENLAATLKELGVTDAVINEAAKVIEHTRKDMLGK
                             IIENLAATLKELGVSDQIIGEAAKVIEHTRKDCLGK
```

FIG. 16. Amino acid sequences of protozoan ciliate Mbs. Each globin is acetylated at the N-terminus and contains a quite different number of histidine residues. Taken from Korenaga *et al*. (2000).

undoubtedly deepen our insight into the Mb and Hb biochemistry, as well as the evolution of these proteins from protozoa to higher animals.

A Shortened Structure of *Tetrahymena* Myoglobin

Primary and Secondary Structures. Figure 16 summarizes the complete amino acid sequences of protozoan Mbs (or Hbs) isolated from three ciliates, *P. caudatum* (Iwaasa *et al*., 1989), *T. pyriformis* (Iwaasa *et al*., 1990), and *T. thermophila* (Takagi *et al*., 1993). As examined so far, protozoan Mbs are all acetylated at the N-terminus and much smaller than mammalian Mbs by 37 residues in *Paramecium* and 32 residues in *Tetrahymena*. However, the overall degrees of sequence similarity are low between *Paramecium* Mb and both *Tetrahymena* proteins (32.2–33.9%). Among these, one of the most interesting features is that the globins from *T. pyriformis* and *T. thermophila* contain six and seven histidines, respectively, in a wide distribution throughout the polypeptide chain, whereas *P. caudatum* Mb has only two histidines at positions 68 and 84. The same positioning of the two histidines was also found in *P. triaurelia* and *P. jenningsi* Mbs (Yamauchi *et al*., 1995), as will be listed later in Table 5.

In such *Paramecium* Mbs the alignment of the two histidine residues is particularly interesting, as the distal (E7) histidine is known to play an important role in the stability of the bound dioxygen. In this respect, there are two possibilities: The simplest one is to place His-84 to the heme-binding proximal one and to arrange His-68 to the distal position. Another alignment is also possible if His-68 is arranged to the heme-binding proximal position. In the latter case, *Paramecium* Mb falls into the globin class lacking in the usual distal histidine residue. In *Tetrahymena* Mb, on the other hand, even if the corresponding His-73 is placed in the heme-binding proximal position, it is still possible to have His-45 as the distal residue. Recent computer-assisted alignments strongly suggest that the distal (E7) and proximal (F8) residues are Gln-41 and His-68 for *P. caudatum* Mb, and Gln-46 and His-73 for *T. pyriformis* Mb (Pesce *et al*., 2000). In the known trHb sequences, however, very few amino acids are strictly conserved; the proximal (F8) His is the only invariant residue, while the distal E7 position is occupied by at least six different residues such as Ala, Leu, Gln, Thr, and His (Wittenberg *et al.*, 2002).

To know the helical contents of protozoan Mbs in solution, CD measurements were carried out in 10 mM buffer, pH 7.0. The resultant mean residue molar ellipticity at 222 nm was $-18{,}900$ deg cm^2 dmol^{-1} for *T. pyriformis* Mb and $-20{,}600$ deg cm^2 dmol^{-1} for *P. caudatum* Mb (Korenaga *et al*., 2000). Consequently, both protozoan Mbs have a considerably low helical content compared with sperm whale Mb, which shows a value of $-24{,}000$ deg cm^2 dmol^{-1}. In solution, some conformational fluctuation would be taking place in these truncated globins accordingly.

Conformational Instability of the Heme Pocket Residues. Probably due to a large number of amino acid deletions, the protozoan Mbs exhibit conformational instability in the heme pocket structure. *Paramecium* Mb, for instance, showed irreversible hemichrome formation at pH values higher than 9.5 (Tsubamoto *et al*., 1990). *Tetrahymena* Mb also forms some unusual ferric species at alkaline pH side. Figure 17 represents such an example for the 8 K electron paramagnetic resonance (EPR) spectra for the oxidation products of *T. pyriformis* myoglobin in 10 mM buffer and in the presence of 50% glycerol. EPR spectra were recorded in a Varian EPR spectrometer operating at 9.0–9.2 GHz over a magnetic field of 0–500 mT at 8.0 K.

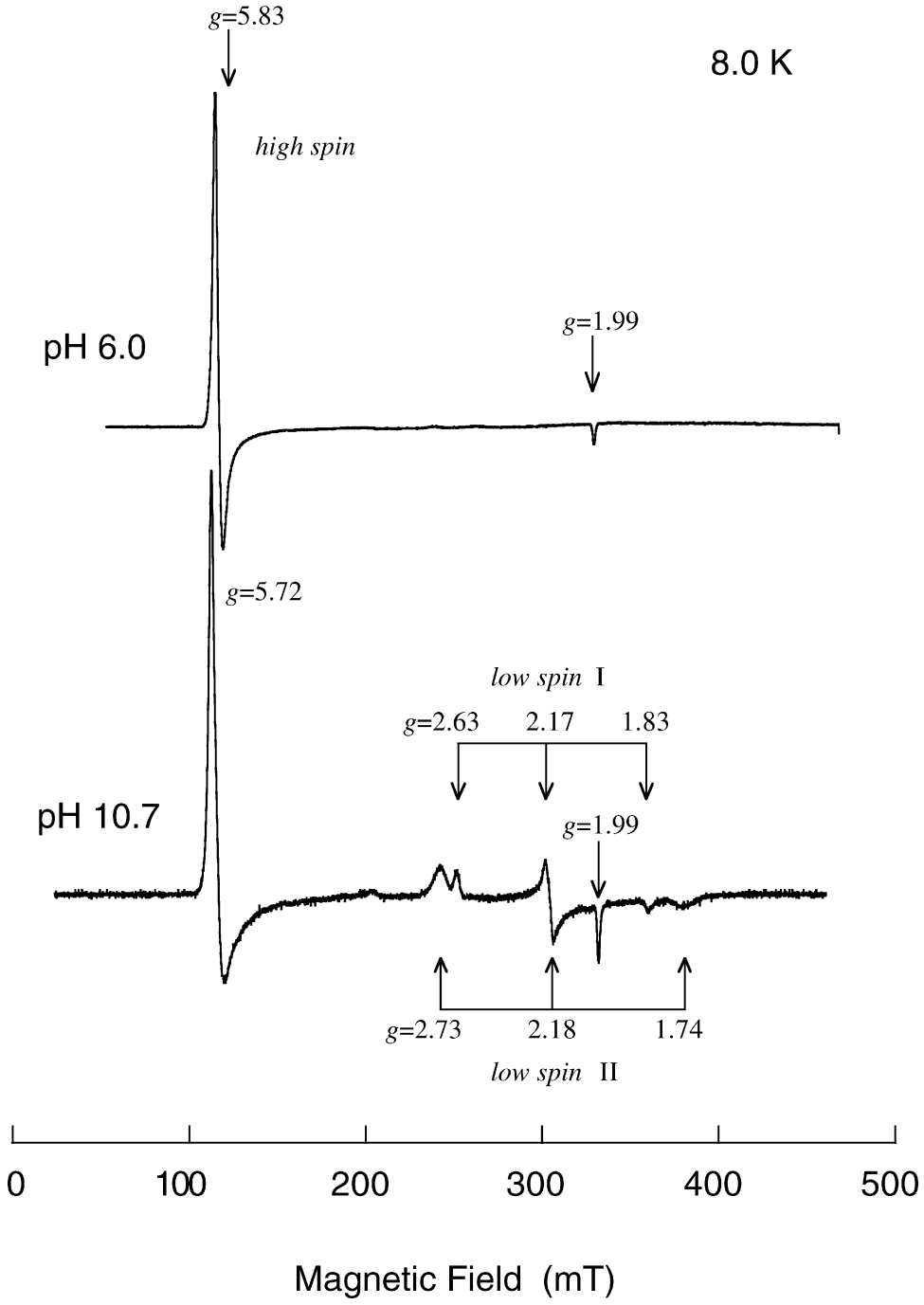

FIG. 17. The 8 K EPR spectra for the oxidation products of *Tetrahymena* Mb in 10 mM buffer at two different values of pH. At pH 10.7, *T. pyriformis* Mb still carried a high-spin aqua met species with *g* values of 5.72 and 1.99. In addition to this, the protein showed two different types of low-spin spectra. One is the low-spin II signal attributed to the usual hydroxide met complex, but the other low-spin I signal with *g* values of 2.63, 2.17, and 1.83 was unique. The buffers used were Mes at pH 6.0 and Caps at pH 10.7. Redrawn from Korenaga *et al*. (2000).

In these spectra, the most interesting point is that even at pH 10.7, *Tetrahymena* Mb still carried a high-spin signal with *g* values of 5.72 and 1.99, both values being similar to those for the aqua-met form observed at pH 6.0. In addition to this, the protein exhibited two other EPR signals. The one named *low-spin II* can be attributed to the normal hydroxide-met complex with *g* values of 2.73, 2.18, and 1.74, but the other signal, *low-spin I*, with *g*

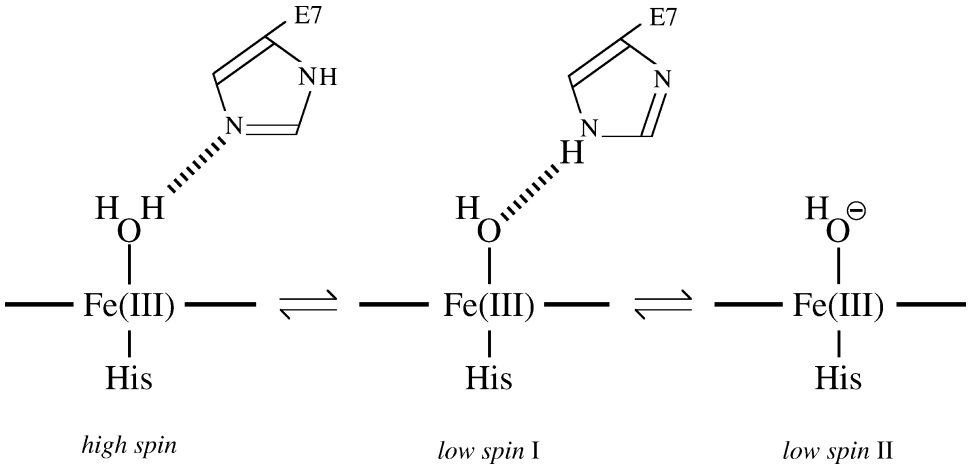

FIG. 18. Schematic representation of multiple subconformations for the heme pocket structure of *Tetrahymena* metMb. The low-spin I species is not a hemichrome but is strongly indicative of association of the distal histidine interaction. Redrawn from Korenaga *et al*. (2000).

values of 2.63, 2.17, and 1.83 was unique. According to the specifications of Rifkind *et al*. (1994), the latter species is not a hemichrome but is strongly suggestive of association of the distal histidine interaction. On the basis of these EPR studies, Figure 18 illustrates a pH-dependent equilibrium between the multiple subconformations for the heme pocket structure of *Tetrahymena* metMb. From the integrated transition probability, we have also estimated the molar fraction of each species (Korenaga *et al*., 2000). As a result, a value of 40% was obtained for the high-spin species even at pH 10.7, while 44% was obtained for the low-spin I and 16% for the low-spin II. When the temperature was raised from 18 K to 130 K, the low-spin I signal overlapped the low-spin II signal.

A Striking Modification of the Classical Globin-Fold. X-ray crystallographic investigations have recently been made by Bolognesi and coworkers with the truncated Hbs from *P. caudatum*, *C. eugametos*, and *M. tuberculosis*, whose three-dimensional structures were determined at 1.54Å, 1.8Å, and 1.9Å, respectively (Pesce *et al.*, 2000; Milani *et al*., 2001). As a result, these proteins were found to receive a striking modification of the conventional globin-fold that can be represented as a three-on-three (or a A/B/E-over-F/G/H) α-helical sandwich fold. In truncated Hbs, their structures accommodate the deletion of the A and D helices, together with part of the H helix, and the concomitant replacement of the crucial heme-binding F helix with an extended polypeptide loop (identified as pre-F), which nevertheless supports the proximal His-68 through a single one-helical turn (identified as F-helix). Accordingly, the antiparallel helix pairs B/E and G/H are the main secondary structure elements that are arranged in a two-on-two sandwich fold. Moreover, an almost continuous hydrophobic tunnel is traversing the protein matrix, from the molecular surface to the heme distal site, and this may provide a path for ligand diffusion to the heme iron (Milani *et al*., 2001; Wittenberg *et al*., 2002). At all rates, such a dramatically simplified 2-on-2 (or a B/E-over-G/H) version strongly indicates that the globin fold has a previously unpredicted structural plasticity in itself.

We have recently studied the three-dimensional structure of *T. pyriformis* Mb at 2.5 Å resolution (M. Saways, Y. Wang, H. Pelletier, K. Shikama, A. Matsuoka, T. Takagi, and R. F. Doolittle, 2003, Crystal structure of a truncated hemoglobin from *Tetrahymena pyriformis* at 2.5 Å resolution, unpublished data), and further refinements are still in progress. As displayed in Figure 19, the protein also adopted the same two-on-two (or a B/E-over-G/H) α-helical sandwich fold as characterized in homologous trHbs. In *Tetrahymena* Mb, its His-45 has been identified as an E6 residue, since computer alignments are used to taking a Gln-46 in the E7 position (Pesce *et al*., 2000). In the crystal structure indeed, the His-45 was found to stick out of the heme pocket into the surrounding solvent. In solution, however, the extended polypeptide pre-F loop would be highly flexible in nature. Consequently, it seems to be possible to place His-45 quite properly in the distal position so as to reach a good accord with the Soret absorption (see Table 1) and EPR spectroscopy of this protein.

Stability Properties of *Tetrahymena* Oxymyoglobin

In view of its contracted or truncated structure, our next concern is to investigate the stability of *Tetrahymena* MbO_2 in terms of the autoxidation rate as a function of pH. According to our standard procedures, the rate of autoxidation of *Tetrahymena* MbO_2 was measured in 0.1 M buffer at

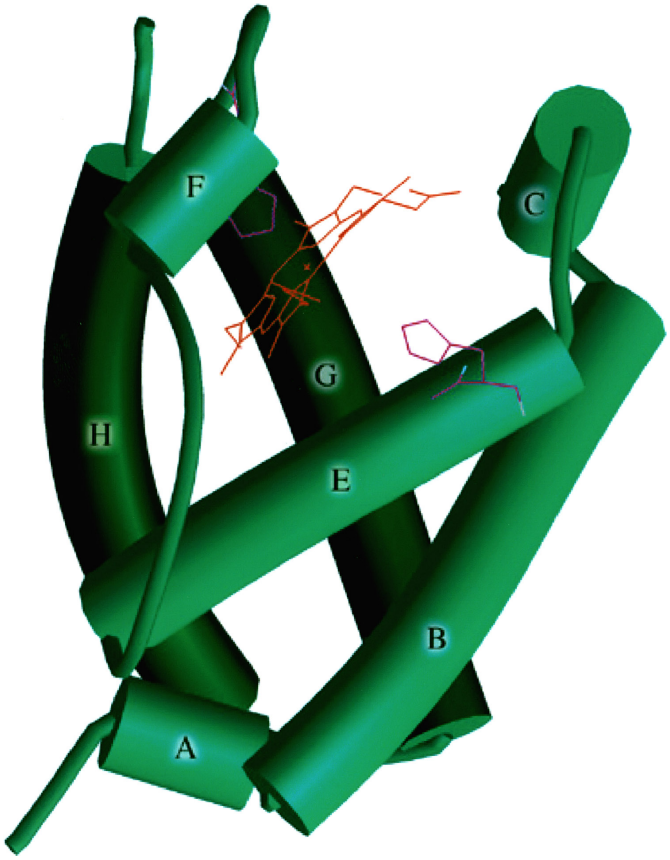

FIG. 19. The 3D structure of *T. pyriformis* Mb. The main α-helical segments are displayed as cylinders labeled according to the topological conventions for the classical globin-fold (see Figure 2). The heme group is shown in red, while the proximal F8-His73 and the distal E6-His45 are both in purple. X-ray analysis was made at 2.5 Å resolution by Saways *et al*. (unpublished data; see text for full citation), and further refinements are still in progress.

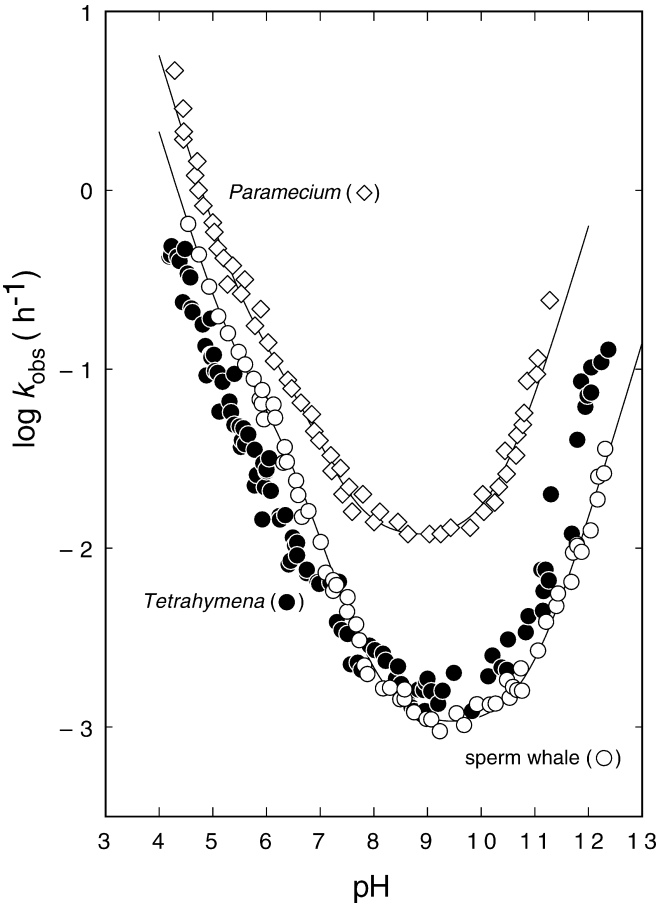

FIG. 20. pH-dependence curves for the stability of *Tetrahymena* MbO_2 and *Paramecium* MbO_2 in 0.1 M buffer at 25°C. The logarithmic values of the observed first-order rate constant, k_{obs} in h^{-1}, for the autoxidation of *T. pyriformis* MbO_2 (•) and *P. caudatum* MbO_2 (◇) are plotted against the pH of the solution. The profile of sperm whale MbO_2 (○) is also shown as a reference. Each computed curve (——) was obtained by a least-squares fitting to the experimental points over the whole range of pH studied, based on Equation (4.2). MbO_2 concentration: 10 μM for *Tetrahymena*; 7.5 μM for *Paramecium*; 50 μM for sperm whale. Redrawn from Korenaga *et al*. (2000).

25°C by the following equation:

$$\frac{-\mathrm{d}[MbO_2]}{\mathrm{d}t} = k_{obs}[MbO_2], \qquad [4.1]$$

where k_{obs} represents the first-order rate constant observed at a given pH value. If the values of k_{obs} are plotted against the pH of the solution, a pH profile of the stability of *Tetrahymena* MbO_2 can be obtained, as shown in Figure 20, with those of *Paramecium* MbO_2 and sperm whale MbO_2 as well (Korenaga *et al*., 2000). This graph clearly indicates that the rate of autoxidation of *Tetrahymena* MbO_2 increases rapidly with increasing hydrogen ion concentration, that a minimum rate appears at pH 9.0, and that a further increase occurs at the higher pH values. When compared with the *Paramecium* protein (Tsubamoto *et al*., 1990), *Tetrahymena* MbO_2 is more resistant against heme oxidation over the whole range of pH studied. Moreover, it was quite surprising that its stability is almost the same as that of sperm whale MbO_2. Accordingly, the pH-dependence curves for the autoxidation rate of two protozoan Mbs can be explained by an "acid-catalyzed two-state model," the same mechanistic model as already described to sperm whale MbO_2 in Section II.

In this model, it is assumed that a single dissociable group, XH with pK_1, is involved in the reaction. Using the rate constants defined previously, the autoxidation reaction of *Tetrahymena* MbO_2, as well as *Paramecium* MbO_2, may

therefore be formulated as follows:

$$k_{obs} = \left\{k_0^A[H_2O] + k_H^A[H_2O][H^+]\right\}(\alpha) + \left\{k_0^B[H_2O] + k_H^B[H_2O][H^+] + k_{OH}^B[OH^-]\right\}(\beta), \quad [4.2]$$

where

$$\alpha = \frac{[H^+]}{[H^+] + K_1},$$

and

$$\beta = (1 - \alpha) = \frac{K_1}{[H^+] + K_1}. \quad [4.3]$$

The kinetic and thermodynamic parameters involved in Equation (4.2) were thus established so as to obtain the best fit to more than 90 experimental points of k_{obs} as a function of pH (Korenaga *et al*., 2000). Table 4 summarizes such rate constants and acid dissociation constants involved in the autoxidation of *Tetrahymena* MbO_2 and *Paramecium* MbO_2 in 0.1 M buffer at 25°C. The corresponding values of sperm whale MbO_2 are also cited as a reference. These results clearly indicate that the proton-catalyzed displacement processes with the rate constants k_H^A and k_H^B are mainly responsible for promoting the autoxidation of protozoan oxymyoglobins. In the proton catalysis, the distal histidine (the dissociable group XH with pK_1) is proposed to participate *via* its imidazole ring by a proton-relay mechanism (Shikama, 1988, 1998; Shikama & Matsuoka, 1994). Table 4 also indicates that in *Paramecium* MbO_2 the rate constant k_0^B is eight times higher than in *Tetrahymena* MbO_2. The higher value of k_0^B implies that the heme pocket structure is open to allow more easier attack of the solvent water molecule on the FeO_2 center, resulting in a more rapid formation of the ferric met species.

At this point, it should be remarked that there is some discrepancy between the proposed crystal structure and the solution properties of *Paramecium* Mb, particularly in the Soret absorption, the acid-catalyzed autoxidation reaction, and the hemichrome formation in alkaline pH side (Korenaga *et al*., 2000). As far as we have examined for a dozen Mbs and Hbs, the proteins lacking the distal (E7) histidine do not manifest any proton-catalyzed process in the autoxidation reaction (Tsuruga *et al*., 1998; Tada *et al*., 1998; Suzuki *et al*., 2000). In the case of *Paramecium* Hb, Das *et al*. (2000) have proposed a model for hydrogen bonding stabilization of the heme-bound O_2 with a pair of Tyr-20 (B10) and Gln-41 (E7), based on the low frequency of Fe–OO stretching in resonance Raman spectra. However, currently little is known about the possibility that such a hydrogen bond network could produce a proton-catalyzed process in the autoxidation reaction of MbO_2 or HbO_2. As a matter of fact, how the modified fold of truncated Hbs is related to their functional properties remains open to future study.

Truncated Globins and Their Genomic Structures

It is well known that the mammalian globin genes have a two-intron and three-exon structure. In seal myoglobin gene, for instance, the first intron was found to be unusual, approximately 4800 bp long, and the second one also contained approximately 3400 bp (Blanchetot *et al*., 1983). In *Paramecium*, Yamauchi *et al.* (1992, 1995) reported that the globin genes from *P. caudatum, P. jenningsi*, and *P. triaurelia* all encoded 116 amino acid residues but were interrupted by a single, extremely short intron of 23, 29, and 29 bp, respectively, at the same position between Arg-62 and Asn-63. On the other hand, Potts *et al*. (1992) derived the homologous protein from genomic DNA analysis of *Nostoc commune* (UTEX 584). This cyanobacterial Mb, referred to as *cyanoglobin*, was encoded by the *glbN*

TABLE 4
Rate constants and acid dissociation constants involved in the autoxidation reaction of *Tetrahymena*, *Paramecium*, and sperm whale oxymyoglobins in 0.1 M buffer at 25°C

Source	State of MbO_2	k_0 (h^{-1} M^{-1})	k_H (h^{-1} M^{-2})	k_{OH} (h^{-1} M^{-1})	pK_1
Tetrahymena MbO_2	A(XH)	0.41×10^{-4}	0.16×10^{3}	—	
	$\uparrow\downarrow K_1$				6.6
	$B(X^-)$	0.25×10^{-4}	0.97×10^{3}	0.34×10	
Paramecium MbO_2	A(XH)	0.35×10^{-3}	0.10×10^{4}	—	
	$\uparrow\downarrow K_1$				6.5
	$B(X^-)$	0.20×10^{-3}	0.57×10^{4}	0.62×10^{2}	
Sperm whale MbO_2	A(XH)	0.78×10^{-4}	0.37×10^{3}	—	
	$\uparrow\downarrow K_1$				6.2
	$B(X^-)$	0.18×10^{-4}	0.20×10^{4}	0.14×10	

Taken from Korenaga *et al*. (2000).

gene, which is positioned between the *nifU* and *nifH* genes essential for nitrogen fixation. DNA sequence analysis of *glbN* gene revealed an open reading frame of 118 codons, with no intron but with a marked amino acid sequence similar to both *P. caudatum* and *T. pyriformis* myoglobins.

In the meantime, Couture *et al*. (1994) isolated two nuclear genes, both encoding a Hb-like protein, from the unicellular green alga *C. eugametos.* DNA sequence analysis of the one gene *LI637* predicted a polypeptide chain of 164 amino acid residues, of which the N-terminal 38 residues constituted a transit or signal peptide for the import into chloroplasts. Thus, the mature globin is composed of 126 amino acid residues. They also showed that the *LI637* gene possesses a three-intron and four-exon structure similar to that of plant leghemoglobin genes, but each positioning of the three introns is quite different between the alga and legume genes. Molecular properties of such truncated Mbs (or Hbs) and their genomic structures are listed in Table 5.

Along with these lines of evidence, we have examined *Tetrahymena* Mbs for their genomic structures. In our studies, the total DNA of each ciliate, almost all of which was derived from macronuclear DNA, was extracted using 2 g of the frozen packed cells. The isolated DNA was then deproteinized according to the standard phenol method. After treatment with RNase, the genomic DNA was subjected to polymerase chain reaction (PCR) amplification, and the globin gene was cloned using the forward and reverse primers, which were synthesized on the basis of each cDNA sequence of *Tetrahymena* Mbs. For *T. pyriformis*, the forward primer was 5′-AAATGAACAAACCCCAAACT-3′ and the reverse one was 5′-ATCATCATCTTCAATAAACG-3′, while the forward of 5′-GTAAAATGAGGAAATAGCCT-3′ and the reverse of 5′-TAAGACATGATAAAACAGAG-3′ were for *T. thermophila*. The reverse primer was complementary to a region 173 bp downstream from the 3′-terminus in *T. pyriformis* and to a region 97 bp downstream in *T. thermophila*. After heating the materials at 95°C for 1 min, PCR amplification was carried out for 30 cycles in the presence of *Ex Taq* DNA polymerase. PCR products were then purified on agarose gel electrophoresis, extracted with Geneclean II kit (Bio 101), and subcloned in pCR2.1 plasmid vector using TA-cloning kit (Invitrogen). The nucleotide sequences of *Tetrahymena* Mb genes were determined by the usual dideoxy chain termination method.

Alignment of the genomic DNA sequence with its corresponding cDNA sequence has clearly indicated that both *Tetrahymena* Mb genes contain no introns (Korenaga *et al*., 2000). Insofar as the genomic structure is concerned, the *Tetrahymena* globin genes are different from the *Paramecium* globin genes, as well as from the *Chlamydomonas* chloroplast Hb gene. Rather, *Tetrahymena* globin genes seem to be related to the cyanobacterial globin gene, as illustrated in Figure 21.

Concluding Remarks: A Distinct Origin

The functional roles of truncated Hbs are little known. Consequently, various biochemical activities other than the conventional O_2 transport and storage have been proposed so far, since O_2 seems to be diffusible by itself into one-celled organisms. For instance, the protein (trHbN) from *M. tuberculosis* has been related to nitric oxide (NO) detoxification, which is considered to be defensive response to the macrophage nitrosative stress exerted on the bacterium in its latent infection stage (Milani *et al*., 2001). In *Tetrahymena* and *Paramecium* species, however, one

TABLE 5
Molecular properties of truncated globins and their genomic structures

Species	Component	Number of amino acids*	Content of histidine (at position)	Position of intron (with bp)	Genomic analysis
Tetrahymena pyriformis		121	6 His (36, 45, 63, 73, 82, 113)	No intron	Korenaga *et al.*
Tetrahymena thermophila		121	7 His (18, 36, 45, 63, 73, 82, 113)	No intron	(2000)
Paramecium caudatum	A-type	116	2 His (68, 84)	62.3 (23 bp)	Yamauchi *et al.*
Paramecium jenningsi		116	2 His (68, 84)	62.3 (29 bp)	(1992, 1995)
Paramecium triaurelia		116	2 His (68, 84)	62.3 (29 bp)	
Nostoc commune (UTEX 584)		118	5 His (22, 46, 70, 79, 86)	No intron	Potts *et al.* (1992)
Chlamydomonas eugametos	LI637	126 (164**)	4 His (73, 79, 84, 91)	20.3 (181 bp) 58.3 (296 bp) 74.3 (755 bp)	Couture *et al.* (1994)

*The amino acid sequence of Mb was determined by Iwaasa *et al.* (1990) for *T. pyriformis*, by Takagi *et al.* (1993) for *T. thermophila,* and by Iwaasa *et al.* (1989) for *P. caudatum.*

**In the precursor, 38 residues are added at the N-terminus as a transit peptide for the import to chloroplasts.

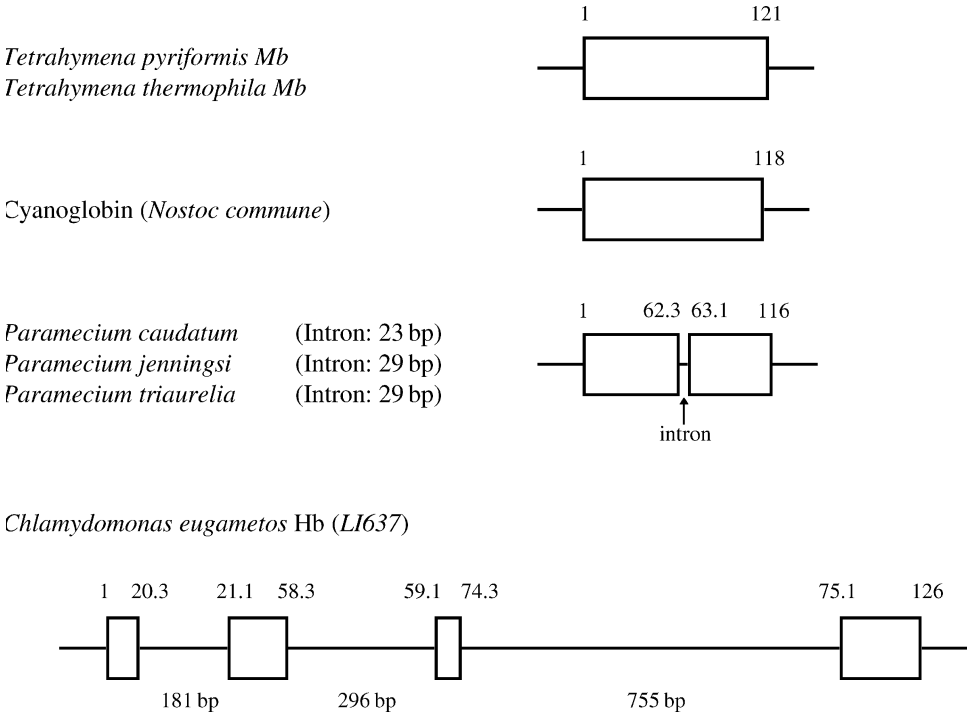

FIG. 21. Structural diversity of the truncated Hb genes from single-celled organisms. The position of the intron is designated by a horizontal line, and the number of 62.3, for example, indicates that the intron is inserted after the third nucleotide of a codon for the amino acid residue at position 62 in the alignment (see Table 5). Redrawn from Korenaga *et al*. (2000).

should recall that these organisms live in full dependence on the ciliary movement, its energy ATP (adenosine triphosphate) being produced mostly by mitochondrial oxidative phosphorylation with very active oxygen consumption. Indeed, electron micrographs clearly indicate that around the basal bodies of cilia, numerous mitochondria are located in a regular array so as to make a characteristic pattern in the cell cortex of *Tetrahymena* as well as in *Paramecium* (Aufderheide, 1979).

Using recombinant *Paramecium* Mb, Das *et al*. (2000) have investigated O_2-binding kinetics at 20°C and pH 7.5, and obtained the rate constants of $k_{on} = 3.01 \times 10^7$ M^{-1} s^{-1} and $k_{off} = 25.2$ s^{-1} that are similar to those of mammalian Mbs (see Equation (2.1) of Section II). In *Tetrahymena* Mb, we have obtained a value of $P_{50} = 0.2$ Torr for the half-saturation O_2 pressure (Korenaga *et al*., 2000). This value is almost comparable to those of $P_{50} = 0.6$ Torr for *Paramecium* MbO_2 (Smith *et al*., 1962) and $P_{50} = 0.51$ Torr for sperm whale MbO_2. In light of such oxygen-binding properties that are similar to mammalian Mbs, the most probable function of ciliate Mbs seems to be the oxygen supply to mitochondria for oxidative phosphorylation. Furthermore, both *Tetrahymena* and *Paramecium* oxymyoglobins show an incredible resistance against heme oxidation; surprisingly, their rates are almost the same as that of sperm whale MbO_2.

We thus conclude that despite the contracted form, protozoan ciliate Mbs have evolved a minimum molecular structure requisite for the reversible oxygen binding. At any rate, the truncated globins found in various single-celled organisms seem to have a distinct origin from other nonvertebrate and vertebrate globins but with marked diversity in their genomic structures.

YEAST FLAVOHEMOGLOBIN FROM *CANDIDA NORVEGENSIS*: AN ENIGMATIC "TWO-DOMAIN" STRUCTURE

Single-Celled Organisms and Flavohemoglobins

In studies of nonvertebrate Mbs and Hbs, we were the first to disclose the very unique structures of a protozoan Mb from *P. caudatum* (Iwaasa *et al*., 1989) and a yeast flavohemoglobin from *Candida norvegensis* (Iwaasa *et al*., 1991, 1992). It is now established that two such different types of globins occur widely in single-celled organisms. A first protein class, referred to as *truncated Hbs*, includes small hemoproteins characterized so far in the protozoan ciliates such as *P. caudatum, T. pyriformis*, and *T. thermophila* (Iwaasa *et al*., 1989, 1990; Korenaga *et al*., 2000), in the unicellular green alga *C. eugametos* (Couture *et al*., 1994), and in the eubacteria such as *N. commune* (Potts

et al., 1992) and *M. tuberculosis* (Couture *et al*., 1999). The second protein group, occurring in bacteria, yeast, and fungi, includes single-chain flavohemoglobins that consist of a N-terminal, heme-containing, oxygen-binding domain and a C-terminal, FAD-containing domain structurally related to NADH or NADPH reductase (Ermler *et al.*, 1995; Ilari *et al*., 2002; Oshino *et al*., 1973a, 1973b; Vasudevan *et al*., 1991; Zhu & Riggs, 1992). Moreover, analysis of the microbial genomic sequences indicates that certain eubacteria, such as *Bacillus subtilis* and *Staphylococcus aureus*, contain both flavohemoglobin and truncated Hb (Pesce *et al*., 2000).

As a matter of course, various biochemical functions have been proposed so far for these ancient hemoproteins, but the precise *in vivo* activity is still unclear. However, recent studies strongly suggest that the most probable role of bacterial flavohemoglobins is in the NO detoxification. In bacteria, NO is a very toxic agent that can be produced by the metabolic reduction of inorganic nitrogen oxides. As to the *Escherichia coli* flavohemoglobin (Hmp), Gardner *et al.* (1998) reported the aerobic conversion of NO to nitrate (NO_3^-). Under anoxic-reducing conditions, this protein was found to bind NO reversibly and to reduce it to NO^-, which resulted in the formation of nitrous oxide (N_2O) *via* a dimeric reaction (Kim *et al*., 1999). These defenses against the nitrosative stress would be analogous to the well-characterized antioxidant systems that protect aerobic organisms from reactive oxygen species.

In baker's yeast, *Saccharomyces cerevisiae,* flavohemoglobin is not always observable, its appearance being dependent largely upon the culture conditions. In another yeast cell, *C. norvegensis*, Oshino *et al.* (1973a) found that flavohemoglobin occurred stably in a large enough amount for isolation and characterization. Taking this advantage, we shall investigate in this section the structural, spectral, and stability properties of *Candida* flavohemoglobin with special focus on the heme iron oxidation (Kobayashi *et al.*, 1995, 2000, 2002). Whatever the possible role of yeast flavohemoglobin may be (or might have been) in, including O_2-buffer, O_2-sensing, O_2^--production, NO-dioxygenation, and oxidative stress response, the reversible binding of molecular oxygen to iron(II) must be the primary event to manifest their physiological functions *in vivo*.

Isolation of *Candida* Flavohemoglobin

The seed cells of *C. norvegensis* (IFO-0734; nonpathogenic) were grown for 30 h at 30°C with constant shaking in a culture medium. The packed cells of 200 g were harvested from the mass culture of 23 l, resuspended in an equal volume of 0.1 M Tris-HCl buffer (pH 7.5) containing 1 mM EDTA, and kept at −80°C until use. The frozen cell suspension was thawed quickly and digested with Zymolyase (β-1,3-glucanase) in the presence of 1 mM PMSF as proteinase inhibitor, and the cells were finally ruptured by sonication. After the lyzed cells were centrifuged down, the supernatant was fractionated with ammonium sulfate between 45 and 75% saturation. The reddish precipitate was then applied to a Butyl-Toyopearl column equilibrated with 1 M $(NH_4)_2SO_4$ in 50 mM Tris-HCl buffer, pH 7.5. After the column was washed with a large volume of the equilibrium solution, elution was made with 50 mM Tris-HCl buffer alone. The resultant Hb solution was further purified by gel filtration on a Sephadex G-75 column.

In our procedures, the essential step was the chromatographic separation of the oxygenated form of yeast Hb on a DEAE-cellulose column, with a linear concentration gradient of Tris-HCl buffer from 5 to 60 mM at pH 7.5. In such elution profile, *Candida* HbO_2 was obtained as two peaks. The first, small peak contained the FAD (flavin adenine dinucleotide)-lacking fraction, while the second, major peak was for the FAD-bound fraction. As for the origin of the FAD-lacking flavohemoglobin, it is not due to a shortage of FAD in the cells. Instead, a large quantity of FAD was released when the Hb extract was subjected to a Butyl-Toyopearl column. As a result, dissociation of the FAD group occurred from *Candida* flavohemoglobin during the course of such a hydrophobic interaction chromatography on Butyl-Toyopearl.

The concentration of *Candida* flavohemoglobin was determined after conversion into cyanomet-form, using an absorption coefficient of 11.2 mM^{-1} cm^{-1} at 540 nm (Kobayashi *et al*., 2002). For each Hb solution, the FAD content was determined, after deproteinized with trichloroacetic acid (TCA), using an absorption coefficient of 10.1 mM^{-1} cm^{-1} at 450 nm. Thus, a value of f_{FAD} = ([FAD]/[Hb]) was defined as the molar ratio of FAD content to the heme iron concentration. Throughout the following description, Hb samples having the values of $f_{FAD} > 0.8$ are referred to as flavohemoglobin (FAD(+)), while those with $f_{FAD} < 0.1$ are used as FAD-lacking flavohemoglobin (FAD(−)).

A "Two-Domain" Structure

Primary Structure. Figure 22 represents the complete amino acid sequence of *Candida* flavohemoglobin. Almost a decade ago, we isolated a Hb-like protein from *C. norvegensis* and found that this flavohemoprotein was composed of 387 amino acid residues with an acetylated serine at the N-terminus and a proline at the C-terminal end (Iwaasa *et al*., 1991, 1992). At the same time, Zhu and Riggs (1992) also characterized a flavohemoglobin from baker's yeast, *S. cerevisiae*. They derived its amino acid sequence of 399 residues from the cDNA analysis. Surprisingly, only 28% sequence similarity was found between *Candida* and *Saccharomyces* flavohemoglobins. More recently, our re-examination of *Candida* flavohemoglobin has revealed

Yeast flavohemoglobin (*Candida norvegensis*)

```
  1                                                                    60
X-SAAKQLFKIV PLTPTEINFL QSLAPVVKEH GVTVTSTMYK YMFQTYPEVR SYFNMTNQKT

 61                                                                   120
 GRQPKVLAFS LYQYILHLND LTPISGFVNQ IVLKHCGLGI KPDQYPVVGE SLVQAFKMVL

121                                                                   180
 GEAADEHFVE VFKKAYGNLA QTLIDAEASV YKTLAWEEFK DFRVTKLVKE AEDVTSVYLT

181                                                                   240
 PVDGFKLKPI IPGEYISFRW DIHNPDITDI QPREYSISQD VKENEYRISV RDIGIVSDYI

241                                                                   300
 NKKLQVGDIV PVHAPVGTMK YDSISKKGKV AVLAGGIGIT PMIPIIEHAL KDGKDVELYY

301                                                                   360
 SNRSYQSEPF REFFSNLEKE NNGKFKLNNY ISAENQKLQV KDLEHINPDE YDVYLLGPVA

361                                389
 YMHEFKTYLV GKGVSDLKME FFGPTDPDC-OH
```

FIG. 22. Complete amino acid sequence of yeast flavohemoglobin from *C. norvegensis*. The single polypeptide chain consists of 389 amino acid residues. Taken from Kobayashi *et al*. (2002).

that the C-terminal Pro is accompanied by the two additional residues of Asp-Cys, so that we must revise the total number of amino acid residues to be 389, as given in Figure 22. Its composition is: 19 Ala, 16 Gln, 31 Leu, 22 Ser, 9 Arg, 27 Glu, 34 Lys, 19 Thr, 17 Asn, 23 Gly, 8 Met, 2 Trp, 23 Asp, 9 His, 20 Phe, 23 Tyr, 2 Cys, 27 Ile, 22 Pro, and 36 Val. This was confirmed by peptide analysis and by cDNA analysis as well (Kobayashi *et al*., 1995).

At any rate, our computer search indicated that the sequence of 155 N-terminal residues has 39% homology with that of a bacterial hemoglobin from *Vitreoscilla* (Wakabayashi *et al.*, 1986). Thus, the N-terminal half of *Candida* Hb seemed to be the heme-containing region that can bind molecular oxygen. On the other hand, the sequence of the remaining 234 C-terminal residues showed a small but notable degree of similarity with that of a metHb reductase found in human red blood cells (Yubisui *et al.*, 1984, 1986). This enzyme is called *NADH-cytochrome b_5 oxidoreductase*, and it is known to have a FAD group that can accept electrons from NADH. In fact, even if yeast flavohemoglobin was oxidized to the ferric met form, it can easily be converted back to the ferrous deoxy form by the addition of NADH, so as to be able to bind molecular oxygen again. In a sense, yeast Hb seems to carry its own "reductase" system within the same molecule. We have thus concluded that *Candida* flavohemoglobin consists of two distinct domains bearing different functions. As depicted in Figure 23, the N-terminal domain is the heme-containing region that binds molecular oxygen, whereas the C-terminal domain may serve as a FAD-containing reductase to convert the former domain from its ferric met form to the ferrous deoxy form in the presence of NADH.

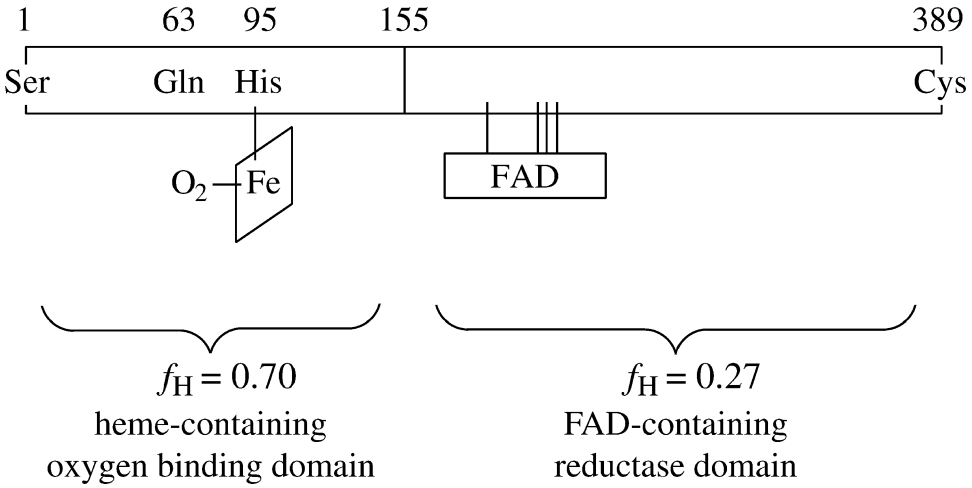

FIG. 23. A structural prediction of *Candida* flavohemoglobin with two distinct domains of different functions. The helical fraction (f_H) was estimated on the basis of CD measurements shown in Figure 25. Redrawn from Kobayashi *et al*. (2002).

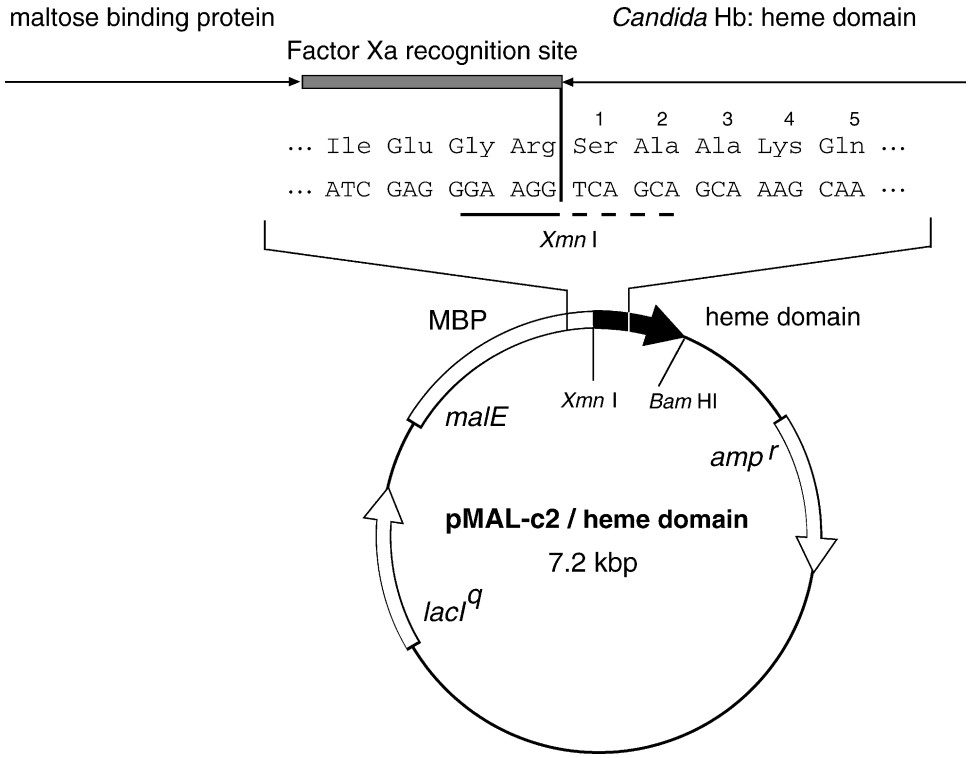

FIG. 24. Construction of a vector pMAL-c2 to express the heme-containing domain of *Candida* flavohemoglobin as a fusion product with maltose-binding protein. The sequence of 155 N-terminal residues is used as the heme domain. Redrawn from Kobayashi *et al*. (2000).

In this prediction, His-95 is assigned to the heme-binding proximal (F8) histidine, while Gln-63 is placed at the distal (E7) position.

Secondary Structure. In relevance to these structural predictions, we have carried out CD measurements of this flavohemoglobin in the far ultraviolet zone. As a result, the mean residue molar ellipticity at 222 nm was found to be $[\theta]^{MRW} = -15{,}000$ deg cm^2 dmol^{-1} in 10 mM buffer, pH 7.2. When compared with a value of $-25{,}400$ deg cm^2 dmol^{-1} for sperm whale Mb, this CD magnitude was surprisingly low, and hence the total helical content was estimated to be 44% or less. In this regard, it was of particular interest to know whether the heme-containing domain carries a common globin-fold or not. Furthermore, if we have the heme-containing region separated from the whole protein, inherent properties of the heme domain of *Candida* flavohemoglobin would be clarified in relevance to other globin molecules. Using plasmid vector pMAL-c2, we have therefore prepared an expression system for the oxygen-binding domain alone in *E. coli* cells.

Expression of the Recombinant Heme Domain. In our construct, the sequence of 155 N-terminal residues of *Candida* flavohemoglobin was designed to be expressed as a fusion product with maltose-binding protein (MBP). The cDNA encoding this heme domain was prepared with a *Xmn*1 site at the 5′ end and a *Bam*H1 site at the 3′ end. As depicted in Figure 24, the gene was ligated into the corresponding restriction sites of pMAL-c2 (New England Biolabs, Inc., Beverly, MA) to construct the expression plasmid, pMAL-c2/heme-domain (7.2 kbp). The expression plasmid was transformed into *E. coli* TB-1 cells, and the cells were grown for 5 h at 37°C in LB (Luria-Bertani) medium containing 100 μg/ml ampicillin and 0.1 mM δ-aminolevulinic acid (ALA). The culture was induced by the addition of isopropyl 1-thio-β-D-galactopyranoside (IPTG), and expression was continued for 10 h with constant shaking. Cells were harvested, washed with 15 mM Tris-HCl buffer (pH 7.5), and kept at -80°C until use. The frozen cells were thawed quickly and sonicated in 2 volumes of 15 mM Tris-HCl buffer (pH 7.5) containing 1 mM EDTA.

The fusion product with MBP was purified from the total lysate by ammonium sulfate fractionation between 30 and 55% saturation, followed by gel filtration on a Sephadex G-75 column, and finally by DEAE-cellulose chromatography. Cleavage between the recombinant protein and MBP was carried out with bovine factor Xa proteinase at 10°C for 24 h. The mixed protein solution was

then subjected to a CM-cellulose column equilibrated with 10 mM Mes-NaOH buffer (pH 6.7) under CO-saturated condition. To protect it from rapid oxidation, the heme domain was finally eluted out completely as the CO-bound form with 30 mM Mes-NaOH buffer at pH 6.7 and immediately stored in liquid nitrogen until use.

The oxygenated species required for autoxidation experiments was produced from the CO form by flash photolysis in O_2-saturated buffer (pH 9.0) and in an ice bath. The concentration of the recombinant heme domain was determined after conversion into cyanomet form, using an absorption coefficient of 10.4 $mM^{-1}cm^{-1}$ at 540 nm.

Domain and Crystal Structures. Figure 25 shows the CD spectra of *Candida* flavohemoglobin and its separated heme-domain in 10 mM buffer, pH 7.2. It thus became evident that the heme-containing domain has a CD magnitude of $-24{,}000$ deg cm^2 $dmol^{-1}$, this being almost identical to that of sperm whale Mb. Consequently, the secondary structure of *Candida* flavohemoglobin may be depicted as follows. In the heme domain, approximately 70% of the residues can exist in a helical conformation. For the remaining FAD-containing domain, its helical content was calculated to be 27% or less. Rather, this region is likely abundant in β-barrel and β-sheet structures, just like that of the bacterial flavohemoglobin from *Alcaligenes eutrophus* whose two-domain structure was already determined at 1.75 Å resolution by Ermler *et al.* (1995). In the *Candida* protein, the probable FAD-binding sites were deduced to be Arg-213, Tyr-215, Ser-216, and Ser-237 based on the sequence comparison with other flavoproteins (Karplus *et al*., 1991; Bredt *et al.*, 1991; Zhu & Riggs, 1992; Ermler *et al.*, 1995).

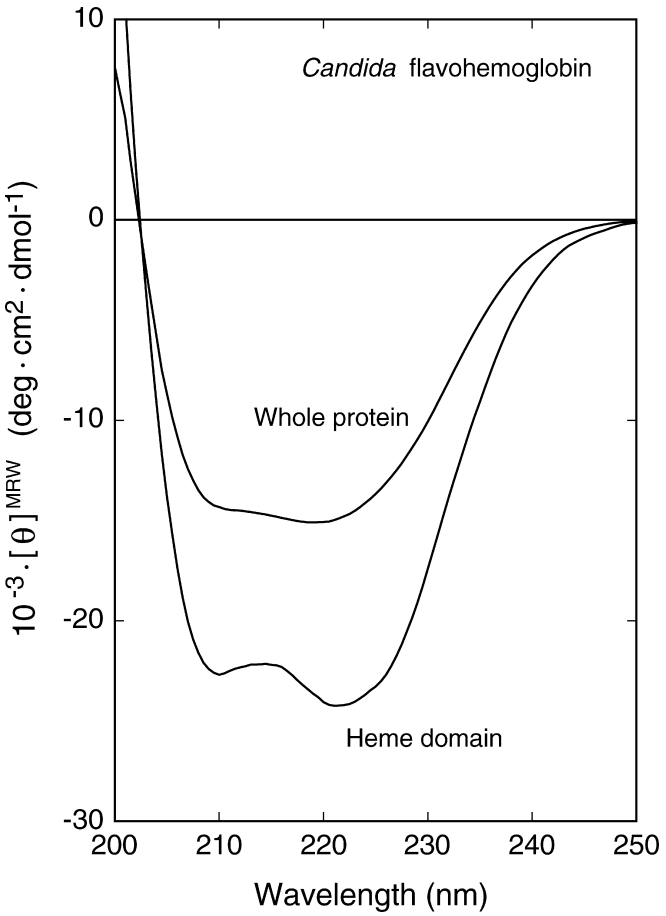

FIG. 25. CD spectrum of *Candida* flavohemoglobin with that of its recombinant heme domain in 10 mM phosphate buffer, pH 7.2. Redrawn from Kobayashi *et al*. (2002).

It should be added here that in *Saccharomyces, Alcaligenes*, and *Escherichia* flavohemoglobins the same pair of Gln-53 and His-85 is aligned to the distal (E7) and proximal (F8) residues, respectively (Zhu & Riggs, 1992; Ermler *et al.,* 1995; Ilari *et al*., 2002). In the *Candida* protein, a different pair of Gln-63 and His-95 corresponds to it. The sequence homology between *Candida* flavohemoglobin and the bacterial proteins from *A. eutrophus* and *E. coli* was 28 and 26%, respectively. Recently, X-ray structure of *E. coli* flavohemoglobin has been solved to 2.2 Å resolution by Ilari *et al*. (2002). They showed that the overall fold of *E. coli* flavohemoglobin (ferric, unliganded) consists of a heart-shaped structure in a manner of positioning the FAD-binding domain at the upper apex, the globin domain on the lower left side, and the NAD-binding domain on the lower right side. They also indicated that the superposition of *E. coli* and *A. eutrophus* flavohemoglobins results in a considerable deviation, despite the high degree of sequence similarity between them. In the *E. coli* protein (Hmp), such a deviation came mainly from a rotation of the NAD-binding module and from a substantial rearrangement of the E helix within the globin domain as well, with respect to the *Alcaligenes* protein.

In view of these structural features, yeast flavohemoglobin is very likely to have been derived from the fusion of two genes, one encoding a globin that binds a heme, and the other encoding a flavoprotein that has a reductase activity. Nevertheless, our comparison of the cDNA and genomic DNA sequences indicated that *Candida* flavohemoglobin contains no introns in it (Kobayashi *et al*., 2002). This result is in good accordance with that of *Saccharomyces* flavohemoglobin by Zhu & Riggs (1992).

Spectral Characterization of *Candida* Flavohemoglobin

Figure 26 represents the absorption spectra of *Candida* flavohemoglobin both in the oxy form (continuous line) and in the acidic met form (broken line). In the oxygenated flavohemoglobin, the α-peak was lower than the β-peak with an absorbance ratio of $\alpha/\beta = 0.76$, this being in

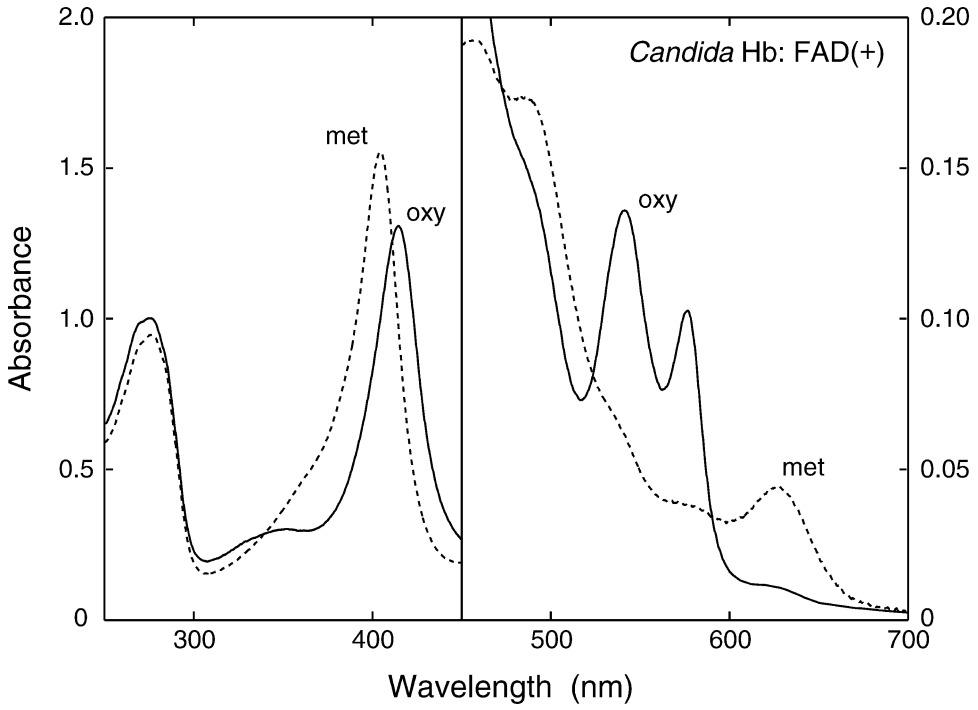

FIG. 26. Absorption spectra of *Candida* flavohemoglobin both in the oxy form (continuous line) and in the ferric met form (broken line). The oxy form was recorded in 10 mM Tris-HCl buffer at pH 7.5, while the met form was in 10 mM phosphate buffer at pH 7.2. The concentration was 10 μM for each form, and the expanded scale was used for visible spectra. Redrawn from Kobayashi *et al*. (2002).

contrast to sperm whale MbO_2 having a value of 1.07. At the same time, a characteristic shoulder appeared at 480 nm, which is indicative of binding of a FAD group (oxidized form). The ultraviolet absorption peak also contains a large contribution from the bound FAD. In fact, this sample had a value of $f_{FAD} = 1.0$. The spectrophotometric parameters of *Candida* flavohemoglobin are summarized in Table 6.

TABLE 6
Spectrophotometric parameters of *Candida* flavohemoglobin

	Absorption maximum (nm) Extinction coefficient (mM^{-1} cm^{-1})				α/β	γ/UV	$\gamma_{met}/\gamma_{oxy}$
oxyHb	α	β	γ	UV			
	576	541	415	275			
	(10.3)	(13.6)	(131)	(100)	0.76	1.31	
metHb	CT^1	CT^2	γ	UV			
	626	—	404	276			
	(4.4)	—	(155)	(94.6)		1.64	1.18

Taken from Kobayashi *et al.* (2002).

The absorption spectra of the FAD-lacking protein ($f_{FAD} = 0.0$) are presented in Figure 27, both in the oxy form and in the ferric met form. Its oxygenated form is almost identical to that of the native FAD-bound protein, except that no shoulder was found at 480 nm. However, the ferric met form was different from that of the FAD-bound protein. In particular, the Soret peak was profoundly blue-shifted and accompanied by a marked decrease in intensity, probably due to a broadening of the spectrum. As a result, the FAD-lacking species showed a value of $\gamma_{met}/\gamma_{oxy} = 0.71$, with a well-developed CT^2 band having maximum intensity of 9.6 mM^{-1} cm^{-1} at 500 nm. The intensity of the CT^1 band was lowered to 2.7 mM^{-1} cm^{-1} at 639 nm. All of these spectral features are characteristic of a pentacoordinate form of ferric high-spin species and are in good accord with our assignment of Gln-63 to the distal E7 position. It follows from these facts that large changes in the heme environment result from loss of the FAD group.

In the native flavohemoglobin (Figure 26), its high value of $\gamma_{met}/\gamma_{oxy} = 1.18$ was decreasing markedly to 0.93 when the temperature was raised to 40°C. This indicates that the vacant-type species could easily be produced from the aqua met form by thermal dissociation of the axial water molecule, as in the case of African elephant Mb having

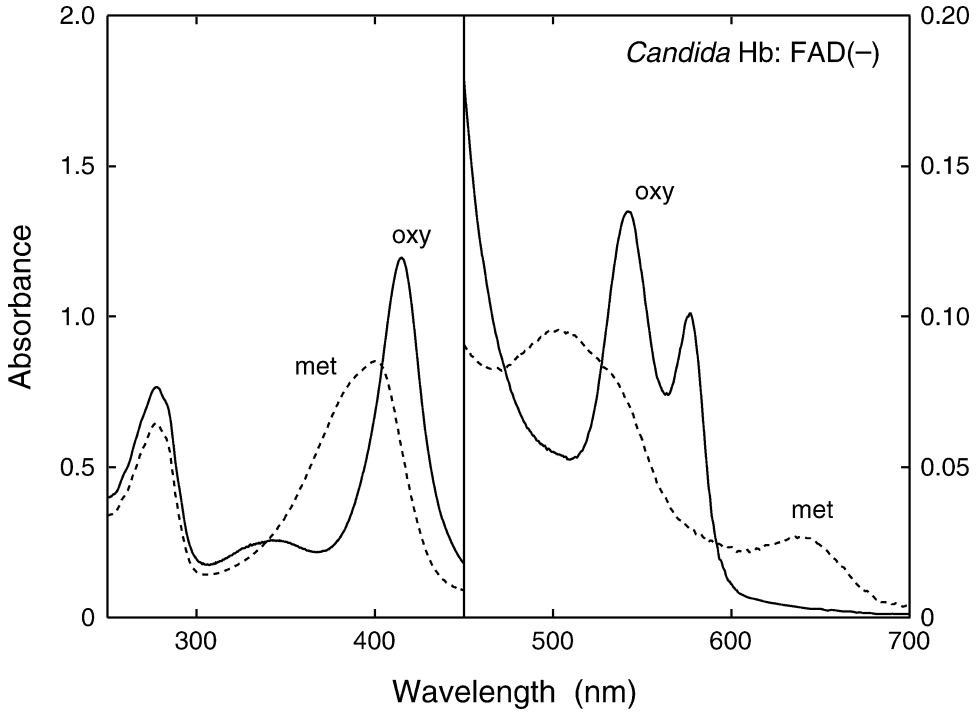

FIG. 27. Absorption spectra of the FAD-lacking flavohemoglobin both in the oxy form (continuous line) and in the ferric met form (broken line). The Soret and CT^2 bands of the ferric met form are characteristic of a pentacoordinate species. The oxy form was recorded in 10 mM Tris-HCl buffer at pH 7.5, while the met form was in 10 mM phosphate buffer at pH 6.0. The concentration was 10 μM for each form, and the expanded scale was used for visible spectra. Redrawn from Kobayashi *et al*. (2002).

Gln-64 as the distal E7 residue (Tada *et al*., 1998). Incidentally, the crystal structure of *Alcaligenes* flavohemoglobin displayed that the sixth coordinate position is vacant in the ferric met form (Ermler *et al*., 1995; Ollesch *et al*., 1999). Similar pentacoordinate structure has been reported in ferric *E. coli* flavohemoglobin as well (Ilari *et al*., 2002).

Stability Properties of *Candida* Flavohemoglobin and Its Heme Domain

Autoxidation. In *Candida* flavohemoglobin, Oshino *et al.* (1973b) reported a value of $P_{50} = 0.01$ Torr for the half-saturation O_2 pressure, but the stability of the heme-bound dioxygen was entirely unknown. This property seems to be of particular importance to consider the possible role of *Candida* flavohemoglobin in relevance to its unique structure. Indeed, the oxygenated form of *Candida* flavohemoglobin is oxidized easily to the ferric met form with generation of the superoxide anion as

$$\mathrm{Hb(II)(O_2)} \overset{k_{\mathrm{obs}}}{\rightharpoonup} \mathrm{metHb(III)} + \mathrm{O_2^-}, \qquad [5.1]$$

where k_{obs} represents the first-order rate constant observed at a given pH value. Accordingly, the rate is given by the following equation:

$$\frac{-\mathrm{d[HbO_2]}}{\mathrm{d}t} = k_{\mathrm{obs}}[\mathrm{HbO_2}]. \qquad [5.2]$$

This process can be monitored by the absorbance changes at α-peak of the oxygenated species (576 nm in the case of *Candida* HbO_2). From the slope of each straight line, the observed first-order rate constant, k_{obs} in h^{-1}, was thus obtained as a most useful measure for the stability of the bound dioxygen.

In 0.1 M buffer at pH 7.2 and 25°C, for instance, its value was 0.24×10^{-1} h^{-1} for *Candida* flavohemoglobin, and 0.26 h^{-1} for the FAD-lacking flavohemoglobin. As a result, *Candida* flavohemoglobin was found to be oxidized somewhat slower than *Paramecium* MbO_2 (0.31×10^{-1} h^{-1}) but several times faster than sperm whale MbO_2 (0.50×10^{-2} h^{-1}). It also becomes evident that a loss of FAD cofactor makes *Candida* flavohemoglobin extremely susceptible to autoxidation with a half-life period ($t_{1/2}$) of 2.6 h. This high oxidation rate was surprising when compared with a value of $t_{1/2} = 29$ h in the FAD-bound native protein. Incidentally, sperm whale MbO_2 was oxidized with a half-life period of 138 h. We have therefore measured the autoxidation rate of *Candida* HbO_2

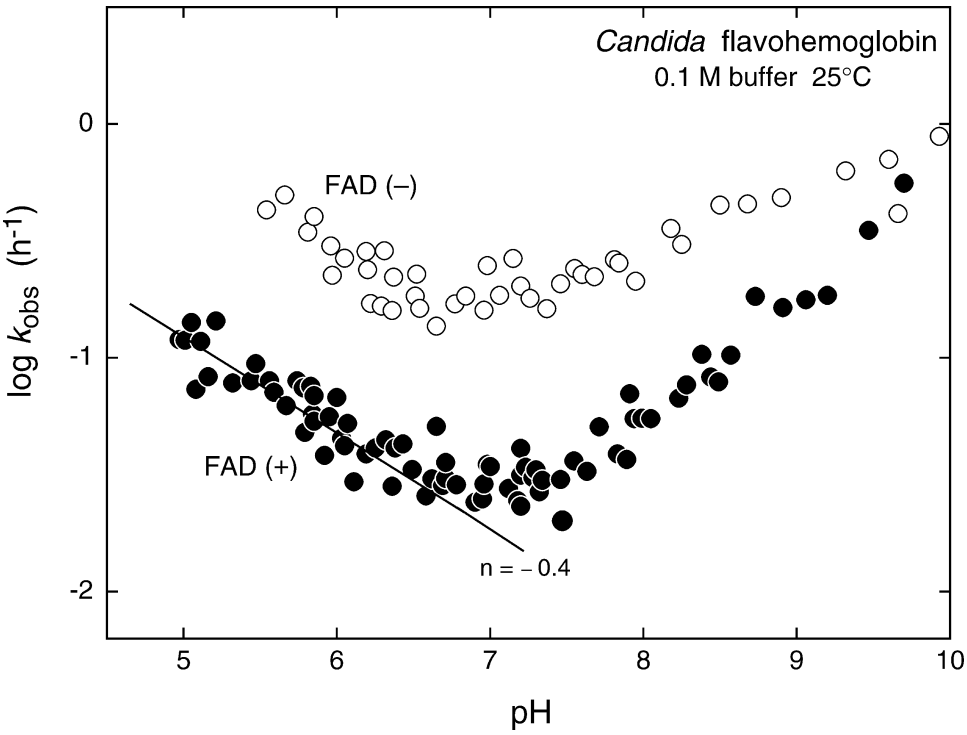

FIG. 28. Plots of log(k_{obs}) *versus* pH for the autoxidation of *Candida* flavohemoglobin and its FAD-lacking species in 0.1 M buffer at 25°C. Rate measurements were carried out with 10 μM protein (as heme) in the presence of 1 mM EDTA. Redrawn from Kobayashi *et al*. (2002).

in 0.1 M buffer at 25°C over a wide range of pH 5–10.

If the values of k_{obs} are plotted against the pH of the solution, a profile of the stability of oxyhemoglobin can be obtained. Figure 28 shows two such profiles, for *Candida* flavohemoglobin and its FAD-lacking species. In the native flavohemoglobin, the rate of autoxidation increased with increasing hydrogen ion concentration, but much less so than in sperm whale MbO_2. In the latter protein, a value close to n = −1 was always found for the slope of log(k_{obs}) *versus* pH, as will be seen again in Figure 29. In *Candida* flavohemoglobin, its slope was less than n = −0.4, exhibiting rather a rate-saturation behavior at extremely low pH values. This is a strong indication that *Candida* flavohemoglobin does not contain any proton-catalyzed process, such as the one that can play a dominant role in the autoxidation reaction of most mammalian oxymyoglobins (or oxyhemoglobins) that have the usual distal (E7) histidine. In *Candida* flavohemoglobin, a minimum rate appeared at pH 7 and a further increase occurred at the higher pH values. At the basic extreme, its rate came up to a level of the FAD-lacking species. Such an abrupt rate increase seemed to result from the concomitant loss of a FAD group from the reductase domain. In fact, the pH at which half of the bound FAD was dissociated from *Candida* flavohemoglobin was 8.6 at 25°C.

At this point, it is of great interest to compare the stability property between the separated heme domain of *Candida* flavohemoglobin and the corresponding sperm whale MbO_2, since both proteins are of a size in amino acid residues (155 and 153, respectively). When the recombinant heme domain was placed in air-saturated buffers, its oxygenated form (with α-peak at 577 nm and α/β-ratio = 0.79) was oxidized very quickly to the final state of run, which was identified as a typical pentacoordinate ferric species. Its Soret peak was profoundly blue shifted and accompanied by a marked decrease in intensity. A very strong CT^2 band also appeared with maximum centered at 505 nm. All such spectral features were similar to the oxidation product of the FAD-lacking flavohemoglobin. In 0.1 M buffer at pH 7.2 and 25°C, for instance, a value of k_{obs} = 0.72 h^{-1} was obtained for the autoxidation rate of the heme domain with a half-life period of $t_{1/2}$ = 58 min.

In this way, a complete pH-profile has been established for the stability of the recombinant heme domain of *Candida* flavohemoglobin in 0.1 M buffer at 25°C. As is clear in Figure 29, the heme domain was extremely susceptible to autoxidation with an unusual pH-dependence. Over the pH range of 7–9, the heme domain was oxidized at an almost constant rate, its value being nearly 1000 times higher than that of sperm whale MbO_2 at pH 9.0. Another

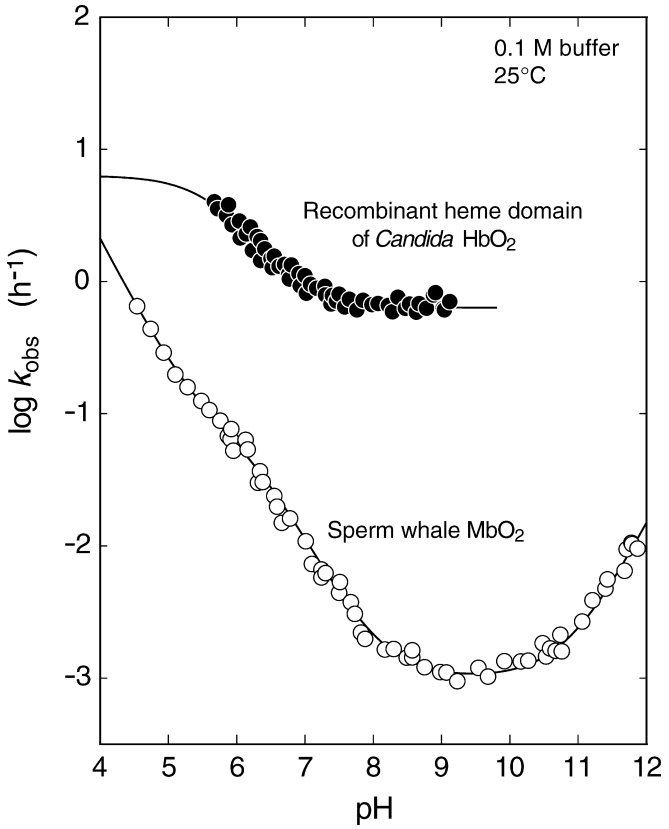

FIG. 29. pH profiles for the stability of the recombinant heme domain of *Candida* flavohemoglobin and the corresponding sperm whale Mb in 0.1 M buffer at 25°C. The computed curve (solid line) was obtained by a least-squares fitting to the experimental points over the whole range of pH studied, based on Equation (2.8) for sperm whale MbO_2 and Equation (5.3) for *Candida* HbO_2, respectively. The protein concentration was 10 μM for *Candida* and 50 μM for sperm whale. Redrawn from Kobayashi *et al*. (2002).

marked difference was also found on the acidic pH side. In sperm whale MbO_2, the rate of autoxidation increases rapidly with increasing hydrogen ion concentration, exhibiting a value close to n = −1 for the slope of $\log(k_{obs})$ *versus* pH. As mentioned previously, this is a definitive indication of the involvement of a very strong acid-catalysis performed by the distal histidine residue (Shikama, 1998; Tsuruga *et al*., 1998; Suzuki *et al,* 2000). In the heme domain alone, the rate also increases with decreasing pH but much less so (n = −0.4) than in sperm whale MbO_2. Rather, the heme domain showed a rate-saturation behavior below pH 6, although the data points could not fully be obtainable because of the protein denaturation at acidic pH extreme.

Kinetic Formulation of the pH Profile. Based on a nucleophilic displacement of O_2^- from the FeO_2 center by an entering water molecule or hydroxyl ion, the pH profile for the autoxidation rate of sperm whale MbO_2 has been formulated completely by an "acid-catalyzed two-state model" involving a single dissociable group (XH) with $pK_1 = 6.2$ (Shikama & Matsuoka, 1986, 1994; Shikama, 1988, 1998). Along with this line of evidence, kinetic formulation was made for the separated heme domain of *Candida* flavohemoglobin. As a result, its pH-dependence could be totally described by the follwing "two-state equation," which contains a single dissociation process (for the group XH with $pK_1 = 5.8$) but no proton-catalyzed process:

$$k_{obs} = \left\{k_0^A[H_2O]\right\}(\alpha) + \left\{k_0^B[H_2O]\right\}(\beta), \qquad [5.3]$$

where

$$\alpha = \frac{[H^+]}{[H^+] + K_1}$$

and

$$\beta = (1 - \alpha) = \frac{K_1}{[H^+] + K_1}. \qquad [5.4]$$

The resulting rate constants and acid dissociation constant involved in the autoxidation reaction of the separated heme domain are summarized in Table 7, with those for sperm whale MbO_2 as a reference. As for the dissociable group XH with $pK_1 = 5.8$, the most probable candidate is a carboxyl group of the heme propionates, just like the case of *Aplysia* MbO_2 lacking the distal histidine residue (Matsuoka & Shikama, 1992).

In essence, the heme domain, if separated from *Candida* flavohemoglobin, undergoes extremely rapid autoxidation. At pH 7.2, for instance, its rate gives a value of $k_{obs} = 0.72\ h^{-1}$ with a half-life period ($t_{1/2}$) of less than 1 h. However, this inherently high oxidation rate was dramatically suppressed in *Candida* flavohemoglobin. Indeed, the half-life period of heme oxidation was prolonged by 2.6 h in the FAD-lacking flavohemoglobin and by up to 29 h in the native flavohemoglobin at pH 7.2. We thus conclude that the binding of FAD as well as the attachment of the reductase domain can produce extensive changes in the distal heme pocket structure of *Candida* Hb so as to block entering water molecules from the FeO_2 center. In this respect, however, we do not know whether the noncovalent presence of the reductase domain would be sufficient or whether the covalent attachment to the heme domain is indispensable. At present, we unfortunately failed to formulate an unusual pH-dependence for the autoxidation rate of *Candida* flavohemoglobin. This is mainly due to the difficulty in including the rate effects caused by the FAD dissociation occurring on the basic pH side. At any rate, the stability of the oxygenated form of *Candida*

TABLE 7
Rate constants and acid dissociation constants obtained from the pH-dependence curves for the autoxidation rate of sperm whale Mb and the recombinant heme domain of *Candida* flavohemoglobin in 0.1 M buffer at 25°C

Source	State of oxy form	k_0 ($h^{-1}M^{-1}$)	k_H ($h^{-1}M^{-2}$)	k_{OH} ($h^{-1}M^{-1}$)	pK_1
Sperm whale	A(XH)	0.78×10^{-4}	0.37×10^{3}	—	
MbO_2	$\Uparrow\Downarrow K_1$				6.2
	$B(X^-)$	0.18×10^{-4}	0.20×10^{4}	0.14×10	
Heme domain of	A(XH)	0.11	—	—	
Candida HbO_2	$\Uparrow\Downarrow K_1$				5.8
	$B(X^-)$	0.11×10^{-1}	—	—	

Taken from Kobayashi *et al.* (2002).

flavohemoglobin is quite different from that of the bacterial flavohemoglobins.

Oxidation-Reduction Cycle. In Mb and Hb molecules, the iron(III) species cannot bind molecular oxygen and is therefore physiologically inactive. In muscle tissues and red blood cells, however, an NADH-cytochrome b_5 oxidoreductase is present that can reduce metMb or metHb to the ferrous form again and thus prevent the continued accumulation of the ferric met-species *in situ*. The enzyme is called *metmyoglobin reductase* (Livingston *et al*., 1985) and *methemoglobin reductase* (Yubisui *et al*., 1984, 1986), respectively, and is known to have a FAD group that can accept electrons from NADH. As a matter of fact, a strong and cyclic reduction of the met form by these enzymes is a basis for the continuity of Mb and Hb functions *in vivo*, since the autoxidation reaction is inevitable in nature for all oxygen-binding heme proteins (Shikama, 1998). From known changes in valency of the heme iron, one can write the functional cycle of Hb as follows:

$$\begin{array}{ccc} \mathrm{HbFe(II)} + \mathrm{O_2} \underset{k_{off}}{\overset{k_{on}}{\rightleftharpoons}} \mathrm{HbFe(II)(O_2)} & & \\ \mathrm{NADH}\nwarrow \qquad\qquad \downarrow \text{autoxidation.} & & [5.5] \\ \mathrm{HbFe(III)} + \mathrm{O_2^-} & & \end{array}$$

In yeast flavohemoglobin, the situation is different. Even if the protein was oxidized to the ferric met form, it can easily be reduced back to the ferrous state by the addition of NADH alone. Figure 30 represents the oxidation and reduction cycles of *Candida* flavohemoglobin, followed up by the absorbance changes at 576 nm (α-peak) in 0.1 M buffer at pH 6.2 and 25°C (Kobayashi *et al*., 2000). At first, *Candida* flavohemoglobin was oxidized gradually to the ferric met-form. When the oxidation reached a 60% level, for example, five equivalents of NADH were added to the solution. The metHb formed was reduced and oxygenated instantaneously to the almost original level of HbO_2. Such reaction cycle could be repeated several times until the globin suffered from denaturation. In the FAD-lacking flavohemoglobin, such an electron transfer from NADH to the ferric heme iron was not observed as a matter of course. In this sense, *Candida* Hb is a molecular system carrying its own reductase within the same molecule.

Concluding Remarks: An Ancient Form of Hemoglobin?

Single-chain flavohemoproteins are now known to occur widely in lower organisms such as bacteria, yeast, and fungi. Among those, bacterial flavohemoglobins have been most extensively studied, and current attention is being paid to the NO detoxification as their function. For yeast flavohemoglobins, on the other hand, little is known about the molecular structure as well as the precise *in vivo* activity. A yeast cell is dozens of times as massive as a bacterial cell, and can grow both in anaerobic and aerobic conditions. When exposed to air, this eukaryotic cell adapts itself to the aerobic form by producing numerous mitochondria in a very short period of time. Thus, a yeast cell changes its energy-yielding process dramatically from fermentation to the oxidative phosphorylation accompanied with very active consumption of molecular oxygen. In *Candida* yeast, more than 65% of the cells are found to be budding out in the logarithmic growth phase. These observations strongly suggest that yeast flavohemoglobin has a different function than the bacterial proteins. Actually, Oshino *et al.* (1973a, 1973b) reported a P_{50} value of 0.01 Torr at pH 7.0 and 23°C. This oxygen affinity was more than fifty times higher than that of sperm whale Mb ($P_{50} = 0.51$ Torr), but was almost equal to that of cytochrome *c* oxidase. From this viewpoint, they suggested that one of the

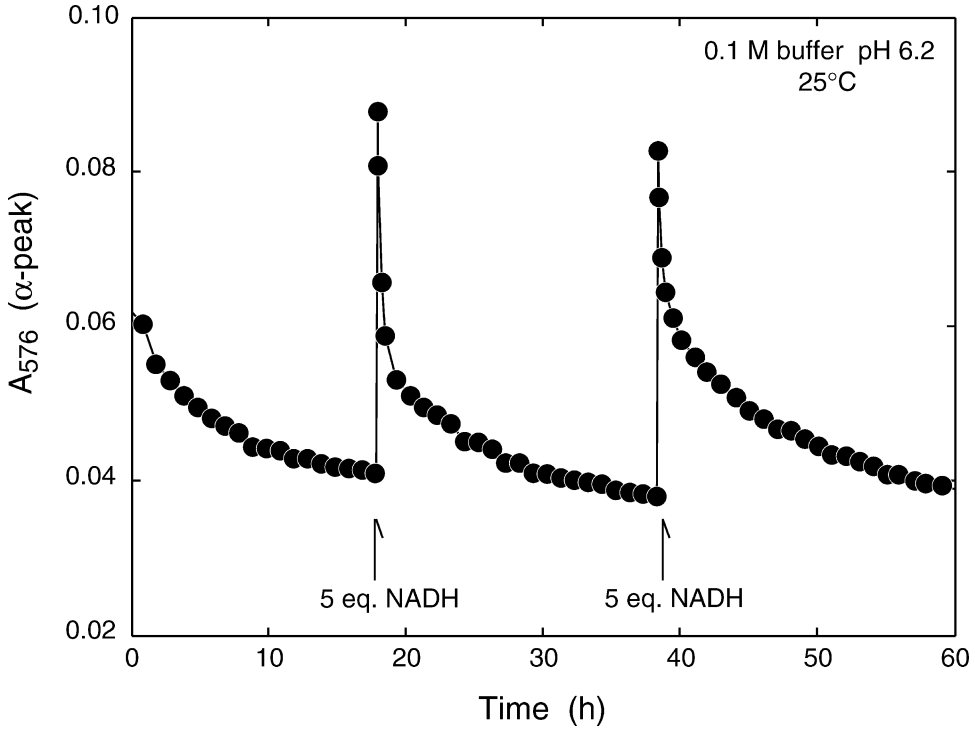

FIG. 30. The oxidation and reduction cycles of *Candida* flavohemoglobin by the addition of NADH in 0.1 M Bis-Tris buffer at pH 6.2 and 25°C. The HbO_2 level was followed up by the absorbance changes at 576 nm for the α-peak. Hb concentration: 10 μM. Redrawn from Kobayashi *et al*. (2000).

possible functions was in an "oxygen buffer" to the respiratory chain of mitochondria.

In this section, we have revealed that the heme domain, if separated from *Candida* flavohemoglobin, becomes extremely susceptible to autoxidation over the whole range of pH studied. At pH 7.2, for instance, its oxidation rate was more than 100 times higher than that of the corresponding sperm whale MbO_2. Consequently, this oxidation rate would be too fast for the protein to play a role in oxygen buffer or oxygen storage. However, a very unique structure of *Candida* flavohemoglobin tells us another strategy to overcome many difficulties in the reversible and stable binding of molecular oxygen, as opposed to the irreversible oxidation of heme iron(II) in aqueous environment. In view of the correspondence of yeast and bacterial flavohemoglobins, Zhu and Riggs (1992) remarked that the two-domain structure has been conserved intact for as long as 1.8 billion years, the estimated time of divergence of prokaryotes and eukaryotes.

At all rates, our kinetic results presented here clearly indicate that *Candida* yeast flavohemoglobin, differently from bacterial flavohemoglobins, can serve as an oxygen storage protein in aerobic condition. This conclusion does not always rule out additional functions, since the autoxidation rate of *Candida* flavohemoglobin is much too slow to interfere with catalytic activities such as NO dioxygenase activity.

CONCLUSION: EVOLUTIONARY IMPLICATIONS

In supporting living organisms on the earth, hemoproteins play a vital role in various life processes. These include the transport and storage of molecular oxygen by Hb and by Mb, the transfer of electrons from respiratory substrates by cytochromes and the terminal oxidation with O_2 by cytochrome *c* oxidase, the decomposition of hydrogen peroxide by catalase, the oxidation of organic substances with H_2O_2 by peroxidase, the hydroxylation of organic substances through dioxygenation by cytochrome P-450, the synthesis of NO from L-Arg by NO synthase, and so forth. As a matter of fact, all of these different functions are based primarily upon the oxidation-reduction properties of the heme iron in itself. Accordingly, it is not so much a surprise that various biochemical functions other than the conventional oxygen transport or storage have been proposed so far for primitive Hbs or Mbs, including O_2 buffer, O_2 sensing, O_2^- production, NO fixation or detoxification, terminal oxidation, and photosynthesis (Couture *et al*., 1999; Kobayashi *et al*., 2002).

In the present review, special emphasis has been placed on the stability properties of the bound dioxygen. Whatever the possible roles of nonvertebrate Mbs and Hbs may be (or might have been), the binding of molecular oxygen to iron(II) must be the primary event to manifest their physiological functions *in vivo*. However, the reversible and stable binding of molecular oxygen to iron(II) is not a simple process. Recent kinetic and thermodynamic studies have revealed that the FeO_2 center of Mb or Hb is always subjected to the nucleophilic attack of an entering water molecule, usually accompanied with a very strong acid-catalysis performed by the distal (E7) histidine residue. The FeO_2 center is also open to the attack of an entering hydroxide anion on the basic pH side. These reactions can cause irreversible displacement of the bound dioxygen in the form of O_2^- so that the iron is converted to the ferric met form.

In a protein-free system, the simple heme compounds are known to undergo an extremely rapid oxidation by O_2, almost within seconds or minutes at ambient temperature. In aqueous solution, Mb and Hb have thus evolved with a globin moiety that can protect the FeO_2 center from easy access of a water molecule (including its conjugate ions OH^- and H^+), as illustrated in Figure 31. In the figure, the distal (E7) histidine is also proposed to play a crucial role in controlling the stability of the bound dioxygen. In these native proteins, however, the globin moiety has still not attained maximal ability to block entering water molecules from the FeO_2 center. Nevertheless, the relative stability of the oxygenated forms, in protic aqueous solution and at physiological temperature, provides the basis for the Mb and Hb functions *in vivo* and differentiates these naturally occurring oxygen carriers from simple heme compounds. This functional stability of Mb or Hb is lost easily by protein denaturation such as in 8 M urea (Sugawara *et al*., 1995). Accordingly, their stability must be linked to the integrity of the native conformation of the globin moiety. In the molecular evolution from simple ferrous complexes to Mb and Hb molecules, we thus conclude that the protein matrix can act as a breakwater of the FeO_2 bonding in aqueous environment (Shikama, 1988, 1998).

In considering such an evolutionary pathway, the occurrence of two different types of plant Hbs may be very suggestive. In contrast to symbiotic leghemoglobins having a traditional pentacoordinate structure similar to Mb, the more recently discovered nonsymbiotic plant Hbs are still a mystery with the heme group coordinated by the distal histidine also. These hexacoordinate proteins cannot facilitate oxygen transport accordingly. Although these proteins are not yet fully understood, Kundu *et al*. (2003) have pointed out that nonsymbiotic hemoglobins predate leghemoglobins, which evolved later in response to the special need for oxygen transport and scavenging in legumes. Consequently, hexacoordinate Hbs in general appear to be of more ancient origin than the pentacoordinate Hbs. In this respect, they also suggested that red blood cell Hb and muscle Mb could well have originated from a hexacoordinate form in a similar evolutionary adaptation (Kundu *et al*., 2003).

At any rate, the very unique structures of protozoan Mb and yeast flavohemoglobin tell us their own different strategies to overcome many difficulties in the reversible and stable binding of molecular oxygen, as opposed to the irreversible oxidation of heme iron(II) in protic, aqueous environment. Despite a shortened structure, on one hand, *Tetrahymena* and *Paramecium* Mbs are quite resistant to heme oxidation, their rates being almost comparable to that of sperm whale MbO_2. Consequently, protozoan ciliates

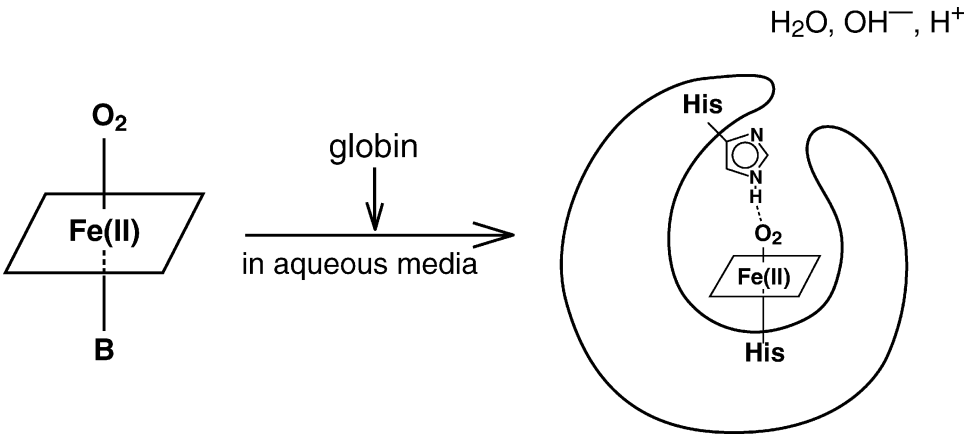

FIG. 31. From simple ferrous complexes to the proteins. Mb and Hb have evolved with a globin moiety that can obstruct access of a water molecule (including its conjugate ions) to the FeO_2 center. The distal (E7) histidine is proposed to participate, *via* its imidazole ring and by a proton-relay mechanism, in controlling the movement of a catalytic proton from the solvent to the coordinated dioxygen. The distal histidine can also stabilize the dioxygen by hydrogen bond formation. Redrawn from Shikama (1988).

must have evolved a globin of minimum molecular structure requisite for its function. In this way, the truncated globins seem to have a distinct origin, although a marked diversity is found in their genomic structures. On the other hand, yeast flavohemoglobin is a molecular system carrying its own reductase domain within the same molecule. In view of the correspondence of yeast and bacterial flavohemoglobins, Zhu and Riggs (1992) remarked that the two-domain structure has been conserved intact for as long as 1.8 billion years, the estimated time of divergence of prokaryotes and eukaryotes.

By the difference-matrix method for amino acid sequences, Dickerson and Geis (1983) indicated that invertebrate globins differ from one another and from all the vertebrate Mbs and Hbs. They also remarked that the vertebrates developed two specialized genes; one for an oxygen-storing Mb, and the other for an oxygen-carrying Hb monomer that later specialized further into genes for α and β chains, leading to the formation of $\alpha_2\beta_2$ tetramer. With recent advances in the field of bioinformatics, we are now in a position to be able to construct easily a phylogenetic tree for any particular class of proteins of interest using suitable programs (such as ClustalW and PAUP) provided on web sites. In this way, Hardison (1998) generated the aligned amino acid sequences of selected Hbs from mammals, invertebrates, plants, protists, fungi, and bacteria and has established a phylogenetic tree of Hbs with the diversity of their proposed functions and regulation. Taking into consideration the intron/exon structures, he also illustrated the Hb gene evolution from bacteria to man.

For the nonvertebrate globins, however, we are still not certain whether their genes evolved from a single, ancestral globin gene, or from the gene(s) for some different but related protein(s) that almost all lines possessed—for instance, cytochromes as the hexacoordinate electron-transferring protein. The horizontal transfer of globin gene was not easy in higher organisms, but it may have been possible in single-celled organisms including bacteria, yeast, algae, and protozoa if they had globins retained to survive the aerobic conditions.

The stabilization of molecular oxygen for transport and storage and the activation of oxygen for use in terminal oxidation are reciprocal but essential functions that support living organisms on the earth. Since the autoxidation reaction of MbO_2 or HbO_2 proceeds through a nucleophilic displacement following one-electron transfer from iron(II) to the bound O_2, this reaction may be viewed as a meeting point of the stabilization and the activation of molecular oxygen performed by hemoproteins (Shikama, 1990). In fact, the heme oxidation is inevitable in nature for all oxygen-binding heme proteins (Shikama, 1998). Thus, the present new views on the nature of FeO_2 bonding and the possible role of globin moiety in stabilizing MbO_2 and HbO_2 provide us with an insight into general principles governing the hemoprotein reactions with O_2 in biological oxidations.

ACKNOWLEDGEMENTS

The materials of our previous publications were used with permission from Publishers, including the following: American Society for Biochemistry and Molecular Biology, Inc. to *J Biol Chem*; Blackwell Publishing Ltd. to *Eur J Biochem*; Cambridge University Press to *Biol Rev*; Elsevier Science Ltd. (Global Rights Department) to *Biochim Biophys Acta*, *Coord Chem Rev*, *Int J Biochem Cell Biol*, and *J Mol Biol*.

REFERENCES

Akiyama, K., Fukuda, M., Kobayashi, N., Matsuoka, A., and Shikama, K. 1994. The pH-dependent swinging-out of the distal histidine residue in ferric hemoglobin of a midge larva (*Tokunagayusurika akamusi*). *Biochim Biophys Acta* **1208:**306–309.

Aufderheide, K. 1979. Mitochondrial associations with specific microtubular components of the cortex of *Tetrahymena thermophila*. I. Cortical patterning of mitochondria. *J Cell Sci* **39:**299–312.

Blanchetot, A., Wilson, V., Wood, D., and Jeffreys, A.J. 1983. The seal myoglobin gene: an unusually long globin gene. *Nature (London)* **301:**732–734.

Bolognesi, M., Coda, A., Gatti, G., Ascenzi, P., and Brunori, M. 1985. Crystal structure of ferric *Aplysia limacina* myoglobin at 2.0 Å resolution. *J Mol Biol* **183:**113–115.

Bolognesi, M., Onesti, S., Gatti, G., Coda, A., Ascenzi, P., and Brunori, M. 1989. *Aplysia limacina* myoglobin: crystallographic analysis at 1.6 Å resolution. *J Mol Biol* **205:**529–544.

Brantley, R.E., Jr., Smerdon, S.J., Wilkinson, A.J., Singleton, E.W., and Olson, J.S. 1993. The mechanism of autooxidation of myoglobin. *J Biol Chem* **268:**6995–7010.

Bredt, D.S., Hwang, P.M., Glatt, C.E., Lowenstein, C., Reed, R.R., and Snyder, S.H. 1991. Cloned and expressed nitric oxide synthase structurally resembles cytochrome P-450 reductase. *Nature* (*London*) **351:**714–718.

Burmester, T. and Hankeln, T. 1999. A globin gene of *Drosophila melanogaster*. *Mol Biol Evol* **16:**1809–1811.

Couture, M., Chamberland, H., St-Pierre, B., Lafontaine, J., and Guertin, M. 1994. Nuclear genes encoding chloroplast hemoglobins in the unicellular green alga *Chlamydomonas eugametos*. *Mol Gen Genet* **243:**185–197.

Couture, M., Yeh, S.-R., Wittenberg, B.A., Wittenberg, J.B., Ouellet, Y., Rousseau, D.L., and Guertin, M. 1999. A cooperative oxygen-binding hemoglobin from *Mycobacterium tuberculosis*. *Proc Natl Acad Sci USA* **96:**11223–11228.

Das, T.K., Weber, R.E., Dewilde, S., Wittenberg, J.B., Wittenberg, B.A., Yamauchi, K., Van Hauwaert, M.-L., Moens, L., and Rousseau, D.L. 2000. Ligand binding in the ferric and ferrous states of *Paramecium* hemoglobin. *Biochemistry* **39:**14330–14340.

Di Iori, E.E., Tavernelli, I., and Yu, W. 1997. Dynamic properties of monomeric insect erythrocruorin III from *Chironomus thummi*

thummi: relationships between structural flexibility and functional complexity. *Biophys J* **73:**2742–2751.

Dickerson, R.E. and Geis, I. 1983. *Hemoglobin*: *Structure*, *Function*, *Evolution*, *and Pathology*. The Benjamin/Cummings Publishing Co., Inc. Menlo Park, CA.

Ermler, U., Siddiqui, R.A., Cramm, R., and Friedrich, B. 1995. Crystal structure of the flavohemoglobin from *Alcaligenes eutrophus* at 1.75 Å resolution. *EMBO J* **14:**6067–6077.

Fermi, G. and Perutz, M.F. 1981. Haemoglobin and myoglobin. In *Atlas of Molecular Structures in Biology*, 2nd ed., pp. 46–47. D.C. Phillips and F.M. Richards, Eds., Clarendon Press, Oxford.

Fukuda, M., Takagi, T., and Shikama, K. 1993. Polymorphic hemoglobin from a midge larva (*Tokunagayusurika akamusi*) can be divided into two different types. *Biochim Biophys Acta* **1157:**185–191.

Gardner, P.R., Gardner, A.M., Martin, L.A., and Salzman, A.L. 1998. Nitric oxide dioxygenase: an enzymic function for flavohemoglobin. *Proc Natl Acad Sci USA* **95:**10378–10383.

Ghiretti-Magaldi, A., Salvato, B., Tallandini, L., and Beltramini, M. 1979. The hemocyanin of *Aplysia limacina*: chemical and functional characterization. *Comp Biochem Physiol* **62A:**579–584.

Giacometti, G.M., Ascenzi, P., Brunori, M., Rigatti, G., Giacometti, G., and Bolognesi, M. 1981. Absence of water at the sixth co-ordination site in ferric *Aplysia* myoglobin. *J Mol Biol* **151:**315–319.

Gotoh, T. and Shikama, K. 1976. Generation of the superoxide radical during autoxidation of oxymyoglobin. *J Biochem (Tokyo)* **80:**397–399.

Hankeln, T., Rozynek, P., and Schmidt, E.R. 1988. The nucleotide sequence and *in situ* localization of a gene for a dimeric haemoglobin from the midge *Chironomus thummi piger*. *Gene* **64:**297–304.

Hardison, R. 1998. Hemoglobins from bacteria to man: evolution of different patterns of gene expression. *J Exp Biol* **201:**1099–1117.

Huber, R., Epp, O., Steigemann, W., and Formanek, H. 1971. The atomic structure of erythrocruorin in the light of the chemical sequence and its comparison with myoglobin. *Eur J Biochem* **19:**42–50.

Ilari, A., Bonamore, A., Farina, A., Johnson, K.A., and Boffi, A. 2002. The X-ray structure of ferric *Escherichia coli* flavohemoglobin reveals an unexpected geometry of the distal heme pocket. *J Biol Chem* **277:**23725–23732.

Irie, T. and Usuki, I. 1980. Disparity of native oxyhemoglobin components isolated from *Paramecium caudatum* and *Paramecium primaurelia. Comp Biochem Physiol* **67B:**549–554.

Iwaasa, H., Takagi, T., and Shikama, K. 1989. Protozoan myoglobin from *Paramecium caudatum*. Its unusual amino acid sequence. *J Mol Biol* **208:**355–358.

Iwaasa, H., Takagi, T., and Shikama, K. 1990. Protozoan hemoglobin from *Tetrahymena pyriformis*: isolation, characterization, and amino acid sequence. *J Biol Chem* **265:**8603–8609.

Iwaasa, H., Takagi, T., and Shikama, K. 1991. Amino acid sequence of hemoglobin from yeast (*Candida norvegensis*). *Zool Sci* (*Tokyo*) **8:**1134.

Iwaasa, H., Takagi, T., and Shikama, K. 1992. Amino acid sequence of yeast hemoglobin: A two-domain structure. *J Mol Biol* **227:**948–954.

Johnson, K.A., Olson, J.S., and Phillips, G.N., Jr., 1989. Structure of myoglobin-ethylisocyanide: histidine as a swinging door for ligand entry. *J Mol Biol* **207:**459–463.

Kamimura, S., Matsuoka, A., Imai, K., and Shikama, K. 2003. The swinging movement of the distal histidine residue and the autoxidation reaction for midge larval hemoglobins. *Eur J Biochem* **270:**1424–1433.

Karplus, M. and McCammon, J.A. 1986. The dynamics of proteins. *Sci Am* **254:**30–39.

Karplus, P.A., Daniels, M.J., and Herriott, J.R. 1991. Atomic structure of ferredoxin-NADP$^+$ reductase: prototype for a structurally novel flavoenzyme family. *Science* **251:**60–66.

Keilin, D. and Ryley, J.F. 1953. Haemoglobin in protozoa. *Nature* (*London*) **172:**451.

Kim, S.O., Orii, Y., Lloyd, D., Hughes, M.N., and Poole, R.K. 1999. Anoxic function for the *Escherichia coli* flavohaemoglobin (Hmp): reversible binding of nitric oxide and reduction to nitrous oxide. *FEBS Lett* **445:**389–394.

Kobayashi, G., Matsuoka, A., Takagi, T., and Shikama, K. 1995. A structural prediction of yeast hemoglobin by CD measurements. *Physiol Zool* **68**(4):82.

Kobayashi, G., Nakamura, T., Ohmachi, H., Matsuoka, A., Ochiai, T., and Shikama, K. 2002. Yeast flavohemoglobin from *Candida norvegensis*: its structural, spectral, and stability properties. *J Biol Chem* **277:**42540–42548.

Kobayashi, G., Ohmachi, H., Nakamura, T., Matsuoka, A., and Shikama, K. 2000. Yeast flavohemoglobin from *Candida norvegensis*. In *Proceedings of the XIIth International Conference on Invertebrate Dioxygen Binding Proteins*, Chap. 11, pp. 1–6. F.H. Lallier, F. Zal, and A. Toulmond, Eds., Roscoff City, France.

Korenaga, S., Igarashi, J., Matsuoka, A., and Shikama, K. 2000. A primitive myoglobin from *Tetrahymena pyriformis*: its heme environment, autoxidizability, and genomic DNA structure. *Biochim Biophys Acta* **1543:**131–145.

Korenaga, S., Miki, K., and Shikama, K. 1996. A myoglobin-like protein from *Tetrahymena pyriformis*: Isolation and characterization. *Eur J Protistol* **32**(Suppl. I):73–78.

Kundu, S., Trent, J.T. III, and Hargrove, M.S. 2003. Plants, humans and hemoglobins. *Trends Plant Sci* **8:**387–393.

Livingston, D.J., McLachlan, S.J., La Mar, G.N., and Brown, W.D. 1985. Myoglobin: cytochrome b_5 interactions and the kinetic mechanism of metmyoglobin reductase. *J Biol Chem* **260:**15699–15707.

Matsuoka, A. and Shikama, K. 1988. *Aplysia* oxymyoglobin with an unusual stability property: involvement of two kinds of carboxyl groups. *Biochim Biophys Acta* **956:**127–132.

Matsuoka, A., Kobayashi, N., and Shikama, K. 1992. The Soret magnetic circular dichroism of ferric high-spin myoglobins. A probe for the distal histidine residue. *Eur J Biochem* **210:**337–341.

Matsuoka, A. and Shikama, K. 1992. Stability properties of *Aplysia* oxymyoglobin: effect of esterification of the heme propionates. *Biochim Biophys Acta* **1118:**123–129.

Milani, M., Pesce, A., Ouellet, Y., Ascenzi, P., Guertin, M., and Bolognesi, M. 2001. *Mycobacterium tuberculosis* hemoglobin N displays a protein tunnel suited for O_2 diffusion to the heme. *EMBO J* **20:**3902–3909.

Nei, M., Stephens, J.C., and Saitou, N. 1985. Methods for computing the standard errors of branching points in an evolutionary tree and their application to molecular data from humans and apes. *Mol Biol Evol* **2:**66–85.

Ollesch, G., Kaunzinger, A., Juchelka, D., Schubert-Zsilavecz, M., and Ermler, U. 1999. Phospholipid bound to the flavohemoprotein from *Alcaligenes eutrophus*. *Eur J Biochem* **262:**396–405.

Oshino, R., Asakura, T., Takio, K., Oshino, N., Chance, B., and Hagihara, B. 1973b. Purification and molecular properties of yeast hemoglobin. *Eur J Biochem* **39:**581–590.

Oshino, R., Oshino, N., Chance, B., and Hagihara, B. 1973a. Studies on yeast hemoglobin. The properties of yeast hemoglobin and its physiological function in the cell. *Eur J Biochem* **35:**23–33.

Pande, U., La Mar, G.N., Lecomte, J.T.J., Ascoli, F., Brunori, M., Smith, K.M., Pandey, R.K., Parish, D.W., and Thanabal, V. 1986. NMR study of the molecular and electronic structure of the heme cavity of *Aplysia* metmyoglobin. Resonance assignments based on isotope labeling and proton nuclear overhauser effect measurements. *Biochemistry* **25:**5638–5646.

Pesce, A., Couture, M., Dewilde, S., Guertin, M., Yamauchi, K., Ascenzi, P., Moens, L., and Bolognesi, M. 2000. A novel two-over-two α-helical sandwich fold is characteristic of the truncated hemoglobin family. *EMBO J* **19:**2424–2434.

Phillips, S.E.V. and Schoenborn, B.P. 1981. Neutron diffraction reveals oxygen-histidine hydrogen bond in oxymyoglobin. *Nature* (*London*) **292:**81–82.

Potts, M., Angeloni, S.V., Ebel, R.E., and Bassam, D. 1992. Myoglobin in a cyanobacterium. *Science* **256:**1690–1692.

Quillin, M.L., Arduini, R.M., Olson, J.S., and Phillips, G.N., Jr. 1993. High-resolution crystal structures of distal histidine mutants of sperm whale myoglobin. *J Mol Biol* **234:**140–155.

Rifkind, J.M., Abugo, O., Levy, A., and Heim, J. 1994. Detection, formation and relevance of hemichromes and hemochromes. *Methods in Enzymol* **231:**449–480.

Rossi-Fanelli, A. and Antonini, E. 1957. A new type of myoglobin isolated and crystallized from the muscles of *Aplysiae*. *Biochimia* (*USSR*) **22:**336–344.

Rozynek, P., Hankeln, T., and Schmidt, E.R. 1988. Structure of a hemoglobin gene cluster and nucleotide sequence of three hemoglobin genes from the midge *Chironomus thummi piger* (Diptera, Insecta). *Biol Chem Hoppe-Seyler* **370:**533–542.

Sato, T. and Tamiya, H. 1937. Über die Atmungsfarbstoffe von *Paramecium*. *Cytologia* **Fujii Jubilee volume**:1133–1138.

Scott, E.E., Gibson, Q.H., and Olson, J.S. 2001. Mapping the pathways for O_2 entry into and exit from myoglobin. *J Biol Chem* **276:**5177–5188.

Shikama, K. 1984. A controversy on the mechanism of autoxidation of oxymyoglobin and oxyhaemoglobin: oxidation, dissociation, or displacement? *Biochem J* **223:**279–280.

Shikama, K. 1988. Stability properties of dioxygen-iron(II) porphyrins: an overview from simple complexes to myoglobin. *Coord Chem Rev* **83:**73–91.

Shikama, K. 1990. Autoxidation of oxymyoglobin: a meeting point of the stabilization and the activation of molecular oxygen. *Biol Rev* (*Cambridge*) **65:**517–527.

Shikama, K. 1998. The molecular mechanism of autoxidation for myoglobin and hemoglobin: a venerable puzzle. *Chem Rev* **98:**1357–1373.

Shikama, K. and Katagiri, T. 1984. *Aplysia* oxymyoglobin with an unusual stability property. *J Mol Biol* **174:**697–704.

Shikama, K. and Matsuoka, A. 1986. *Aplysia* oxymyoglobin with an unusual stability property: kinetic analysis of the pH dependence. *Biochemistry* **25:**3898–3903.

Shikama, K. and Matsuoka, A. 1989. Spectral properties unique to the myoglobins lacking the usual distal histidine residue. *J Mol Biol* **209:**489–491.

Shikama, K. and Matsuoka, A. 1994. *Aplysia* myoglobin with unusual properties: another prototype in myoglobin and haemoglobin biochemistry. *Biol Rev (Cambridge)* **69:**233–251.

Shikama, K., Matsuoka, A., and Iwaasa, H. 1995. The unique structures of protozoan myoglobin and yeast hemoglobin: an evolutionary diversity. *Int J Biochem Cell Biol* **27:**1107–1115.

Shikama, K., Suzuki, T., Sugawara. Y., Katagiri, T., Takagi, T., and Hatano, M. 1982. *Aplysia* myoglobin with an unusual heme environment. *Biochim Biophys Acta* **701:**138–141.

Shiro, Y. and Morishima, I. 1984. Modification of the heme distal side in myoglobin by cyanogen bromide. Heme environmental structures and ligand binding properties of the modified myoglobin. *Biochemistry* **23:**4879–4884.

Smith, M.H., George, P., and Preer, J.R., Jr. 1962. Preliminary observations on isolated *Paramecium* hemoglobin. *Arch Biochem Biophys* **99:**313–318.

Springer, B.A., Sligar, S.G., Olson, J.S., and Phillips, G.N., Jr. 1994. Mechanisms of ligand recognition in myoglobin. *Chem Rev* **94:**699–714.

Steers, E., Jr. and Davis, R.H., Jr. 1979. Purification and characterization of the myoglobins of *Paramecium tetraurelia*. *Comp Biochem Physiol* **62B:**393–402.

Steigemann, W. and Weber, E. 1979. Structure of erythrocruorin in different ligand states refined at 1.4Å resolution. *J Mol Biol* **127:**309–338.

Sugawara, Y., Matsuoka, A., Kaino, A., and Shikama, K. 1995. Role of globin moiety in the autoxidation reaction of oxymyoglobin: effect of 8 M urea. *Biophys J* **69:**583–592.

Suzuki, T. 1986. Amino acid sequence of myoglobin from the mollusc *Dolabella auricularia*. *J Biol Chem* **261:**3692–3699.

Suzuki, T. 1987. Autoxidation of oxymyoglobin with the distal (E7) glutamine. *Biochim Biophys Acta* **914:**170–176.

Suzuki, T., Muramatsu, R., Kisamori, T., and Furukohori, T. 1988. Myoglobin of the shark *Galeus nipponensis*: identification of the exceptional amino acid replacement at the distal (E7) position and autoxidation of its oxy-form. *Zool Sci* **5:**69–76.

Suzuki, T., Takagi, T., and Shikama, K. 1981. Amino acid sequence of myoglobin from *Aplysia kurodai*. *Biochim Biophys Acta* **669:**79–83.

Suzuki, T., Watanabe, Y.-h., Nagasawa, M., Matsuoka, A., and Shikama, K. 2000. Dual nature of the distal histidine residue in the autoxidation reaction of myoglobin and hemoglobin: comparison of the H64 mutants. *Eur J Biochem* **267:**6166–6174.

Tada, T., Watanabe, Y., Matsuoka, A., Ikeda-Saito, M., Imai, K., Ni-hei, Y., and Shikama, K. 1998. African elephant myoglobin with an unusual autoxidation behavior: comparison with the H64Q mutant of sperm whale myoglobin. *Biochim Biophys Acta* **1387:**165–176.

Takagi, T., Iida, S., Matsuoka, A., and Shikama, K. 1984. *Aplysia* myoglobins with an unusual amino acid sequence. *J Mol Biol* **180:**1179–1184.

Takagi, T., Iwaasa, H., Yuasa, H., Shikama, K., Takemasa, T., and Watanabe, Y. 1993. Primary structure of *Tetrahymena* hemoglobins. *Biochim Biophys Acta* **1173:**75–78.

Takagi, T., Tobita, M., and Shikama, K. 1983. Amino acid sequence of dimeric myoglobin from *Cerithidea rhizophorarum*. *Biochim Biophys Acta* **745:**32–36.

Tentori, L., Vivaldi, G., Carta, S., Antonini, E., and Brunori, M. 1968. Amino-acid composition of *Aplysia* myoglobin. *Nature* (*London*) **219:**487.

Tentori, L., Vivaldi, G., Carta, S., Marinucci, M., Massa, A., Antonini, E., and Brunori, M. 1973. The amino acid sequence of myoglobin from the mollusc *Aplysia limacina*. *Int J Peptide Protein Res* **5:**187–200.

Tian, W.D., Sage, J.T., and Champion, P.M. 1993. Investigations of ligand association and dissociation rates in the "open" and "closed" states of myoglobin. *J Mol Biol* **233:**155–166.

Tsubamoto, Y., Matsuoka, A., Yusa, K., and Shikama, K. 1990. Protozoan myoglobin from *Paramecium caudatum*: its autoxidation reaction and hemichrome formation. *Eur J Biochem* **193:**55–59.

Tsuruga, M., Matsuoka, A., Hachimori, A., Sugawara, Y., and Shikama, K. 1998. The molecular mechanism of autoxidation for human oxyhemoglobin: tilting of the distal histidine causes nonequivalent oxidation in the β chain. *J Biol Chem* **273:**8607–8615.

Ungaretti, L., Bolognesi, M., Cannillo, E., Oberti, R., and Rossi, G. 1978. The crystal structure of met-myoglobin from *Aplysia limacina* at 5 Å resolution. *Acta Crystallogr* **B34:**3658–3662.

Vasudevan, S.G., Armarego, W.L.F., Shaw, D.C., Lilley, P.E., Dixon, N.E., and Poole, R.K. 1991. Isolation and nucleotide sequence of the *hmp* gene that encodes a haemoglobin-like protein in *Escherichia coli* K-12. *Mol Gen Genet* **226:**49–58.

Wakabayashi, S., Matsubara, H., and Webster, D.A. 1986. Primary sequence of a dimeric bacterial haemoglobin from *Vitreoscilla*. *Nature (London)* **322:**481–483.

Weber, R.E. and Vinogradov, S.N. 2001. Nonvertebrate hemoglobins: functions and molecular adaptations. *Physiol Rev* **81:**569–628.

Weber, R.E., Braunitzer, G., and Kleinschmidt, T. 1985. Functional multiplicity and structural correlations in the hemoglobin system of larvae of *Chironomus thummi thummi*(Insect, Diptera): Hb components CTT I, CTT II, CTT III, CTT IV, CTT VI, CTT VIIB, CTT IX and CTT X. *Comp Biochem Physiol* **80B:**747–753.

Wilps, H. and Zebe, E. 1976. The end-products of anaerobic carbohydrate metabolism in the larvae of *Chironomus thummi thummi J Comp Physiol* **112:**263–272.

Wittenberg, B.A., Brunori, M., Antonini, E., Wittenberg, J.B., and Wyman, J. 1965. Kinetics of the reactions of *Aplysia* myoglobin with oxygen and carbon monoxide. *Arch Biochem Biophys* **111:**576–579.

Wittenberg, J.B., Bolognesi, M., Wittenberg, B.A., and Guertin, M. 2002. Truncated hemoglobins: a new family of hemoglobins widely distributed in bacteria, unicellular eukaryotes, and plants. *J Biol Chem* **277:**871–874.

Yamauchi, K., Ochiai, T., and Usuki, I. 1992. The unique structure of the *Paramecium caudatum* hemoglobin gene: the presence of one intron in the middle of the coding region. *Biochim Biophys Acta* **1171:**81–87.

Yamauchi, K., Ochiai, T., and Usuki, I. 1995. Structure and evolution of *Paramecium* hemoglobin genes. *Biochim Biophys Acta* **1264:**53–62.

Yamazaki, I., Yokota, K., and Shikama, K. 1964. Preparation of crystalline oxymyoglobin from horse heart. *J Biol Chem* **239:**4151–4153.

Yasuda, J.-P., Ichikawa, T., Tsuruga, M., Matsuoka, A., Sugawara, Y., and Shikama, K. 2002. The $\alpha 1\beta 1$ contact of human hemoglobin plays a key role in stabilizing the bound dioxygen: further evidence from the iron valency hybrids. *Eur J Biochem* **269:**202–211.

Yubisui, T., Miyata, T., Iwanaga, S., Tamura, M., and Takeshita, M. 1986. Complete amino acid sequence of NADH-cytochrome b_5 reductase purified from human erythrocytes. *J Biochem (Tokyo)* **99:**407–422.

Yubisui, T., Miyata, T., Iwanaga, S., Tamura, M., Yoshida, S., Takeshita, M., and Nakajima, H. 1984. Amino acid sequence of NADH-cytochrome b_5 reductase of human erythrocytes. *J Biochem (Tokyo)* **96:**579–582.

Zhao, X., Vyas, K., Nguyen, B.D., Rajarathnam, K., La Mar, G.N., Li, T., Phillips, G.N., Jr., Eich, R.F., Olson, J.S., Ling, J., and Bocian, D.F. 1995. A double mutant of sperm whale myoglobin mimics the structure and function of elephant myoglobin. *J Biol Chem* **270:**20763–20774.

Zhu, H. and Riggs, A.F. 1992. Yeast flavohemoglobin is an ancient protein related to globins and a reductase family. *Proc Natl Acad Sci USA* **89:**5015–5019.